AD

EDR 4669

LITHIUM-CHLORINE ELECTROCHEMICAL ENERGY STORAGE SYSTEM

Interim Technical Report
13 December 1965—13 June 1966

Edited by: E. H. Hietbrink
Advanced Power Systems

5 July 1966

U. S. Army Research and Development Laboratories
Fort Belvoir, Virginia

Contract DA-44-009-AMC-1426(T)

Allison Division • General Motors
Indianapolis, Indiana

AD

EDR 4669

LITHIUM-CHLORINE ELECTROCHEMICAL ENERGY STORAGE SYSTEM

Interim Technical Report
13 December 1965—13 June 1966

Edited by: E. H. Hietbrink
Advanced Power Systems

5 July 1966

U. S. Army Research and Development Laboratories
Fort Belvoir, Virginia

Contract DA-44-009-AMC-1426(T)

Allison Division • General Motors

Indianapolis, Indiana

FOREWORD

This interim technical report was prepared by the Allison Division of General Motors, with support from the Defense Research Laboratories of General Motors, to present the technical work conducted for the U.S. Army Engineer Research and Development Laboratories under Contract No. DA-44-009-AMC-1426(T) during the period 13 December 1965 to 13 June 1966. Research and systems investigations are being accomplished to determine the feasibility of a lithium-chlorine electrically rechargeable electrochemical energy storage system.

Management direction at Allison included Mr. T. F. Nagey, Manager, Research and Advanced Projects, Aerospace Products; Dr. F. G. Myers, Director of Research, Aerospace Products; Dr. J. L. Hartman, Chief, Advanced Power Systems; and Mr. N. H. Triner, Section Chief, Terrestrial Power Systems. Mr. E. H. Hietbrink is the Project Manager. Dr. F. Schuler is the manager at Defense Research Laboratories for their contribution to this contract. Acknowledgement is also made of the contributions to this report by the following individuals:

Allison Division	Defense Research Laboratories
Dr. R. E. Henderson	Ronald Guidotti
Dr. D. A. Swinkels	G. A. Sheppard
H. R. Karas	Edward Zeitner
D. L. Dimick	
J. P. Kern	

SUMMARY

Work was conducted in several areas to investigate the feasibility of a lithium-chlorine electrochemical energy storage system for vehicle propulsion. The system investigated had a high energy density, high power density, and fast charge capability for use in military vehicles which can be recharged by a mobile reactor powerplant.

Task I effort involved determining methods for charging a system in a 20-min time interval. Previous experimental work has established the occurrence of an anode effect. At high charging current densities, the cell efficiency drops significantly due to polarization of the Cl_2 electrode. A reverse current pulsing concept for eliminating this phenomenon was experimentally investigated. Different types of carbon were utilized for the Cl_2 electrode and various electrode geometries were analyzed. Experimental results indicate that both geometry and material selection are important in the electrode design and that reverse pulsing enhances the electrode performance, allowing a higher charging current density.

Task II and III effort involved fabricating and operating a test cell using Li and Cl_2 as reactants. This cell, designated as Mark IV, contains approximately 1600 amp-hr of Li. Design modifications were completed on the cell cooling system to allow for higher charge rates. An electrical short terminated the first cell test before meaningful data could be obtained. Required design modifications are presently being incorporated into the design.

Task IV effort involved performing system design studies on the proposed Li-Cl_2 system for Army vehicle propulsion. During this report period, two cell concepts were investigated. The first was an advanced concept of the Mark IV experimental cell currently being tested. The second was a cylindrical cell design using vertical electrodes. The latter cell was selected as the most advantageous and was developed into several engine system concepts. A modular engine system comprised of ten replaceable modules was developed to meet the duty cycle requirements specified by ERDL. This system, weighing approximately 1250 lb, will provide 200 kw-hr of energy. System analysis and trade-off studies on a fast charge system concept are in progress and only partial results are reported.

Task V effort involved determining the feasibility of Cl_2 adsorption on charcoal. Adsorption kinetics and recycle characteristics were experimentally determined. No specific conclusions were reached regarding this work.

TABLE OF CONTENTS

BLANK PAGE

LIST OF ILLUSTRATIONS

LIST OF TABLES

I. INTRODUCTION

This interim technical report was prepared by the Allison Division of General Motors, with support from the Defense Research Laboratories of General Motors, under U.S. Army Engineer Research and Development Laboratories Contract DA-44-009-AMC-1426(T) for the period 13 December 1965 to 13 June 1966. Effort was directed toward determining the feasibility of a regenerative cell using Li and Cl_2 as reactants.

Initial feasibility studies carried out by the Army have indicated a number of possible methods of utilizing nuclear energy for powering Army ground vehicles. The immense weight of a reactor system precludes any possibility of direct use of nuclear energy on a vehicle. As a result, those systems that have been investigated utilized the thermal output from a mobile reactor plant by converting this energy through some intermediate system to mechanical power at the wheel of the vehicle.

From the initial feasibility studies, three systems have been selected as the most promising for further study. These systems all consider use of electrical power generated by reactor heat. Those selected are:

- Production of anhydrous ammonia and its use in conventional engines
- Production of anhydrous ammonia and its use in ammonia-air fuel cells
- Charging and discharging of electrical power using a regenerative cell

The concept of the regenerative cell is inherently a simple one. Much like the automobile battery, it involves the storage of electrical energy by chemical means. The regenerative cell is thus a secondary battery with high energy storage capability. The cell is charged by connecting it to leads from an electrical power source. Electrolytic separation of the stored chemical compound into its reactive constituents takes place within the cell. On discharge, these constituents recombine electrolytically within the cell to produce the electrical power required.

A lithium-chlorine cell is an example of such a regenerative cell. Figure 1 is a schematic illustration of this cell. Lithium and Cl_2 are fed through their respective electrodes into the power section of the cell. The Li atom gives up an electron at the Li electrode, and the ion migrates through the electrolyte to the vicinity of the Cl_2 electrode. Here it combines with a Cl-ion to form a LiCl molecule. The electron, flowing in the external circuit, provides the desired electrical power. The potential, v, across these external electrodes is a function of the free energy of reaction of the constituents used and the cell losses. In charging the cell, a sufficiently large voltage is applied to the external leads to electrolytically separate the LiCl and regenerate the original constituents.

The purpose of this effort is to carry out investigations, experiments, and design studies of a lithium-chlorine regenerative energy storage system. The ultimate objective of this work is to obtain suitable data to determine the feasibility of this energy storage system. The application envisioned is for use in a vehicle propulsion system where the energy for recharging the power system will be provided by mobile reactor powerplants.

Program effort was divided into the following five tasks:

- Task I—Chlorine Electrode Charge Performance—Investigation of alternative means for increasing the charge rate of the Li-Cl_2 cell
- Task II—Construction of Cell Model—Construction of a cell for feasibility testing
- Task III—Experimental Evaluation of Energy Efficiency—Performance testing of the experimental Mark IV cell

BLANK PAGE

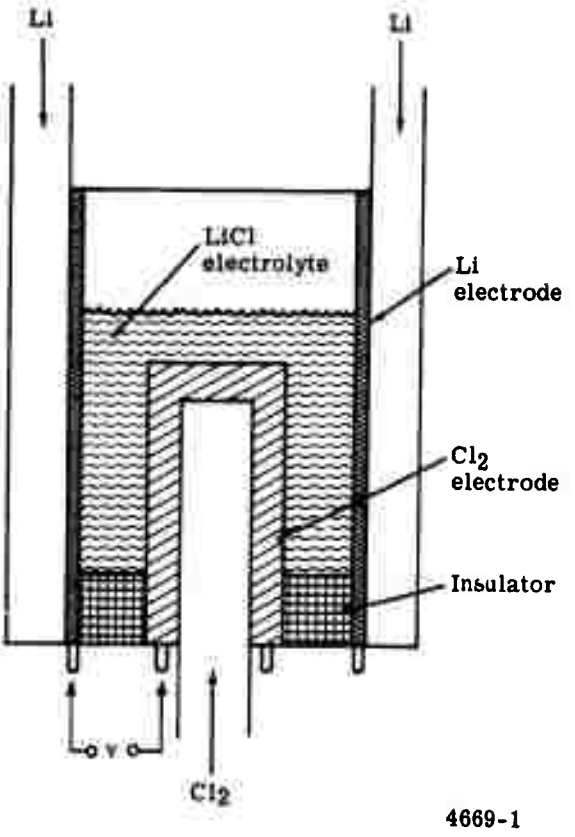

Figure 1. Lithium-chlorine cell schematic.

- Task IV—System Analytical Studies—Evaluation of potential vehicle electrochemical engine systems
- Task V—Chlorine Adsorption Investigation—Experimental investigation of the potential use of charcoal adsorption for Cl_2 storage

The Defense Research Laboratories of General Motors conducted the work which is reported for Tasks 1 and 5.

II. CHLORINE ELECTRODE CHARGE PERFORMANCE (TASK I)

OBJECTIVE

The purpose of this task was to develop methods for maintaining high charge rates in a lithium-chlorine cell without being limited by the anode effect at the Cl_2 electrode.

INVESTIGATION

Initial investigations of the anode effect were completed in the Allison Research Laboratory prior to tne contract by Dr. D. Swinkels and R. Seefurth.* It was concluded from these investigations that reverse current pulses during charge would be effective in depositing Li on the graphite electrode and form Li_2C_2. The Li_2C_2 would then diffuse through the electrolyte and cause it to wet the graphite to a relatively high degree allowing high critical charge current densities. It was concluded, therefore, that the anode effect studies should be focused on the current reversal concept described in the following Statement of Work.

- The effect of current reversal on the appearance of the anode effect will be determined at one atmosphere. Factors to be considered are frequency of current reversal, duration of the reversal, and the ratio of forward-to-reverse current density. The use of a dummy electrode for current reversal should also be investigated. In all cases, steady-state conditions must be determined.
- The materials to be studied should include both porous and dense carbon and graphite materials which are presently used in the construction of Li-Cl_2 cells (FC-11 porous graphite, Graph-i-tite A, PO3 dense graphite, and pyrolytic graphite). For diagnostic purposes, other grades of graphite may, however, be investigated.
- The effect of increasing the total system pressure on the appearance of the anode effect will be studied. The optimum conditions of current reversal will be tested at 5 and 10 atmospheres on the materials evaluated.
- The long-time effects of the optimum current reversal technique will be studied. Possible damage to the electrode and accumulation of products in the electrolyte will be investigated.

Other methods for obtaining high rates of Cl_2 evolution in the lithium-chlorine system may be studied if time and manpower are available—e.g., pressure reduction behind the electrode to remove Cl_2 bubbles as they form.

EXPERIMENTAL EFFORT

Experimental effort to date has been focused on one-atmosphere studies. A concise Statement of Work completed is as follows:

- The anode effect was first investigated in molten LiCl between 660 and 675°C at 1 atm of Cl_2 pressure. The Cl_2-Cl_2 cell consisted of an aqueous LiCl solution as the electrolyte. Various electrode configurations were investigated for relative comparison of limiting current densities using the same anode materials studied in the molten LiCl. Current-voltage data were obtained for each anode material studied in an attempt to accurately characterize the anode effect in molten LiCl.

*Dr. D. Swinkels and R. Seefurth, Anode Effect Studies, Part I and II, Allison Division, General Motors, ACS Report No. 65-55 (29 September 1965) and 65-65 (6 December 1965).

- Limiting current densities were studied for the various anode materials tested in both fused and aqueous systems. The effect of current reversal on the limiting density was noted for several anode materials.
- Work was resumed on fused LiCl. Preliminary studies of pressure reduction behind the anode were performed.

The system used to study the anode effect in fused LiCl at 650°C was a Cl_2-Cl_2 refining cell enclosed in a furnace. The cell contained a counter-electrode with a Cl_2 supply, where the reaction was $1/2\ Cl_2 + e \rightarrow Cl^-$, and a test anode, where the reaction was $Cl^- - e \rightarrow 1/2\ Cl_2$. The cell used associated circuitry to manually increase the cell voltage and record the current-voltage data until the anode effect was observed.

A modification was also used (i.e., aqueous 50% saturated LiCl at room temperature) with a similar Cl_2-Cl_2 cell, so that visual observation of the gas film formation could be correlated with the current-voltage data.

Various tests were conducted during this report period. The pertinent features of the tests are described in the following paragraphs.

Circuit Diagram

The circuit diagram is shown in Figure 2 and discussed in the Generalized Operating Procedure section.

Cl_2-Cl_2 Electrode Configurations

Two designs of the overall apparatus used in the study are shown in Figures 3 and 4. These cutaway drawings show the details of the Cl_2-counter electrodes and the Cl_2-test electrodes which consisted of either nonporous graphite or porous graphite cemented to nonporous rods.

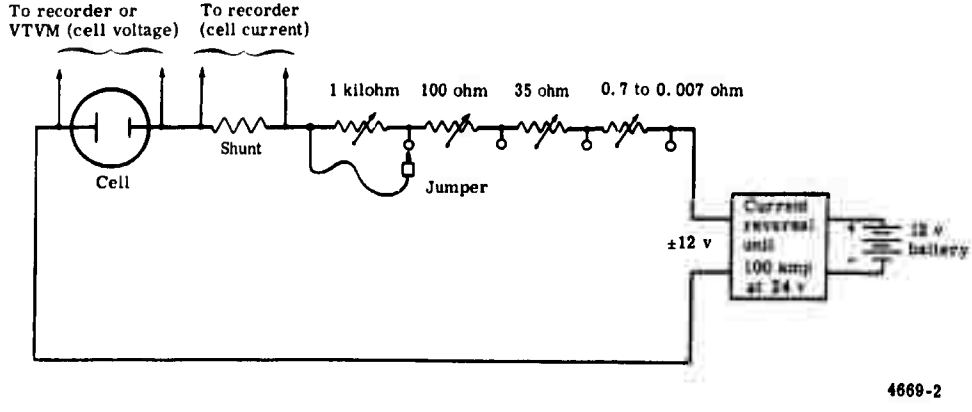

Figure 2. Circuit diagram for the fast charge investigation.

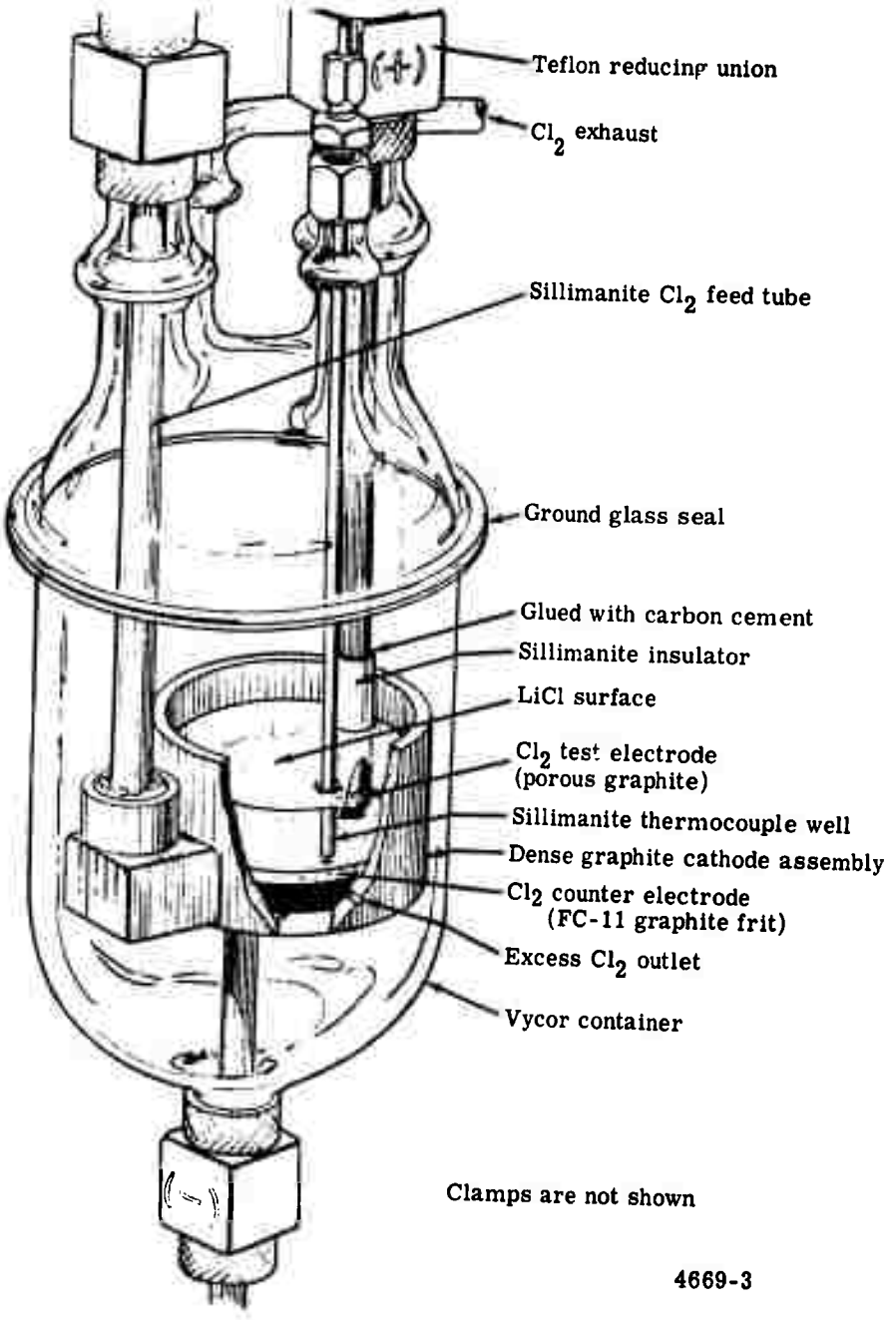

Figure 3. First model of the Cl_2-Cl_2 cell.

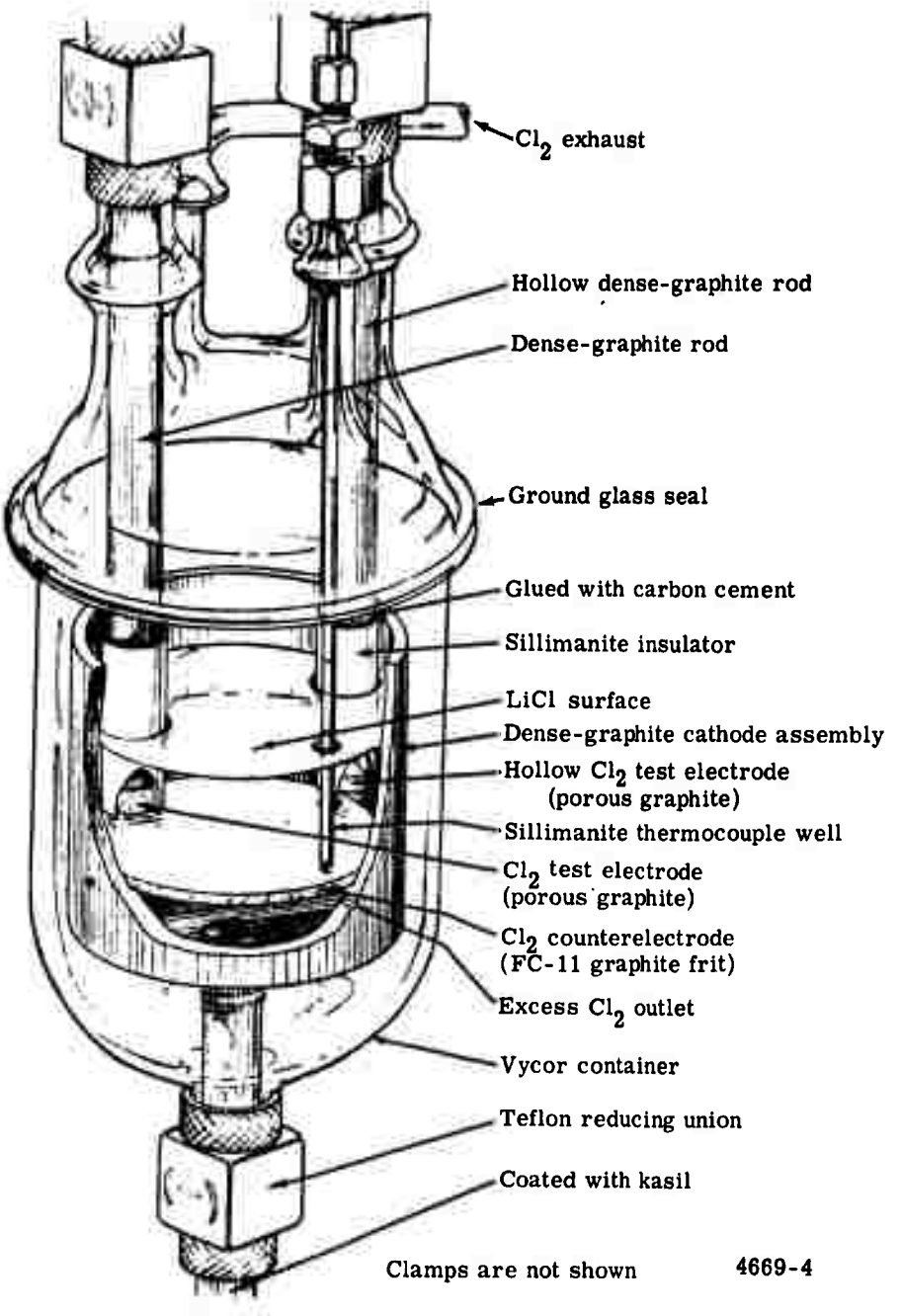

Figure 4. Second mode of the Cl_2-Cl_2 cell.

In the aqueous LiCl solution studies, other configurations were used. These are schematically shown in Figure 5. In the early experiments, scale-down difficulties were encountered with configuration D of Figure 5. The Statement of Work tended to minimize this aspect and stress current reversal and the effect of increased Cl_2 pressure. However, the problem of scale-down (this part of the study is really a scale-down experiment relative to a proposed power module) is well known in the electrochemical field.*

Materials Used

The porous graphites investigated were FC-11 and FC-13 (Pure Carbon Company). The dense graphite studied was Speer Carbon 886, which is similar to Pure Carbon Company's AGR in its physical properties.

Generalized Operating Procedure

1. Construct a Cl_2-Cl_2 cell—The cathode, which supplied Cl_2 to the system, had a body of dense graphite (Speer Carbon 890) and a porous bottom (Pure Carbon FC-11). This cathode body was the container for the electrolyte; however, another container was sometimes used. The cathode was not "dead-ended" but had several small holes in its side (1/32-in. dia) for excess Cl_2 flow.

   The anode area was restricted to the end of the electrode rod by use of an insulating sleeve. Other designs could have special geometries, but all have this area restriction technique when using an insulator.

   Sillimanite (Mullite) was the usual insulating material. It was glued to the electrode rod with C-9 carbon cement (National Carbon Company). This cement was cured at both 100 and 150°C for several days. It was given a higher temperature cure in the cell when the cell was brought to operating temperatures with Cl_2 flushing through it.

   The electrolyte melt temperature was measured with a thermocouple which was sheathed by a Sillimanite tube and inserted into the melt.

2. Assemble the associated circuitry—The current through the cell was measured as a voltage drop across a known resistance shunt. The voltage of the cell in the initial studies was measured with a Hewlett-Packard VTVM (Model 410C). The voltage drop across the shunt was recorded on a Sargent strip-chart recorder (Model SR). A Moseley dual-pen strip-chart recorder (Model 7100B) was used in later studies to record both cell current and voltage at the same time. A 1750w Jagabi rheostat (Biddle Company) was used for the final adjusting of current at the higher levels.

   The current reversal unit (Rapid Electric Company, Periodic Reverser, Model 266933) could be used as an on-off switch with or without reversing the current. The forward or reverse time could be adjusted from 120 sec to less than 1 sec.

   A 12-v battery was adequate for most studies.

3. Melt the LiCl—The LiCl (Lithium Corporation of America) was melted in the dry box (Vacuum Atmospheres Corporation, Model VAC-LAB-HE-233-16) and poured into graphite molds to form salt plugs.

*R. B. MacMullin, "The Problem of Scale-Up in Electrolyte Processes", Electrochemical Technology, January-February 1963, pp 5-17.

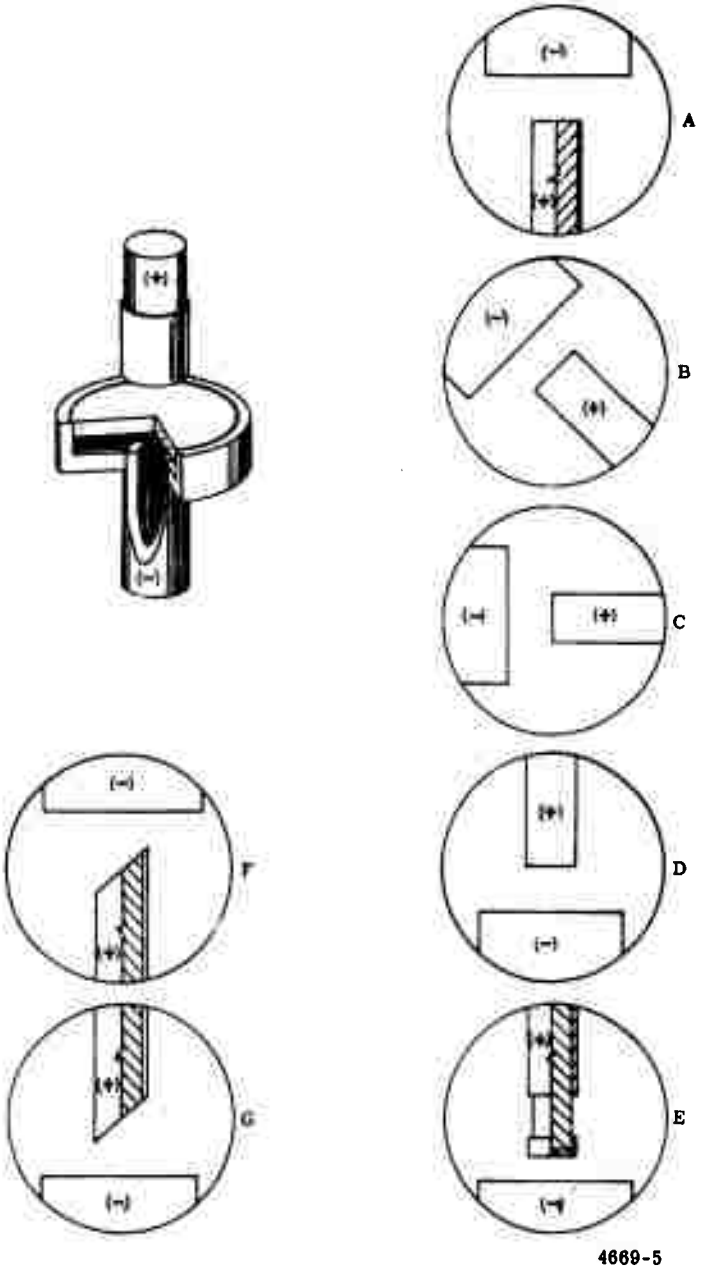

Figure 5. Cl_2-Cl_2 electrode configurations.

4. Purge the cell—The cell was first flushed with Ar for an hour and the LiCl plug quickly transferred from the dry box to the cell; the cell was then flushed for an additional 30 to 40 min. The cell was next flushed with Cl_2 while being heated in a muffle furnace to the operating temperature.

5. Lower the anode into melted LiCl—Once the LiCl had been melted and the cell had been flushed an additional 30 min, the anode was lowered into the melt to begin a run.

   At the end of the day, the anode was raised above the salt and the cell was allowed to cool to room temperature. The cell was then flushed overnight with Cl_2 to maintain a Cl_2 atmosphere.

6. Start testing—To start a run, the rheostats were turned to their maximum resistance position. Starting with the 1 kilohm rheostat and working down to the Jagabi rheostat (bypassing each rheostat with the jumper cable when it had reached its minimum resistance position), the current through the cell was gradually increased until an anode effect was observed (i.e., the cell current would drop to a very low value and the cell voltage would climb to that of the power supply maximum).

7. Keep the Cl_2 flow constant—The Cl_2 supplied to the cell passed through a flowmeter which had been calibrated for Cl_2. A 100% excess of Cl_2 over that required for a specific current flow was maintained at all times.

8. Stop testing—The jumper was removed and the rheostats returned to their maximum resistance positions before the next run was made.

Saturated Aqueous LiCl Study, Cl_2-Cl_2 Electrode

A Pyrex beaker with a tight-fitting plastic lid was used in the aqueous anode-effect study at room temperature and 1 atm of Cl_2. The anode and cathode could be interchanged easily and the beaker tilted so that various configurations (see Figure 5) could be obtained. The electrolyte was 50% saturated aqueous LiCl solution prepared by diluting a saturated solution 1:1 with distilled water. The solution was cooled by means of an immersed Pyrex coil through which cold water was circulated. The Sillimanite sheath was cemented to the graphite with General Electric RTV-102 silicone adhesive. A Teflon sheath was taped to the graphite with Mystik tape.

Preliminary Fused Salt Study, Cl_2-Cl_2 Electrode

Cell Design and Geometries

The anode effect was studied using a Cl_2-Cl_2 cell in LiCl at 1 atm of Cl_2. Both a dense graphite (Speer 886) and a porous graphite (FC-11) were investigated. The 1/4-in. dia anodes were insulated with Sillimanite (Mullite) sleeving so that the anode faces were down and parallel to the FC-11 cathode (Cl_2-Cl_2 electrode configuration D of Figure 5). This cell (see Figure 3) was used in the early studies with the small anodes (1/4-in. dia). It had provisions for only one test electrode at a time. The area of the cathode was about 10 cm^2 while the small anode was 0.32 cm^2. The temperature range was 660 to 673°C.

The cell of Figure 4 is similar to that of Figure 2 but is larger and has provisions for several test electrodes (1/2-in. dia). The area of the cathode in this case was 32 cm^2 while the anode was 1.26 cm^2.

This cell was also used in the preliminary study of pressure reduction behind the anode as a means of improving the limiting current density. A pressure differential across a hollow anode was provided by H_2SO_4 bubblers of different heights.

A thermocouple was also inserted so that the temperature at the anode surface could be measured during the anode effect.

Open Circuit Measurements

Open circuit voltages were observed for both the dense and porous graphites. With the dense graphite, open circuit voltages of 15 to 25 mv were observed (the anode was positive). With FC-11, somewhat lower open circuit voltages were observed—sometimes close to zero and at other times 10 to 15 mv.

Cell Resistances and Start-up

The cell resistances of the smaller cells ranged from 0.47 to 0.54 ohm for the dense graphite anodes and 0.57 to 0.87 ohm for the FC-11 anodes. The largest part of the resistance was caused by the graphite. The resistance of cells with FC-11 anodes was much higher initially and these cells did not reach equilibrium as rapidly (i.e., attain a stable cell voltage at a given current) as did the cells with dense-graphite anodes. This is probably caused by the O_2, N_2, and other gases initially adsorbed on the FC-11 which is replaced by Cl_2 as the cell operates.

These adsorbed gases caused considerable trouble in initiating current flow in cells with FC-11 anodes. A gas film must have been present initially, causing the cell to exhibit a pseudo-anode effect at current densities as low as 0.02 to 0.08 amp/cm^2. These difficulties were generally not observed with the dense-graphite anodes.

Current-voltage Curves and Anode Effect

With dense-graphite anodes, the voltage versus time and current versus time curves were constant until the anode effect occurred. After this, the voltage suddenly rose to the battery voltage and the current dropped to nearly zero. This was observed in several cases with FC-11. However, as the anode effect was beginning to take place, the cell voltage gradually increased much faster than the cell current decreased until the anode effect occurred. At this point, the changes were abrupt as with the dense-graphite anodes. Where the anode effect could be seen taking place with the FC-11, it occurred without warning in every instance with the dense graphite.

Current-voltage plots for the dense-graphite anodes were very linear at medium current densities (15 amp/cm^2). At low current densities (0 to 0.25 amp/cm^2), there was a knee or bending of the line. At high current densities (15 to 30 amp/cm^2), the line curved away toward a more positive voltage. In other cases, the line continued to be linear in this region.

In the case of the FC-11, the current densities reached were much lower. The current-voltage plots for the FC-11 were more linear in the lower current region but began to deviate gradually at current levels near anode effect to higher voltages and lower currents. The anode effect was generally first observed between 3.0 and 4.0 amp/cm^2 after several minutes, but at other times, even currents below the original level could not be maintained very long.

Recovery After Anode Effects—Nonreproducible

After occurrence of an anode effect with the dense-graphite anode, vibration of the anode with the power on would not return the current to its original level. Instead, only short current spikes were observed. Once the cell had recovered and the open circuit voltage was between 15 and 25 mv, the current began to pass again. It was observed during this time that the charge-time at high current densities where anode effect occurred could not be repeated at each current level. Sometimes the charge-time was longer than that at which the anode effect first occurred, while at other times the anode effect took place almost immediately after the power was switched on.

With FC-11, the time-to-anode effect for a given current level was more erratic than for the dense graphite. Even when the open circuit voltage of the cell had returned to normal, attempts to switch the power on to the previous level where the anode effect had occurred would sometimes result in an immediate anode effect. It was not possible, therefore, to know whether or not the characteristics of the cell were the same each time a run was made. If the current level was approached more gradually, however, the charge-time at this level was usually longer or closer to the original charge-time at the level where the anode effect first occurred. After the cell with the FC-11 electrode had been subjected to anode effects many times over a period of 4 or 5 hr, it became more and more difficult to maintain even the lower current densities for a fraction of their previous times.

Indirect Observations

Bubble formation at the anode was observed in an indirect manner at low currents by the periodic rise and fall of the cell voltage. The period decreased as the current increased. This was observed for both FC-11 and dense-graphite anodes.

Anode Effect—Nonreproducible

With the Cl_2-Cl_2 electrode (configuration D of Figure 5), a reproducible quantity that characterized the anode effect (e.g., voltage and/or current) could not be measured in a realistic manner by experimental means. There were too many variables—the manner in which anode was prepared, the past history of each anode, and the changing characteristics during the experiment. As a result, it was difficult to repeat an experiment to obtain the same current-voltage plot. This was more common for the FC-11 than for the dense-graphite anodes. However, there was general agreement between different anodes and different runs.

TEST RESULTS

The results of the anode effect studies in molten LiCl with the smaller anodes (1/4-in. dia) are presented in Table I. Results with the larger anodes are listed in Tables II and III. Typical current-voltage density plots for dense (886) and porous (FC-11) graphite are shown in Figure 6 (low current densities) and Figure 7 (high current densities). The data for the aqueous anode-effect study is presented in Table IV.

DISCUSSION

Certain operational and technical problems were encountered in this investigation, specifically with the Cl_2-Cl_2 electrode design.

Table I.
Anode-effect studies in molten LiCl (1/4-in. dia anodes and temperature range between 660 and 673°C).

Current density (amp/cm^2)	Duration	Anode effect	Open circuit voltage (mv)	Cell resistance (ohm)
		Speer Carbon 886		
30 to 33	10 to 15 sec	Yes	15 to 25	0.47 to 0.54
18	20 min	No		
20	25 min	No		
		Pure Carbon FC-11		
6.0 to 8.0	< 1 min	Yes	0 to 15	0.57 to 0.87
3.0 to 4.0	3 to 4 min	Yes		
2.6 to 2.5	after 25 min	No		
2.6 to 2.4	after 25 min	No		
2.5	35 min	No		
0.80	1 hr	No		

Table II.
Anode-effect studies in molten LiCl (1/2-in. dia FC-11 and FC-13 anodes).

Current density forward (amp/cm^2)	Current density reverse (amp/cm^2)	Forward-to-reverse time (sec)	Duration (min)	Anode effect	Melt temperature (°C)	Remarks
		FC-11				
3.77	—	—	2	Yes	660 to 670	Good cell recovery
5.15	4.56	30 to 5	3	No	660 to 670	—
7.95	7.15	30 to 5	5	No	660 to 670	Cell condition worsening
14.3	12.7	30 to 2	5	No	660 to 670	Cell voltage not stable
		FC-11 (pressure reduction behind anode was 0.12 atm)				
>20 to 0.40*	14.0	30 to 5	10	Yes	650 to 690 (at anode)	Anode effect occurring every cycle
10.3	8.6	30 to 5	5	No	690 to 715 (at anode)	Cell voltage stable
14.7	11.9	30 to 5	5	No	720 (at anode)	Temperature rise of 50°C every time current switched forward
15.5	13.9	30 to 5	1	Yes	740 (at anode)	Cell condition worsening
		FC-13 (pressure reduction behind anode was 0.12 atm)				
1.98 to 2.06	—	—	3	Yes	660 to 670	Cell condition worsening
1.60	—	—	2	Yes	660 to 670	Cell condition deteriorated; anode effect occurring at 0.6 to 0.7 amp/cm^2
0.87	0.87	30 to 1	2	No	660 to 670	Cell condition improved
4.36	4.60	30 to 0.3	7	No	660 to 670	Cell voltage not stable; current reversal off
7.90	—	—	0.5	Yes	660 to 670	Cell condition deteriorated

*Values are for each cycle

Table III.
Variation of current densities with various forward/reverse times for FC-13 anodes in LiCl at 660°C.

Forward-to-reverse time (sec)	Forward cell voltage* (v)	Forward current density* (amp/cm^2)	Reverse cell voltage* (v)	Reverse current density* (amp/cm^2)	Duration (min)
30 to 5	1.12 to 1.20	1.35 to 1.27	0.80	1.40	2
30 to 2.5	1.00	1.35 to 1.31	0.80	1.40	2
30 to 1	0.90 to 0.86	1.31	0.70	1.40	2
30 to 5	0.90 to 0.96	1.35 to 1.28	0.80	1.40	2
30 to 2.5	0.88	1.33	0.72	1.40	2
30 to 1	0.84	1.34	0.72	1.40	2
30 to 0.5	0.81	1.34	0.68	1.43	3
30 to 0.3	0.78 to 0.73	1.35	0.65	1.43	3

*Values are for each cycle

Table IV.
Limiting current densities for the electrode configurations presented in Figure 5 in aqueous LiCl* at 25°C (1/4-in. dia anodes).

Type anode	Current densities** for Figure 5 electrode configurations (amp/cm^2)						
	D	C	B	A	E	F	G
886, Sillimanite	10.6 to 11.3	—	12.9	13.7	9.94	14.0	12.4
886, Teflon	5.65 to 5.82	8.88	10.3	11.2	6.55	—	—
FC-11, Sillimanite	9.70	10.7	11.6	12.9	—	—	—
886, Sillimanite, saturated LiCl solution	16.0	—	—	—	—	—	—

*50% saturated aqueous LiCl solution diluted 1:1 with distilled water.
**The maximum current densities that could be maintained for several minutes before observing anode effect.

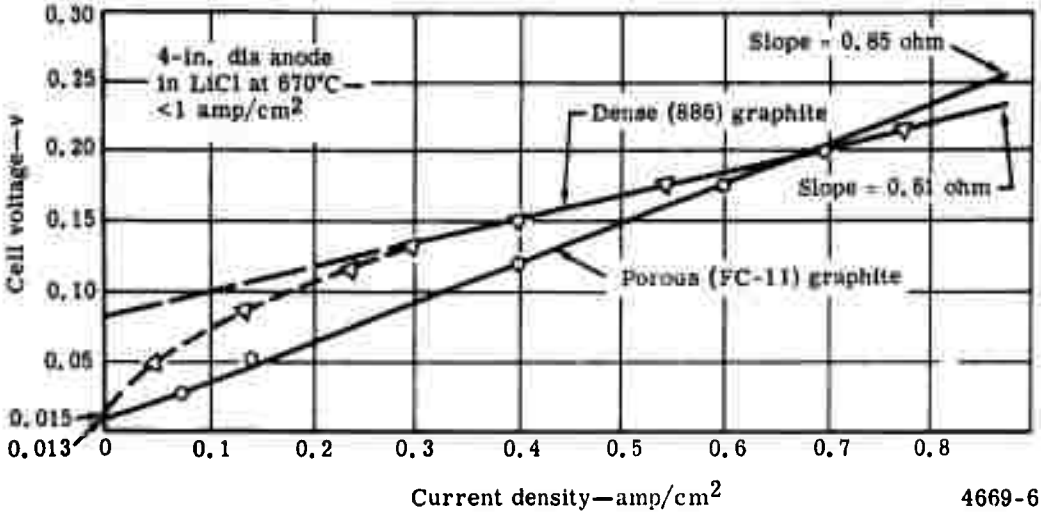

Figure 6. Cell voltage versus current density.

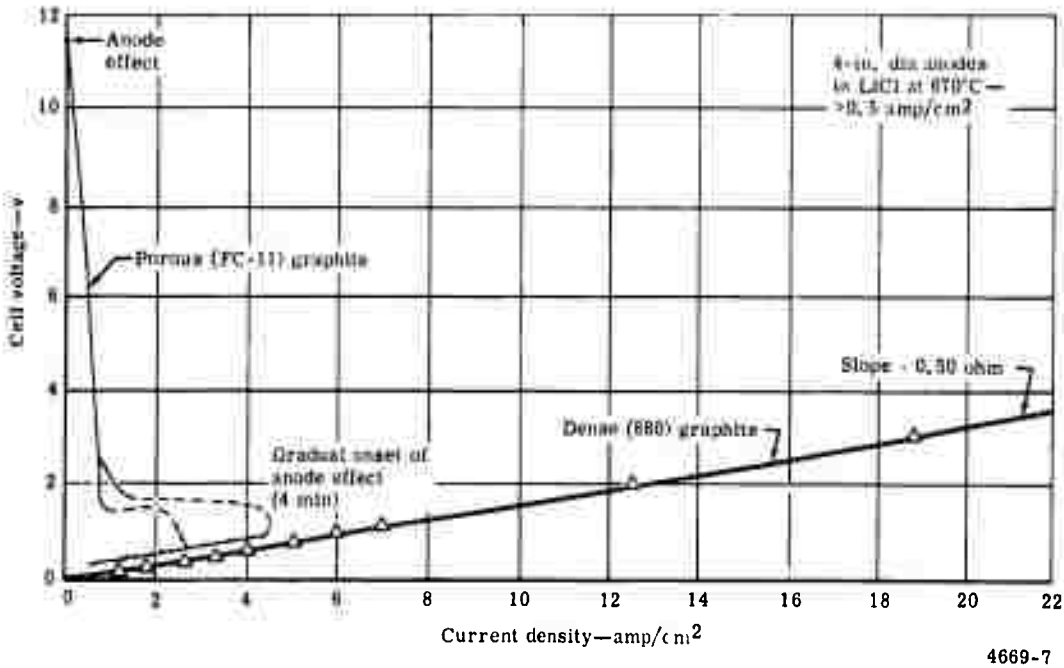

Figure 7. Cell voltage versus current density.

The anode effect study involved a problem in scale-down. The vehicle cell must be scaled down to a convenient experimental size to provide more meaningful data. Other problem areas relevant to fast charging are:

- Effect of gas bubbles on conductivity
- Thermal conductivities and heat transfer coefficients for electrolytes and all materials
- Wetting and nonwetting of Cl_2 electrode
- Edge effects of electrodes
- Configuration—vertical, horizontal, etc

The purpose of the following paragraphs is to emphasize that limited and restricted experimental cell designs may not prove directly applicable to a vehicle system.

Little difficulty was experienced in initiating current flow at the start of a run with cells using the dense-graphite anodes. These cells reached equilibrium rapidly. However, it was more difficult to begin a run with the porous-graphite anodes. At equilibrium, cell resistances became less than 1 ohm, but resistances of 5,000 ohms could be initially encountered with cells using FC-11 anodes. A cell resistance of 200,000 ohms was observed several times.

A gas film was thought to be initially present since the cells sometimes exhibited a pseudo-anode effect at current densities between 0.02 and 0.08 amp/cm^2. The use of the Sillimanite insulating sleeve contributed to the gas film as a result of the foreign gases (O_2, N_2, etc) trapped in the space between the graphite rod and the insulating sleeve.

When a graphite anode was used without the insulating sleeve, no difficulties were encountered in initiating current flow and no pseudo-anode effect was observed. More difficulty was encountered with the FC-13 anodes than with the FC-11. The porosity appeared to be a factor (FC-13, 47% porosity and FC-11, 35% porosity). Less difficulty in initiating current was observed for the porous 1/2-in. dia anodes than for the 1/4-in. dia anodes. The larger anodes also seemed to show a better recovery after anode effect than the smaller ones.

It sometimes required an hour or more for the porous electrodes to reach equilibrium after being inserted into the LiCl. The open circuit voltages dropped to 15 mv or less (anode was positive) while the dense graphite anodes exhibited open circuit voltages of 15 to 25 mv.

After an anode effect had occurred with the smaller anodes, the cell open circuit voltage decreased exponentially from 300 to 500 mv with a sudden decrease to the original stable open circuit voltage again after several minutes.

Mechanical vibration of the anode usually caused this to occur almost immediately. This indicated the release of the gas film or bubble covering the anode surface after occurrence of the anode effect. This bubble release from the anode surface was also observed at low current densities (0.1 to 0.2 amp/cm^2) by the gradual build-up and sudden decay of the cell voltage with time. This occurred periodically and became more frequent as the current density was increased.

This was seen to take place very clearly in the aqueous LiCl system. At low current densities, the gas bubbles formed so slowly that they did not escape freely but tended to become physically trapped at the anode surface until they coalesced to form larger bubbles

which then escaped. This caused a periodic fluctuation of the cell voltage. At medium current densities, the bubbles formed faster and were able to escape with less difficulty, as observed visually, and by reduction in oscillation of cell voltage. At high current densities, the bubbles formed so rapidly that they had less opportunity to escape, tending instead to coalesce to form large bubbles which resulted in the eventual onset of the anode effect.

With the dense-graphite anodes, the cell voltage remained fairly constant at a given current density near anode effect. The occurrence of anode effect was always sudden and without warning. With the porous-graphite anodes, however, the onset of anode effect was gradual at a given current density near anode effect. The cell voltage gradually increased with time, but much faster than cell current decreased over the same period, until anode effect finally occurred. This is shown graphically in Figure 7. Plots of cell voltage versus current density are shown in Figure 6 for FC-11 and 886 graphite at current densities less than 1 amp/cm^2. The data for the 886 graphite anode generally exhibited a rounding at very low current densities (< 0.25 amp/cm^2).

The time required for occurrence of anode effect at a given current density appears to be random. Measurements of time required for anode effect to occur at a given current density with dense-graphite anodes varied to a factor of ten or more. The porous-graphite anodes tended to be more erratic in this respect. It was not possible to determine if the anode had the same characteristics before each trial. They probably changed during the course of the experiments. When the current density was increased above that at which anode effect was first observed, the time until occurrence of anode effect decreased. When this point was approached gradually, the original current could sometimes be maintained for a longer period of time. The performance of cells with porous-graphite anodes tended to worsen after being subject to many anode effects over a period of time, while those with dense-graphite anodes did not (without using current reversal). Anode effect occurred at increasingly lower current densities until densities which had been maintained over an hour could not be maintained for several minutes. When limiting current densities are referred to with respect to anode effect, the duration of this current density is stated. For example, in Figure 5 current densities of 30 amp/cm^2 were maintained for 10 or 15 sec while a level of 20 amp/cm^2 was maintained for 25 min.

The dense graphite (886) was able to sustain 6 to 7 times the current density that the FC-11 could sustain over a similar period of time without anode effect occurring (no current reversal). The data of the larger FC-11 anodes agreed, within experimental error, to those of the smaller anodes. Relative to the FC-13, the FC-11 anodes were able to sustain about 50% higher current density over the same length of time before anode effect occurred.

The use of current reversal with the porous-graphite anodes was quite helpful. Anode effect occurred in one case with FC-11 at about 3.8 amp/cm^2 after several minutes, but after reversing the current for 5 sec every 30 sec forward, current densities of 14.3 amp/cm^2 were maintained for 5 min without observing an anode effect. However, while the cell voltage and current density in the reverse direction were quite stable at this level, they were not as stable in the forward direction. Each time current was switched to the forward direction, a large current spike was observed (> 20 amp/cm^2) for a few seconds before the current density returned to a relatively stable value (14.3 amp/cm^2).

The use of pressure reduction behind the anode was not significantly helpful in increasing the limiting current density. The porous-anode area available behind the anode for Cl_2 to

pass during discharge was not very large (a 29/64-in. dia hole was drilled through the 1/2-in. dia rod which was glued to the FC-11 or FC-13 being tested). The small flow area coupled with the flow resistance of the frit resulted in no significant amount of gas flowing through the anode during Cl_2 discharge.

The amount of gas flowing through the anode varied little with the current density at the anode. Also, there was a problem of Cl_2 diffusing through the dense-graphite rod. A coating of Kasil (a silicate solution) effectively sealed the graphite externally, but this was not satisfactory under internal cell conditions.

A thermocouple at the anode surface was used to measure the temperature of an FC-11 anode during anode effect and current reversal (Table II). By applying sufficient power to the cell, anode effect was produced while reversing the current (30 sec forward to 5 sec reverse). Each time the current was switched forward, a sudden increase of 50°C was noted at the anode tip, but this decreased after the initial current pulse. This is conservative since there is a thermal delay due to the wall thickness of the thermocouple sheath. After 10 min, the steady-state temperature had risen by 40°C. After decreasing the power to the cell, a stable current density of 10.3 amp/cm^2 was maintained and increased to 15.5 amp/cm^2 over 10 min. The temperature during this time rose from 690 to 740°C and the cell condition began to deteriorate.

With the FC-13 anodes, the use of current reversal resulted in increasing the limiting current density by more than a factor of two relative to that sustained without the use of current reversal over a similar period of time. However, this level was much less than that obtained using FC-11. When current reversal was discontinued, the cell showed a large increase in resistance, relative to that during current reversal, and a gradual deterioration—i.e., the cell voltage began to increase while the current density decreased with time. Subsequent use of current reversal again returned the cell to its original stable condition. The use of current reversal was also helpful for improving the condition of a cell that had begun to worsen after experiencing anode effects without the use of current reversal.

The effect of forward-to-reverse time during current reversal at a given current density on the performance of an FC-13 anode is shown in Table III. Reduction of the forward-to-reverse time from 30 to 5 sec to 30 to 1 sec resulted in stabilizing the cell current density and cell voltage—i.e., the cell resistance became less. Increasing the ratio to 30 to 5 sec again caused the cell to become unstable. The best results were observed using a ratio of 30 to 0.3 sec. Limitations of the reversal unit prevented reducing the reverse time any lower than 0.3 sec.

For a relative comparison of the onset of anode effect for various anode configurations, an aqueous LiCl system was chosen for ease of study and observation. The results are presented in Table IV. The anode configuration presently being used in the molten salt studies was the worst case. The limiting current density for the FC-11 was less than that for the 886, though the difference was not as great as that observed in the molten salt study.

The use of an insulating sleeve of Teflon rather than Sillimanite produced relatively large differences in the observed limiting current densities. This was due to the difference in physical properties. The Cl_2 adhered to the Teflon tenaciously but only slightly to the Sillimanite. This was especially apparent in the vertical, face down, anode position.

III. CONSTRUCTION OF CELL MODEL (TASK II)

OBJECTIVE

The purpose of this task was to modify an existing research cell so that it was capable of accepting a fast charge. Allison is currently operating fourth generation cells which have been designated as the Mark IV type. A complete description of this cell and the required modifications for fast charge are presented in this section.

MARK IV CELL DESIGN

The Mark IV cell design, shown schematically in Figure 8, incorporates the experience acquired into a series stackable cell. Electrical leads are attached to the stainless steel Li electrode container and to the porous graphite Cl_2 electrode. The cell is filled about 3/4 full with LiCl. The cell is then charged by passing a direct current through it with the Li becoming the cathode and the carbon becoming the anode. Lithium is deposited on the stainless steel frit and retained by surface tension. A small differential pressure, not identified in Figure 8, is placed across the frit in such a direction that the Li as it is formed accumulates in the Li chamber. The Cl_2 released exits through the Cl_2 exit lines. A connection is made between the bottom of the Li chamber and the electrolyte section so that the LiCl displaced by the Li is transferred into the electrolyte area. When the Li chamber is filled, the charge is stopped. The capacity of this chamber is 1600 amp-hr of Li. To discharge the cell, a load is placed across the electrical leads. Chlorine is fed through the porous graphite which now becomes the cathode until a small excess of Cl_2 is noted venting through the exit line. Current can now be drawn from the cell. The Li, as it is consumed to form LiCl, is replaced by the electrolyte. The LiCl as it is formed will be forced into the LiCl chamber through the passageways connected to the electrolyte area. When all of the Li has been consumed, the process of charge and discharge can be repeated.

A front view of the assembled cell is shown in Figure 9. The Cl_2 inlet in the center just below the flange area was chosen as the locating point for the front. Figure 10 is a left side view of the assembled cell. In this illustration, the two buss bars for electrical connections are shown. The Li electrode buss is located near the bottom of the cell. The Cl_2 electrode buss is connected just above the flange area. The two large tubes, one opposite the other, extending from the cell housing just above the flange area are the Cl_2 outlet tubes. The two 1/4-in. dia tubes which enter the housing on either side of the Li buss are for the heater in the Li storage area.

Figure 11 shows insulators for the flange bolts and an insulating spacer. The first two items are a stainless steel retaining washer and mica insert for the bolt heads on the lower flange. The third item is an alumina sleeve to insulate the bolts through the holes on the lower flange. The fourth item is an alumina spacer which fits between the carbon and the metal skirt of the Li electrode housing. This item was changed from alumina to beryllia prior to the run.

Figure 12 shows the ceramic tubing and metal bellows for the Cl_2 inlet and outlets. The small end of the metal bellows is brazed on the dark metallized area of the tube behind the threads. The lower tube is the Cl_2 inlet, and the upper tube is one of two chlorine outlets. The large tubes projecting from the Cl_2 inlet and outlets, Figures 9 and 10, are used to house the metal bellows.

The geometrical area of the porous graphite Cl_2 electrode is approximately 125 cm^2. Additional reaction area is produced by grooving the electrode. Outside the porous area and down the skirt to the BeO is an additional area of approximately 150 cm^2 which is active

BLANK PAGE

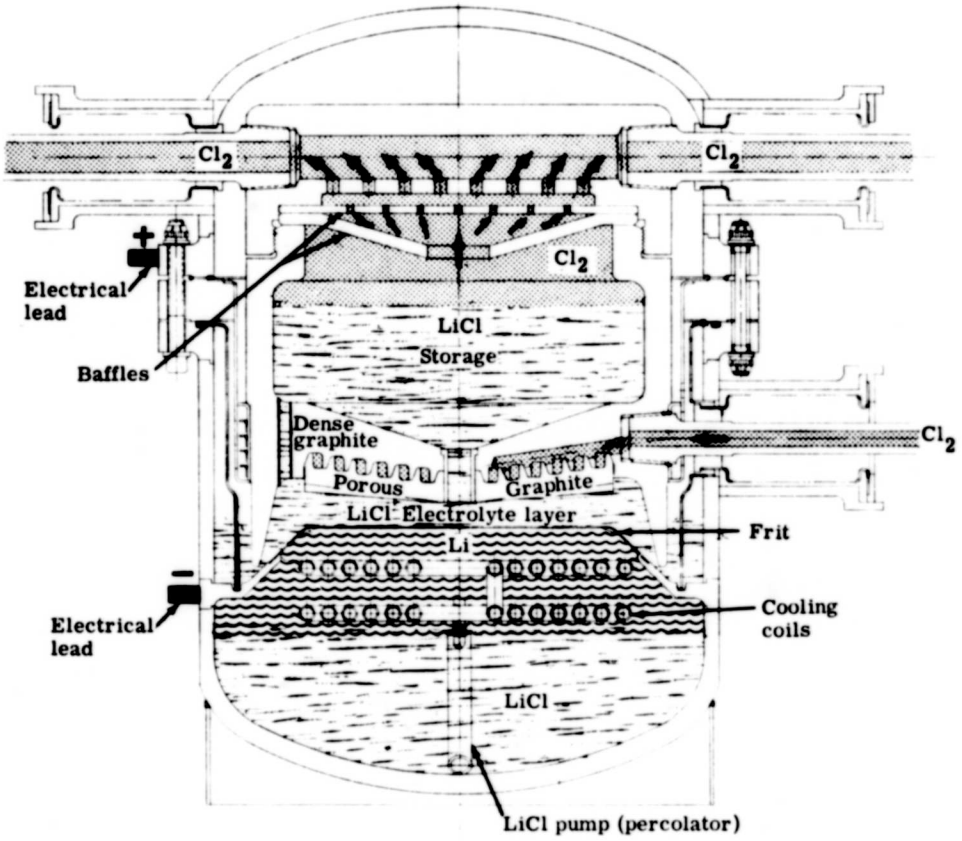

Figure 8. Laboratory Mark IV cell design.

on the charge cycle. The total area on charge, therefore, is 275 cm^2. The Li electrode screen is approximately 125 cm^2, with an additional area of approximately 100 cm^2 outside the screen which is active only on the charge cycle.

All metal parts, with the exception of the nickel blocks and the tubing of the graphite cooler and the metal O-ring, are type SS 316.

MARK IV CELL COMPONENTS

Figure 13 shows the graphite housing for the Cl_2 electrode. The flat machined areas with the small threaded holes are for the nickel cooling blocks. The larger threaded hole in between the two smaller holes is the Cl_2 inlet. The hole which goes through the cap at the top is for the Cl_2 outlets. Figure 14 is a view of the interior of the cap showing the small Cl_2 exit holes. Baffle plates not shown are used inside the cap to strip electrolyte from the Cl_2. Figure 15 shows the Cl_2 electrode area with the radial grooves. The holes at the outside dia of the frit are for excess Cl_2 removal and the convective flow of electrolyte. The Cl_2 electrode housing was made from Graphitite A (Basic Carbon Corporation), and the porous electrode frit was made from FC-11 graphite (Pure Carbon Company). The porous electrode frit was joined to electrode housing with C-9 cement (National Carbon Company).

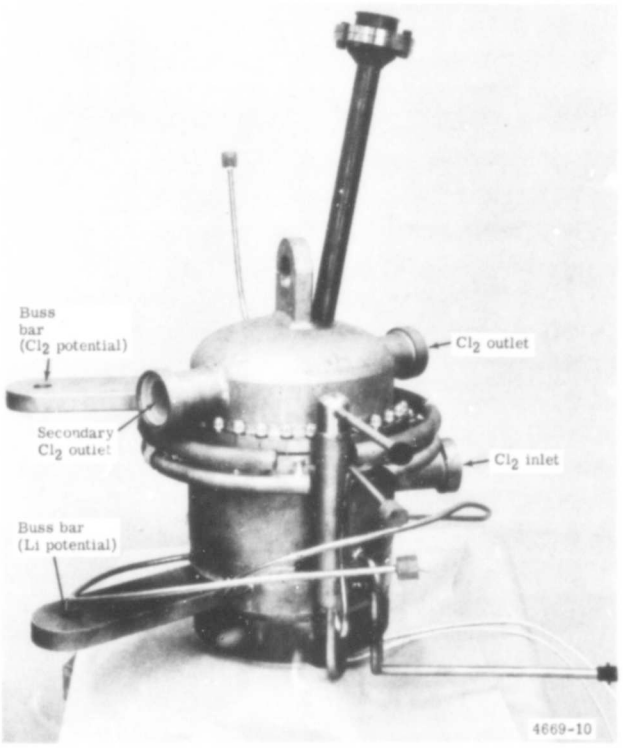

Figure 9. Mark IV cell—front view.

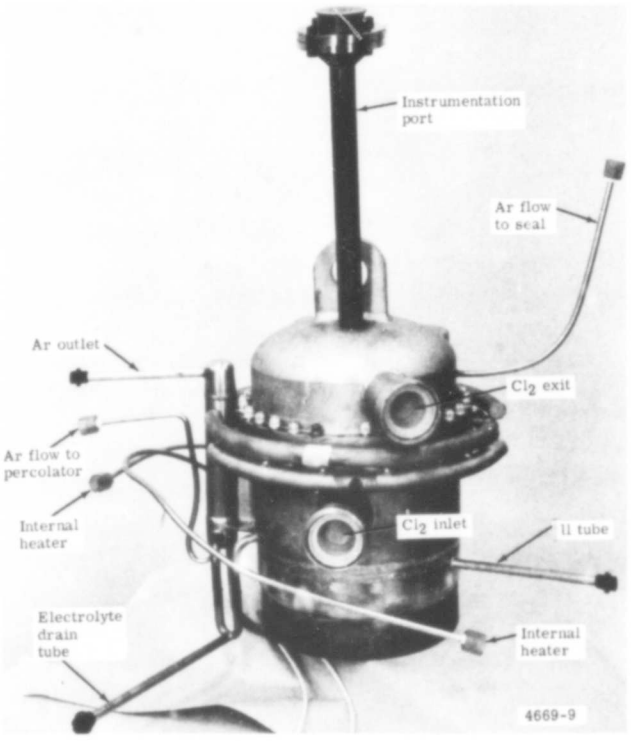

Figure 10. Mark IV cell—side view.

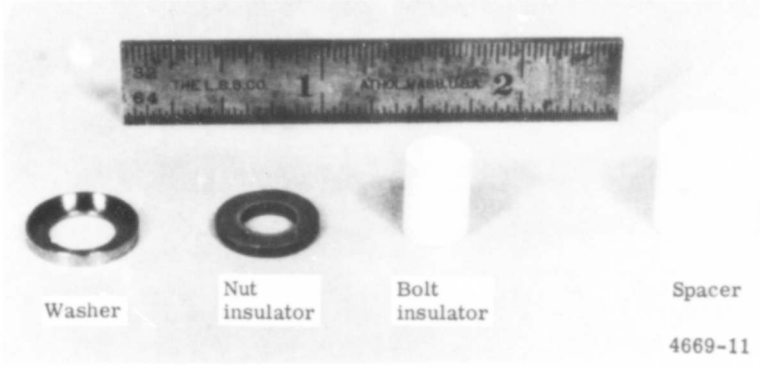

Figure 11. Flange bolt insulators and spacers.

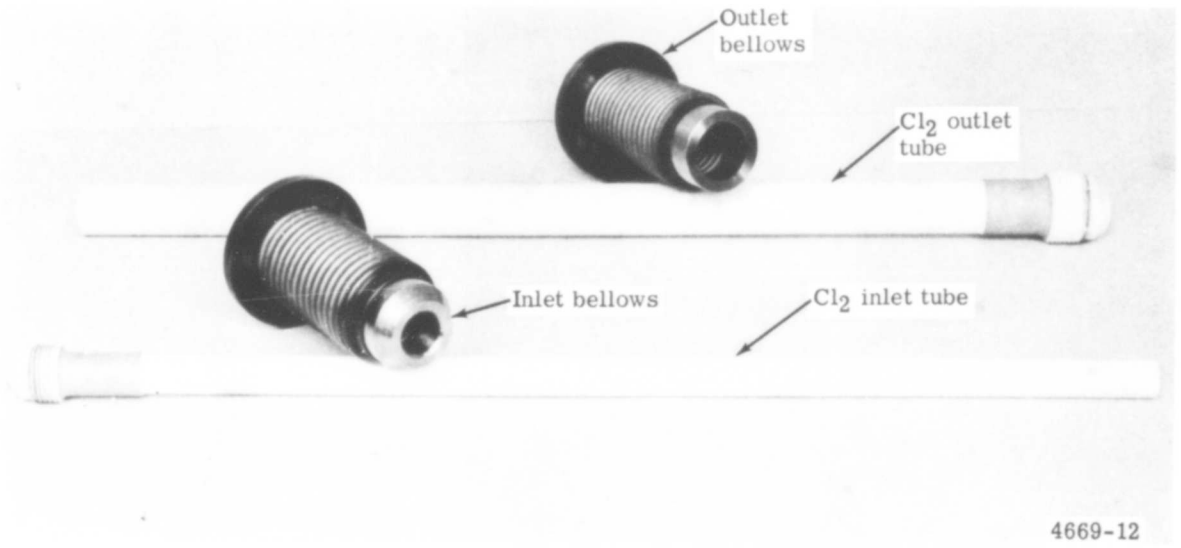

Figure 12. Chlorine lines.

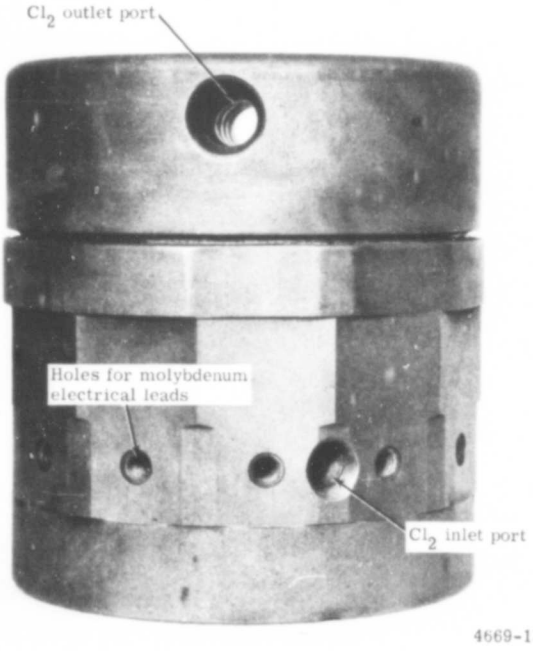

Figure 13. Graphite housing for Cl_2 electrode.

Figure 14. Chlorine electrode cap.

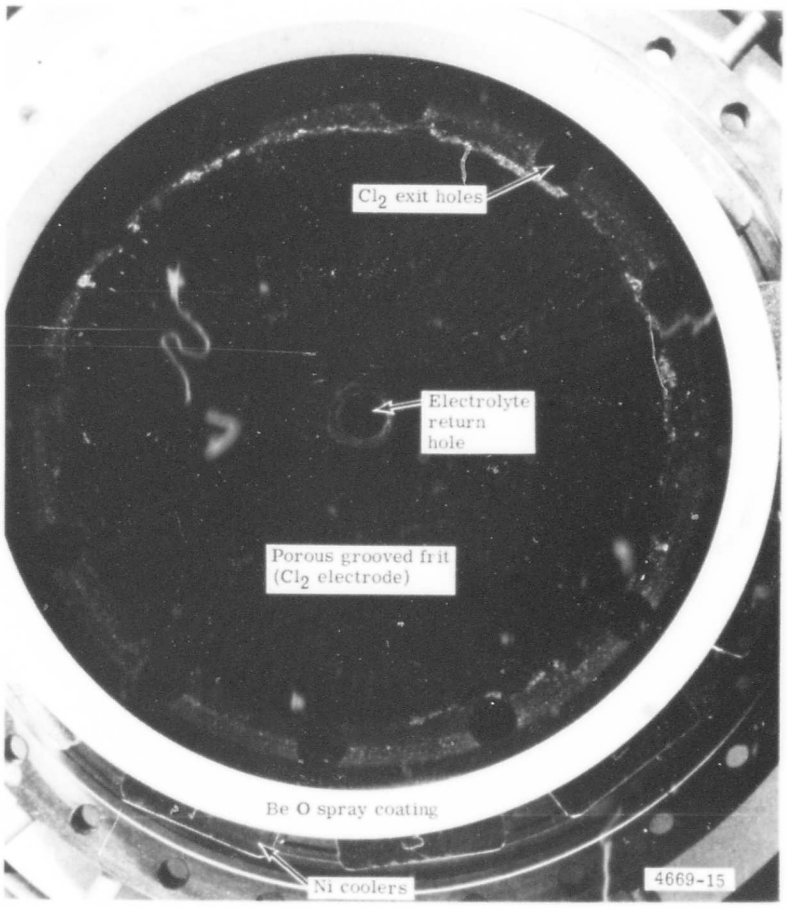

Figure 15. Chlorine electrode face.

Figure 16 shows an assembly consisting of the Cl_2 electrode housing, nickel cooling blocks, intermediate flange, and inlet and outlet manifolds for the Ar coolant. The nickel cooling blocks also provide support and electrical connection for the Cl_2 electrode housing. Inside the bolt circle on the intermediate flange is the O-ring groove. In this case, a nickel plated steel O-ring was used for a permanent seal. In the Mark III design, the seal was achieved only at cell operating temperature with a glass O-ring. The glass ring also provided electrical insulation. The white area on the graphite is the beryllium oxide spray, which is designed to reduce electrochemical activity in unwanted areas.

Figure 17 shows the Li electrode housing with the sidearm attached. The large round hole projecting from the front just below the flange is for the Cl_2 inlet tube. The 3/8-in. dia tube extending at the right is the LiCl fill line. The 3/8-in. dia U-shaped tube attached near the bottom of the sidearm and to the housing at the same level is the electrolyte equalizer tube. The 3/8-in. dia tube which comes from the bottom of the cell and enters the bottom of the sidearm is the percolator tube. This tube extends into the sidearm 3.28 in. The 1/4-in. dia tube which enters the bottom of the sidearm and extends along side of it is the percolator Ar supply tube. Inside the sidearm, this tube enters the percolator tube at a point 2.4 in. from the top.

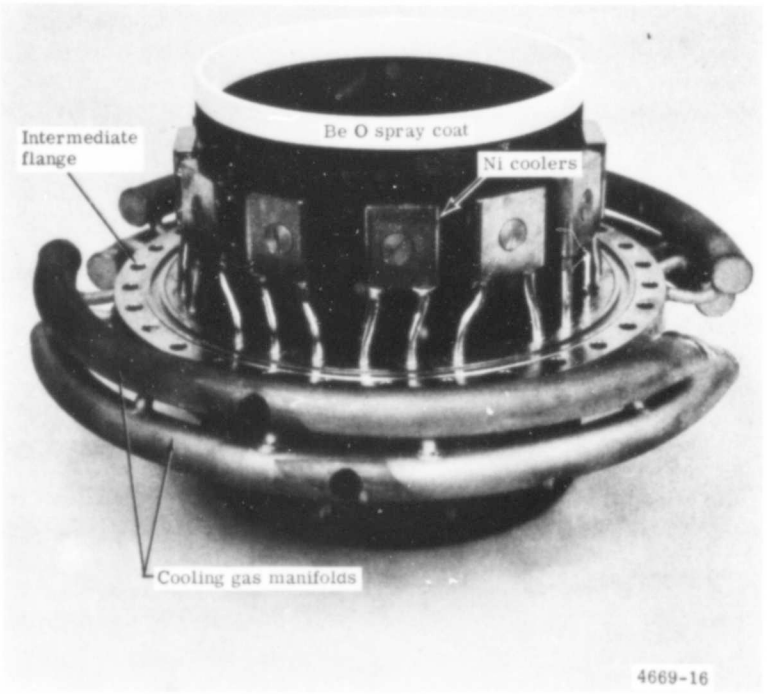

Figure 16. Chlorine electrode housing w/cooling system.

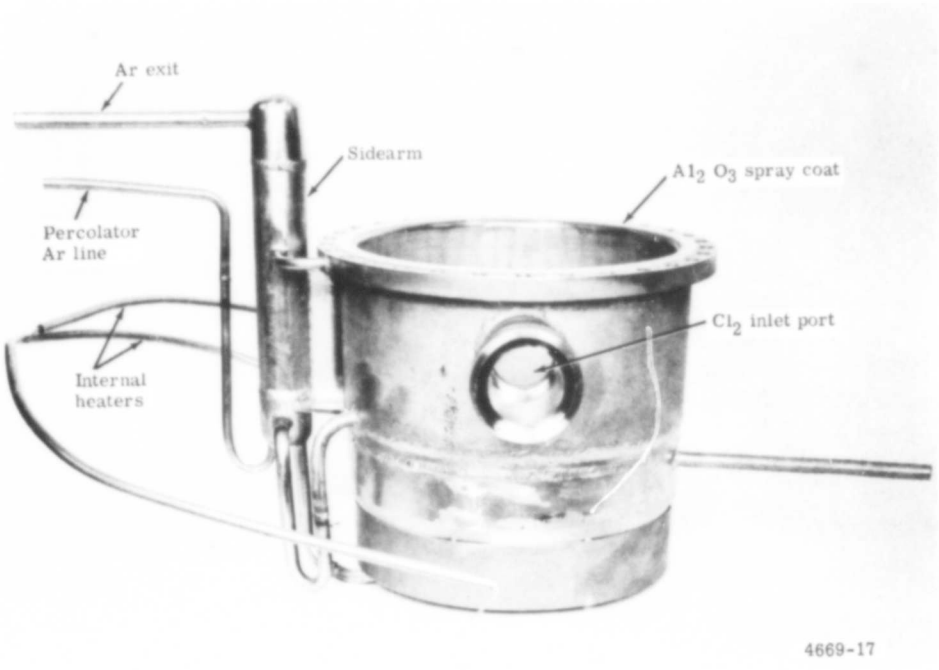

Figure 17. Lithium electrode housing.

The 1/4-in. dia tube shown attached to the flange and entering the sidearm at the same level is the seal Ar outlet for the cell. This tube extends to a 3.4-in. depth inside the sidearm, bringing the tube opening to the same level as that of the graphite skirt inside the cell.

Figure 18 is an interior view of the Li electrode housing showing the Li electrode screen. The Li electrode screen is perforated type SS 316 with 1109 holes/in.^{2}. The screen is 0.009-in. thick and the holes are 0.016-in. in dia. A sheet metal skirt attached to the flange extends down to the outer base of the Li electrode. The holes which can be seen near the bottom of this skirt are outlets for the seal Ar. The seal Ar is exhausted from behind this skirt through a 1/4-in. dia tube in the flange into the sidearm. When assembled, these holes are slightly higher than the bottom of the carbon skirt of the Cl_2 electrode housing. This arrangement permits the seal Ar to exhaust behind the metal skirt rather than under the carbon skirt and into the main electrode area. The grey or white band on the flange just inside the bolt circle is sprayed alumina which is the electrical insulator between the Li and Cl_2 electrodes.

MARK IV CELL COOLING MODIFICATIONS

The original Mark IV design called for a rated power of 200 w electrical output at 3 v. The thermal dissipation on discharge was then set at 67 w (ΔH = 4 v for 2 Li + $Cl_2 \rightarrow$ 2 LiCl. No requirement existed at the time of the original design for high charge rates, therefore, the thermal design was based on the discharge conditions.

With the advent of this contract, high charge rates became a mandatory design requirement. For this reason, the advanced design cooler shown in Figure 16 was developed. Cooler

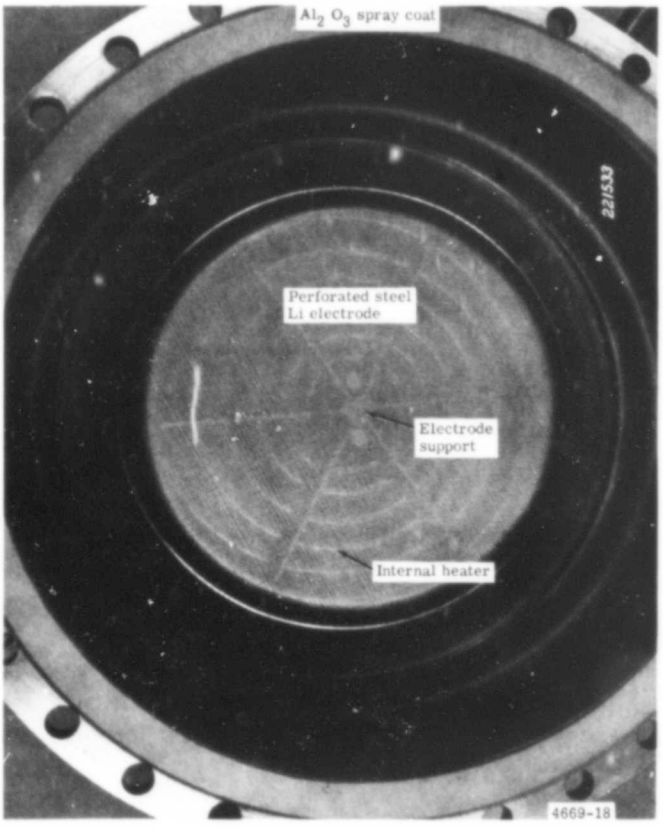

Figure 18. Lithium electrode housing—internal view.

testing shown in Figure 19 was carried out to determine the thermal conductance of this finned cooler as a function of the cooling Ar flow. It was found that the cooler could handle a flow rate of 1.5 gm/sec. At this maximum flow rate, the thermal conductance was 0.50 w/°C. From geometrical considerations, the thermal conductance from the electrode assembly to the heat exchanger was 0.78 w/°C.

Assuming that an arithmetical mean temperature can be used to calculate the temperature drop through the heat exchanger, the heat flux at 1.5 gm/sec Ar flow, Q, is

$$Q = 0.78\,(T_c - T_h) = 0.5\left[T_h + (T_{ar} - T_{amb})\right]/2 = m\,C_p\,(T_{ar} - T_{amb}) = \sim 155\ w$$

where

T_c = cell temperature, 650°C
T_h = heat exchanger center line temperature, 448°C
T_{ar} = Ar outlet temperature, 240°C
T_{amb} = ambient temperature, 45°C
m = Ar flow rate, 1.5 gm/sec
C_p = Ar specific heat, 0.53 joule/gm

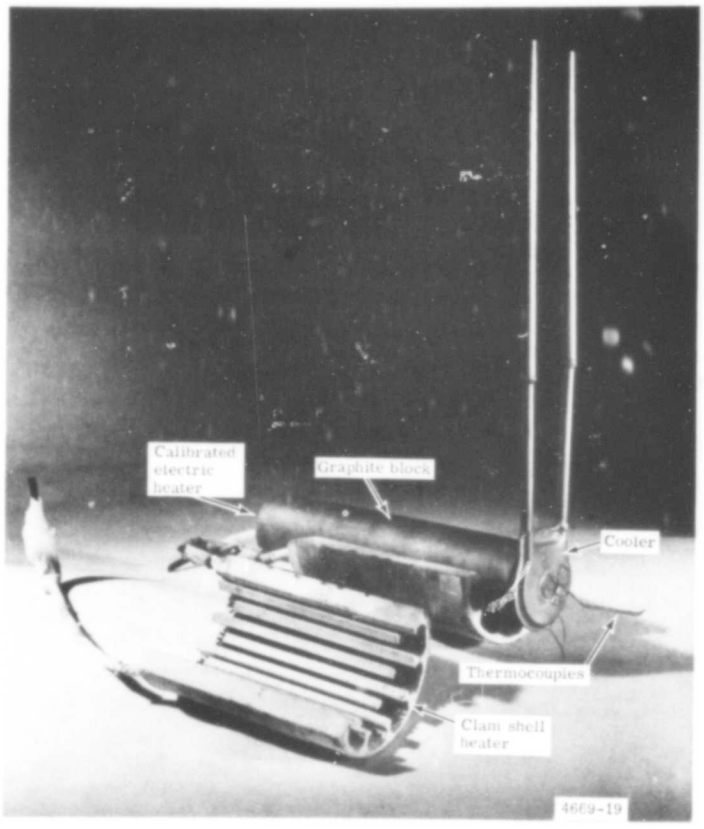

Figure 19. Advanced design cooler.

Since there are 12 coolers per cell, this means that an 1860-w heat load can be sustained. The resulting current through the cell can be calculated from

$$I^2R - (T\Delta S)_{cool} I = 1860$$

where

$$(T\Delta S)_{cool} = 0.5 \text{ v}$$

$R = 0.0024$ ohm for a Mark IV single cell

This results in a limiting current based on the heat dissipation during charge of 984 amp. Since the theoretical capacity of the Li chamber in the Mark IV cell is 1600 amp-hr, a charge time capability of about 1.6 hr can be projected for a current efficiency of 100%.

IV. EXPERIMENTAL EVALUATION OF ENERGY EFFICIENCY (TASK III)

OBJECTIVE

The purpose of this task was to evaluate and prove the newly designed Mark IV cell and to obtain experimental data to evaluate the charge and discharge efficiency as a function of charge time.

The new design features evaluated were:

- Capability of high pressure operation
- Ceramic-to-metal brazed joints (including the use of metal bellows to connect ceramic tubing to the cell housing)
- Sprayed alumina for electrical insulation
- Permanent flange seal for the full range of temperature (ambient to cell operation)
- Cooler to remove heat from cell during high performance operation and to cool the flange
- Sidearm to separate effluent Cl_2 and Ar and compensate expulsion pressure of seal argon
- New Cl_2 electrode design for improved removal of Cl_2 during charge and increased electrode area
- Heating coils in the Li storage area
- New design of thread and tapered flange for ceramic-to-carbon joint
- A low resistance electrical connection to the graphite pot utilizing a nickel-graphite-molybdenum braze

CELL OPERATION

Figure 20 shows the cell installed in a California hood with the associated gas system and instrumentation. A schematic of the gas system is shown in Figure 21.

The cell was operated for 8.2 hr. During this time it was on charge for 4.1 hr for a total of 208 amp-hr. There was no discharge obtained because of the inability to obtain a seal on the Li electrode screen, therefore, no lithium could be stored. This was caused by fluctuations in the seal-to-percolator pressures which affected the differential pressure across the screen. There were indications that a seal did occur but only at very high charge rates.

The cell test was terminated because of a major short in the cell. Presumably this short was caused by LiCl getting into the flange area which resulted in the deposition of Li on the lower flange. Bridging of the Li to the intermediate flange would cause a direct short. Although Ar seal pressure was maintained to hold the molten LiCl level outside the electrode area near the bottom of the carbon skirt, there was evidently sufficient LiCl creep up the walls of the container. A design modification will be made prior to the next test to ensure that the flange area is maintained below the freezing temperature of the LiCl. This will freeze the electrolyte reaching the flange area and prevent a short, since frozen LiCl is nonconductive.

CELL OPERATING PROCEDURE

The start-up procedure is begun by purging the complete system with Ar. Argon is introduced into the cell through all inlets except through valve 34 in Figure 21. All gas going into the system leaves through the exit bubblers.

BLANK PAGE

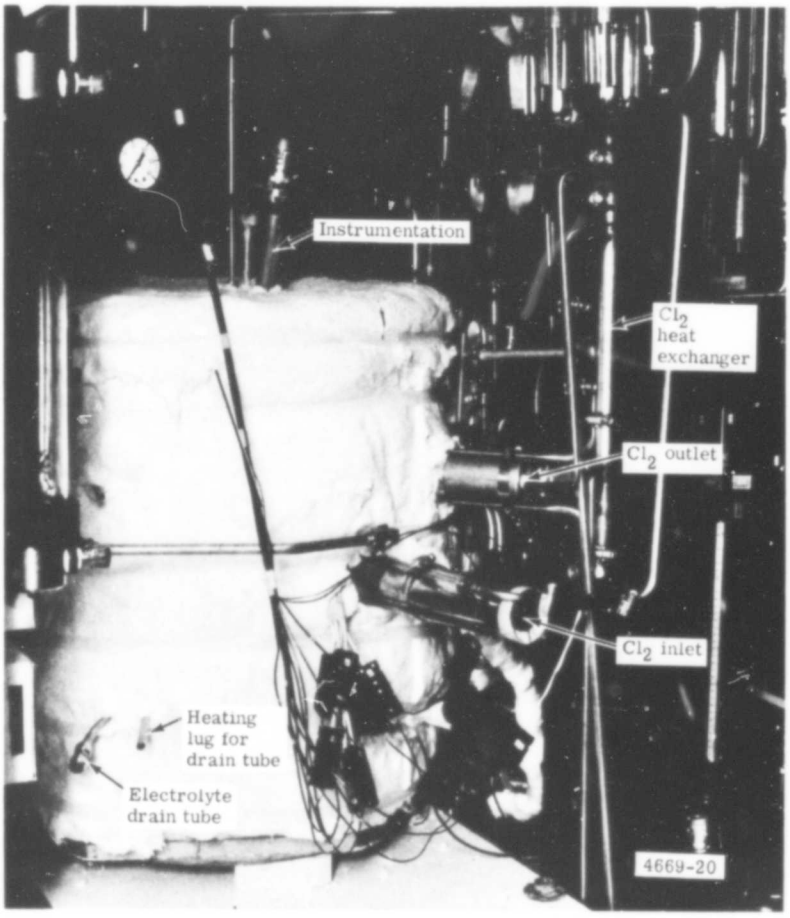

Figure 20. Mark IV cell installed in a California hood with the associated gas system and instrumentation.

After several hours of purging, the furnaces for the cell and the fill system are turned on. The cell temperature is gradually raised to 675°C, and the fill pot temperature raised to 700°C to ensure that all of the electrolyte is molten.

To proceed with the fill, the Ar flow rates to the cell are adjusted for filling the cell, and the line between the E pot and the fill separator is heated by passing current through its length. When the fill line is to temperature, transfer pressure is applied to the E-pot gas space to force electrolyte into the fill separator. The electrolyte then flows by gravity into the Li cavity of the cell.

After the cell is filled, the Ar flow rates to the cell are adjusted for running and a low cell charge (50 amp) is started. Shortly after starting the cell charge, argon flow to the Cl_2 inlet is interrupted and Cl_2 introduced in its place.

After a few amp-hr of charge, the Li screen is observed on the percolator monometer to seal. After a programmed charge is completed, the cell open circuit voltage is checked and the Cl_2 flow rate is increased to the amount required for discharge. After the Cl_2 flow rate is established, the discharge is started and continued until the lithium screen is unsealed as detected on the percolator monometer. At this point, the discharge is stopped,

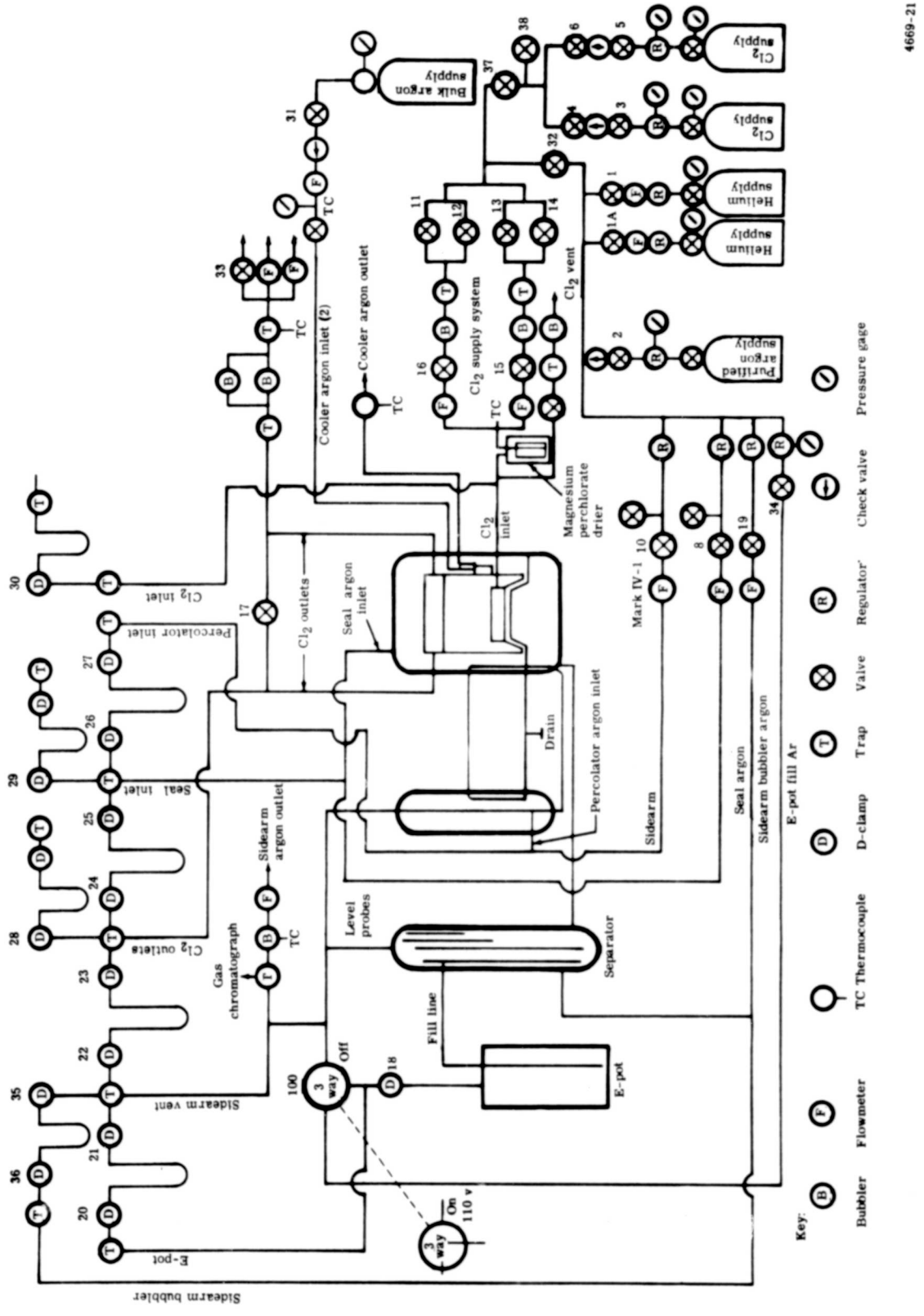

Figure 21. Schematic of the gas system used with the Mark IV cell.

the chlorine flow reduced to idle level, and a charge is initiated to begin the next charge-discharge cycle.

Temperature, pressure, voltage, and current data are normally taken every 15 min during each cell run. After the cell run is completed, the upper portion of the cell may be gravity drained by attaching a container to the drain line of the cell and heating the line to the melting temperature of the electrolyte. Before draining and cooling the cell, an Ar purge is introduced into the Cl_2 inlet to protect the cell during cool down.

TEST RESULTS

Because of the short life of the cell, no experimental data were obtained to evaluate the charge-discharge efficiency. However, the following significant results were obtained in terms of proving several features of the Mark IV cell design.

- The sprayed alumina provided sufficient electrical insulation until the cell shorted out. It is believed that the shorting occurred via a bypass of the alumina and not through it.
- The brazing of the ceramic tubes to the metal bellows which were welded to the cell housing appeared to work very satisfactorily. Also, the thread and tapered flange for the ceramic-to-carbon joint appeared to work well.
- The metal O-ring functioned satisfactorily. A flat place was discovered in the O-ring after disassembly which was probably caused by localized heating at the time of the short.
- The fill system operated satisfactorily so that no difficulties in loading LiCl are anticipated in future tests.

V. SYSTEM ANALTYICAL STUDIES (TASK IV)

OPERATIONAL CONCEPTS

The use of a regenerative cell Energy Depot concept requires the production of only electrical power by a mobile reactor powerplant. This electrical power, produced in some area at the rear of the forward edge of the battle area, can be transported to the using vehicles by the methods illustrated in Figure 22. The three basic modes of operation illustrated are:

- Module replacement
- Engine replacement
- Fast charge

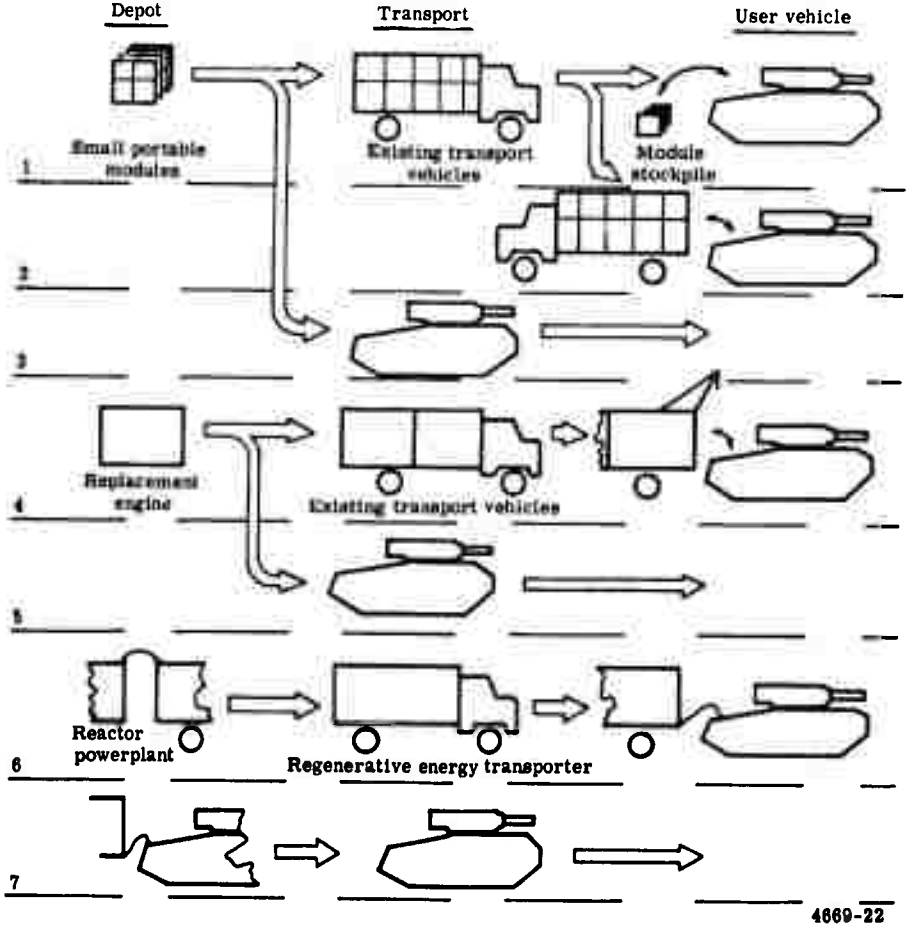

Figure 22. Operational alternatives for the electrochemical Energy Depot.

Module Replacement Mode

The module replacement mode of operation can be used in any of the operational schemes illustrated in Figure 22 as alternatives 1, 2, and 3. This concept would envision the use of a portable module which could be handled by one or two men. Each module would be a self-contained regenerative cell. These cells would be connected in series or series-parallel arrangements in vehicular engine systems. Each module, once depleted, would then be removed from the vehicle and replaced by a charged module. This could be accomplished at some prearranged stockpile, as illustrated in alternative 1, or the transporting vehicle could deliver replacement modules to the combat vehicle, as shown in alternative 2. Alternative 3 shows the further possibility of vehicles returning to the depot for module exchange.

Engine Replacement Mode

A second mode, similar to the module replacement mode, is illustrated as alternatives 4 and 5 in Figure 22. This system would make use of modular engines which could be changed at the depot and exchanged for depleted engines either at the depot or in the field. Due to the engine weight, some provision would have to be made for hoisting the engine in the field. This could be accomplished by means of a winch and frame on the delivery vehicle.

Fast Charge Mode

The last mode considered is a fast charge mode, illustrated in Figure 22 as alternatives 6 and 7. In this mode, neither the electrochemical engine nor its components would be removed from the vehicle. The vehicle would be charged either at the depot or in the field. For field charging, a regenerative energy transporter would have to be developed. This would be a vehicle which would have integral to it a large regenerative cell. This unit would then act in the same manner as the currently used fuel truck; however, it would carry stored electrical power.

ERDL SPECIFICATIONS

The Engineering Research and Development Laboratories of the U. S. Army (ERDL) has furnished certain data to Allison to perform a systems analysis of the lithium-chlorine regenerative cell. The size of the electrochemical engine has been determined to meet a given Army duty cycle.

Energy Storage

The required amount of stored energy is 200 kw-hr, deliverable at approximately 200-v dc over the specified duty cycle.

Full Power

The full power requirement is 50 kw; however, a peak power of 75 kw is required for short periods of time.

Duty Cycle (Discharge)

An 8-hr discharge sequence was provided which is equivalent to four full power hours for the 50 kw vehicle. The sequence is as follows and is graphically presented in Figure 23.

50 kw for 1 hr	75 kw for 20 min	10 kw for 2 hr	50 kw for 1 hr
25 kw for 1 hr	45 kw for 40 min	Open circuit for 2 hr	

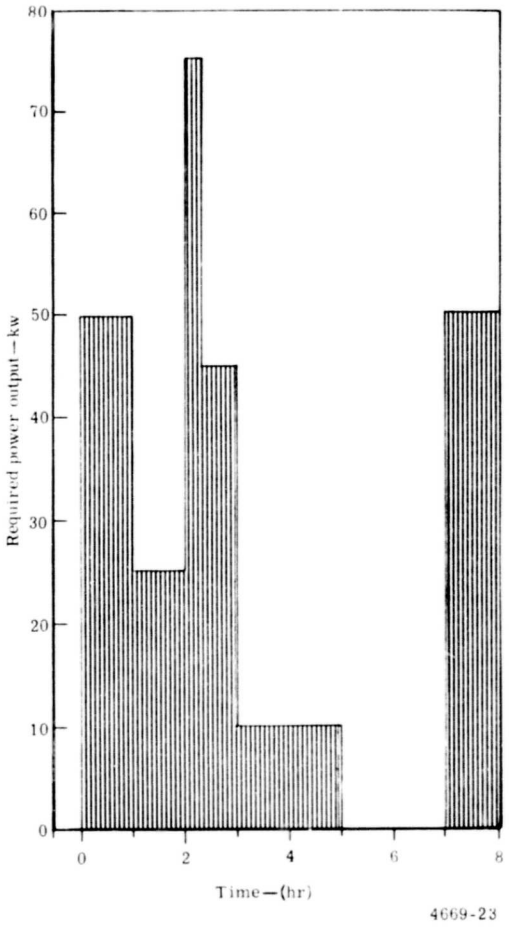

Figure 23. Required output versus time for the ERDL duty cycle.

Charge Times

Different charge times were specified for the alternative modes of operation. The module replacement mode requires a 6-hr charge time, while the fast charge mode requires a 1-hr charge time at design point with 20-min charge capability at the sacrifice of efficiency.

Electrical Energy Efficiency

It is desired that the overall electrical energy efficiency during the charge-discharge cycles specified be as high as possible. An overall efficiency of 50% is considered a minimum and 70% desirable.

Construction Materials

All construction materials must be of a nature that they would not be unavailable or prohibitively expensive for wide scale application as the power source in military vehicles.

Weight and Volume

Weight and volume should be minimized. An energy storage density greater than 0.2 kw-hr/lb is desired.

Reactants

All reactants must be contained within the system.

Self-Discharge (Allison Requirement)

A self-discharge requirement was placed on the system design after discussion with ERDL. Self-discharge is defined as the loss of stored energy which occurs during standby and discharge modes of operation. It includes loss of chemically stored energy by nonelectrochemical reactions and any loss of useful energy required to maintain it in operable condition—e.g., to provide heating for a high temperature system. Since the lithium-chlorine cell operates at an elevated temperature, some of the stored energy is required to maintain the operating temperature particularly during standby operation and open circuit.

The goal is to keep the energy loss by self-discharge at less than 5%/day.* This can also be expressed in terms of "hot time", which is defined as that period of time when the entire amount of stored energy is consumed to keep the system at operating temperature during standby operation. Thus, 5% self-discharge per day is equivalent to a 20-day "hot time".

Miscellaneous

Long-life, high reliability and low maintenance requirements are desired.

MODULE REPLACEMENT MODE

The operational concept considered in this section is the module replacement mode previously described. In this mode of operation, the engine consists of a number of individual power modules which can be separately removed from the using vehicle when they are discharged and recharged at a remote mobile nuclear powerplant. This mode of operation allows the using vehicles to be out of service for a minimum time so that charged modules can be supplied to the using vehicle at the user location in a manner analogous to current refueling using conventional fuels. In addition, the charging time for the modules can be selected so that efficient charge rates can be maintained, and scheduling can be arranged to allow optimum use of the electrical power generation equipment.

A number of conceptual designs of modular systems have been investigated to determine one which is operationally attractive and has engineering practicality. This section presents a description of the resulting system concept which has been evaluated for the module replacement mode of operation. It consists of ten modules comprised of seven cells each. The cells are vertical type cells utilizing a wick electrode. In the basic design, Cl_2 is stored external to the modules in a single storage container. Separate Cl_2 storage within each module has also been evaluated and is described in a latter portion of this section. An alternative system using a horizontal type cell is also described.

*Initially the requirement was for a self-discharge of approximately 6 1/2%, and a part of the systems studies have used this basis.

System Description

A conceptual lithium-chlorine electrochemical engine incorporating a vertical cell design is shown in Figure 24. The system consists of a power section which includes ten modules, each containing seven cells, and an accessories section which includes the Cl_2 storage, cooling system, electrical system, and controls. The power section is designed to remain as a unit while the auxiliary section components can be moved to areas in the vehicle which are available to house these assemblies.

An alternative engine system using a horizontal cell has also been investigated. This engine concept, which is based more on existing laboratory type cells, is described in Appendix 2.

The engine conceptual design shown in Figure 24 has been developed to allow system analysis and evaluation of the module replacement mode of operation. All system components have been included; however, design details have not been developed for all components. If the concept is operationally attractive, detailed design and analysis will be carried out in future programs. The engine specifications used to establish the cell and system characteristics were supplied by ERDL and described previously.

The engine is designed to furnish 50 kw with overload capability at 75 kw. The system has an energy capacity sufficient to deliver 200 kw-hr in accordance with the required duty cycle.

The general system schematic shown in Figure 25 presents the major subsystems, excluding instrumentation and control. The ten-power modules, connected in series by the power

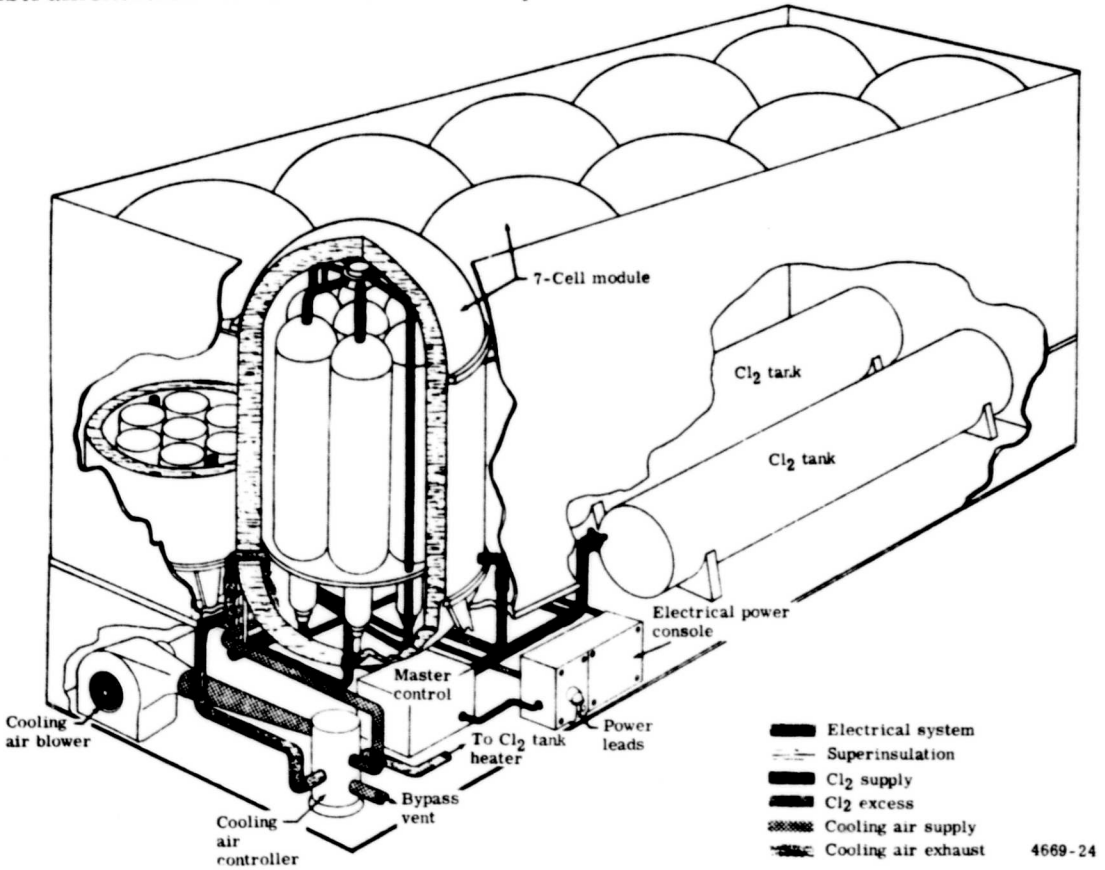

Figure 24. Conceptual engine design for the module replacement mode.

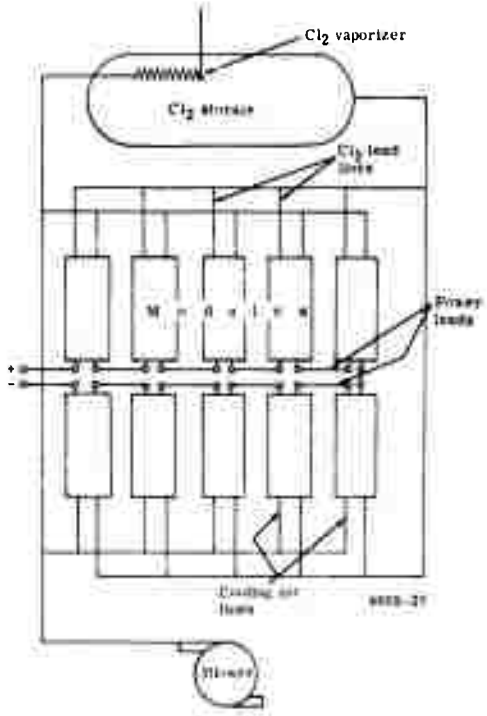

Figure 25. General system schematic of the module replacement mode.

leads, furnish the variable power required by the electric drive system. The power furnished will be at varying voltages according to the required power level. The Cl_2 feed system consists of a Cl_2 storage tank containing liquid Cl_2. A control system will feed the Cl_2 to the modules as required by the load current. The third major system is the cooling air system which is also manifolded to each module. This same ambient air will also be used, when required, to vaporize the Cl_2 in the Cl_2 storage tank.

In the discharge mode, the system will be assembled as shown in Figure 24 and used for power production on the vehicle. Once the modules are fully discharged, quick disconnect couplings will allow each module to be separately removed from the system. The empty Cl_2 storage tanks can also be individually removed by means of zero leakage disconnects. The modules and tanks can then be replaced with charged power modules and filled Cl_2 storage tanks. The discharged modules will be recharged at the charging station by an electrical power source. The generated gaseous Cl_2 is liquefied and the Cl_2 storage tanks refilled.

System Operating Conditions

The following five operating conditions are considered for the electrochemical engine:

- Startup
- Standby
- Discharge (power generation)
- Shutdown
- Charge

The normal duty cycle for the electrochemical powerplant will consist of standby and discharge during vehicle operation. Although not routine, start-up from a frozen condition (ambient temperature) to the standby state (1200°F) and complete shutdown to the frozen state must be considered in planning the control, instrumentation, and mechanical design of the system. Charging of the powerplant is also a condition of operation which would be routine at the completion of each module discharge and dictated by the applicable powerplant duty cycle.

The conditions of standby and power generation correspond to idling and driving conditions, respectively, of a vehicle. In the standby condition, the cells are kept at operating temperature and in a ready state to deliver power. A variation of standby exists when it is desired to keep the cells at operating temperatures for extended periods without maintaining a ready state. This would be for powerplant storage rather than short-term parking or stop and go driving.

Component Description

A brief description of the electrochemical engine system components shown in Figure 24 is presented in the following paragraphs. A more detailed presentation of these components and supporting design analysis is presented in Appendix 1. An alternative horizontal cell system has also been investigated and is described in Appendix 2.

Vertical Cell

The fundamental power source for the electrochemical engine is an advanced vertical cell which is designated as the "D" cell to differentiate it from alternative Allison design concepts. This vertical cell is shown conceptually in Figure 26. The cell consists of two basic sections—the reactant storage section and the power production section. Detailed design of this cell, as presented in Appendix 1, was arrived at by means of the parametric trade-off studies described in Appendix 3. It is emphasized that this is currently a cell concept based on several projections of technology. Programs are currently in progress at Allison to develop the necessary new technologies.

When the cell is discharging, chlorine enters the bottom of the Cl_2 electrode and reaches the electrode-electrolyte interface after passing through the feed holes and the porous carbon electrode. The Li electrode is a feltmetal wick which also transports the Li from the storage compartment by wicking action. This is based on the greater wetting capability of Li relative to LiCl. The excess Cl_2 flow during discharge, along with that evolved during charge, is kept away from the Li electrode by the Cl_2 separator and removed at the top of the cell.

The Li is stored in the Li storage chamber. During cell discharge the Li is continuously consumed and the remaining Li stays at the top of the Li storage chamber floating on the LiCl that is being generated as the reaction product. About twice as much LiCl (by volume) is generated as the Li is consumed during cell discharge; therefore, additional storage space is provided for the excess LiCl. The excess Cl_2 flow during discharge and evolved Cl_2 during charge passes up through the center tube and through the LiCl storage chamber to be removed at the top of the cell.

There are several advantages to this design concept.

- The cell can operate with relatively large variations in attitude since there are no large horizontal fluid interfaces to be controlled.

- Chlorine gas removal from the reaction zone is aided by its material buoyance in vertically rising to the Cl_2 collection manifold.
- The Li storage chamber is designed to take full advantage of its natural tendency to float on top of LiCl.
- Good heat transfer is available from the reaction zone for cell cooling during high current rates.

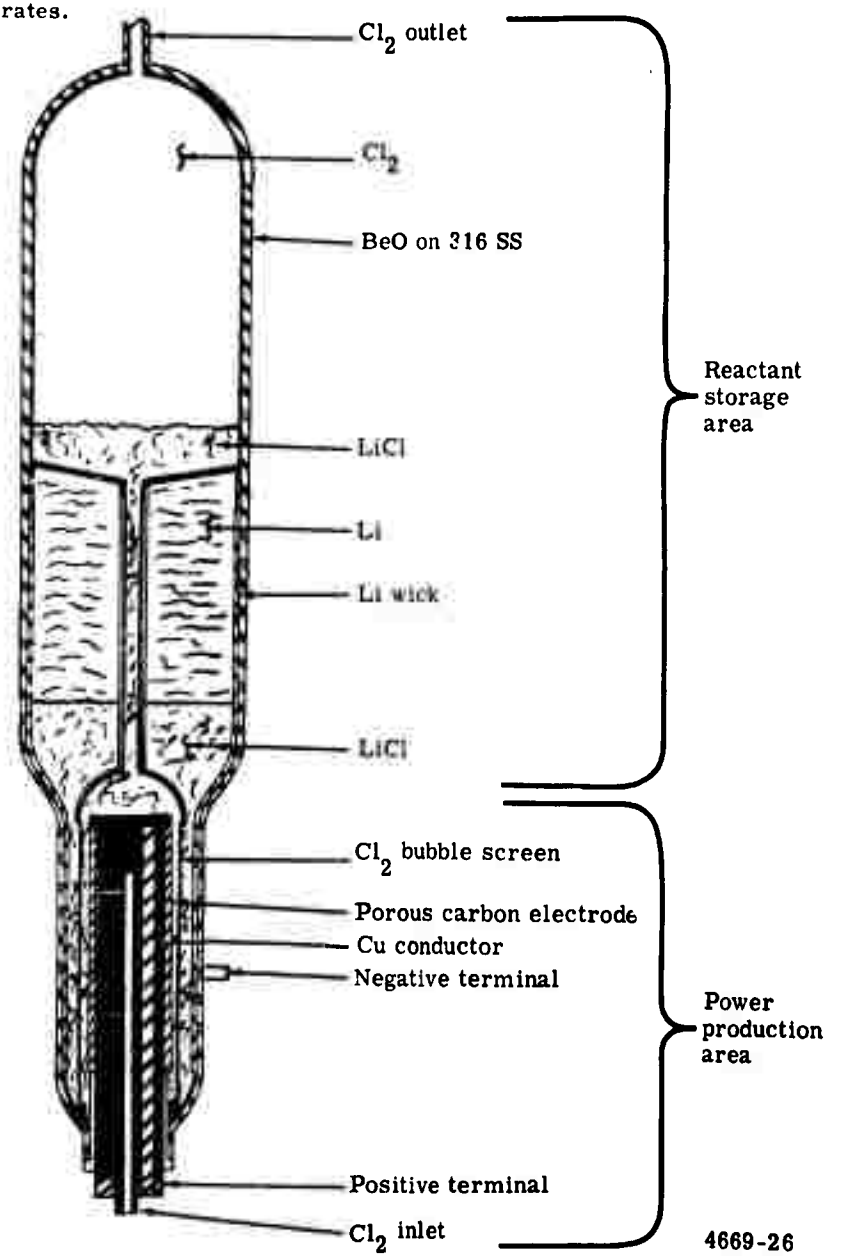

Figure 26. Vertical "D" cell.

Engine Module

The engine module is the exchangeable package of cells in the module replacement mode of operation. The engine module, aside from its function as a packaging device, provides thermal insulation for the cells to maintain cell operating temperature. An illustration of the engine module is shown in Figure 27.

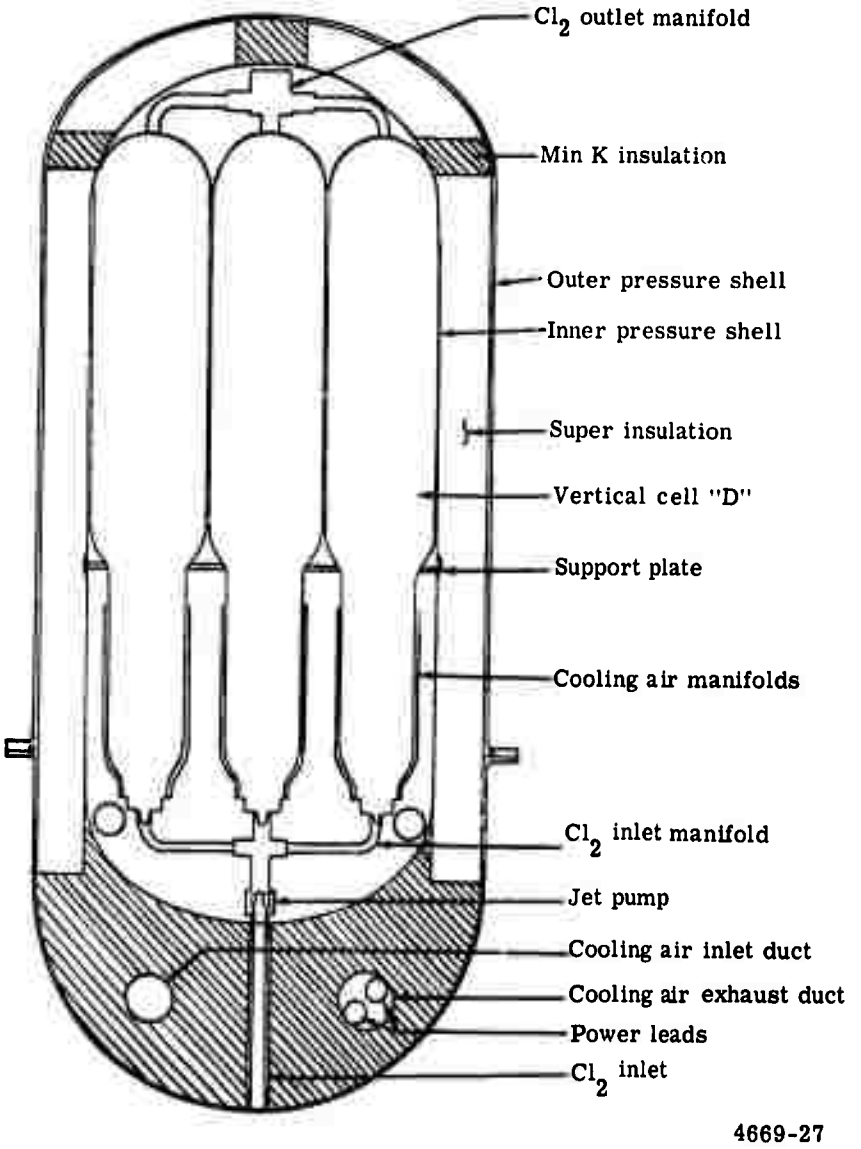

Figure 27. Engine module with evacuated insulation.

The engine module has been designed for a 15-day "hot time" which corresponds to approximately a 6 1/2% self-discharge rate. Two types of insulation, as shown in Figure 27, have been used in the design—Linde Superinsulation for nonloadbearing portions of the module and Johns-Manville Min-K for loadbearing portions of the module.

An inner and outer pressure vessel allow retention of these insulating materials in a vacuum of approximately 10^{-4} mm Hg. To conserve weight, the upper portion of the outer vessel is fabricated from aluminum. The remainder of the vessel along with the entire internal vessel is fabricated from type SS 316.

The overall module will be approximately 11.25 in. in dia and 29.5 in. high. It will weigh approximately 30 lb, excluding the contained cells, leads, and plumbing.

Inside the module, the seven cells will be retained by two perforated disks inserted in the inner pressure vessel. The cells will be manifolded inside the module for Cl_2 feed and excess Cl_2 flow. A jet pump will recirculate excess Cl_2 through the cells.

Cooling air channels are provided into and out of the module through the Min-K at the bottom. Electrical leads are brought into the module through the cooling air exhaust line and are connected to the cells which are interconnected in series.

The total module with its contained seven cells and necessary interconnections weighs approximately 90 lb. This also considers the design for the 15-day "hot time". If a lesser self-discharge rate is desired, the module weight will be increased somewhat.

Cooling System

A forced air cooling system has been designed to cool the cells during discharge and provide the necessary heat for vaporization of the chlorine. The cooling system is comprised of the following components:

- Blower, motor, and filter
- Ducting
- Controls
- Chlorine tank heater

The motor/blower, which will provide 300 cfm of ambient air at 4 in. of water pressure, will be on at all times during discharge. An air control damper will direct the cooling air either to the modules or through a module bypass duct. In either case, the cooling air will continue to the exit manifold where necessary amounts will be ducted to the Cl_2 tanks for Cl_2 vaporization.

Chlorine System

In this design concept, chlorine is stored in the liquid phase by two pressurized storage cylinders. These cylinders are placed in a protected place in the vehicle. The two storage cylinders are 12 in. in dia and 29 in. long with a 0.1-in. wall thickness. Internal design pressure is 225 psia which allows liquid Cl_2 storage at 125°F.

The Cl_2 tank contains approximately 200 lb of Cl_2. This is sufficient to provide 200 kw-hr of electrical energy over the ERDL duty cycle and includes 5% excess chlorine. The tank contains an excess volume of 25% for gaseous Cl_2 accumulation.

The following alternative Cl_2 storage systems are being investigated to provide additional safety:

- Storage as a Cl_2 rich compound that could be decomposed when needed
- Storage as a gas adsorbed on activated carbon
- Liquid storage surrounded by a reactant

Integral storage of Cl_2 within each module to make the module a self-contained energy furnishing unit has been investigated. Because of the weight penalty, however, this concept was rejected in favor of the separate Cl_2 storage system described previously.

Instrumentation and Controls

Control and instrumentation will be provided so that an operator can control all modes of powerplant operation or, alternatively, will be able to allow automatic system operation. The lithium-chlorine system is expected to be load following, that is power will be provided as required by the load (see Appendix 4). The power will be furnished, however, at lower voltages as power increases.

Lithium wicking action within the cell is expected to provide the necessary amount of Li in the reaction or power section of the cell to meet demand power requirements. Chlorine is provided to the cells by maintaining 5 atm pressure in the input manifold. This manifold pressure is maintained by Cl_2 tank pressure through two pressure regulating valves—one set at 5 atm and the second at 1 atm. The 5 atm valve will control Cl_2 pressure during all discharge conditions. During standby, this valve is bypassed and approximately 1 atm pressure will be maintained in the system by the second pressure regulating valve.

Cell temperatures must remain above 610°C so that the LiCl does not solidify. In the standby or shutdown condition, the chemical recombination of the reactants is expected to provide sufficient heat of formation to retain molten LiCl in the cell. During discharge the cells must be cooled so the temperature does not rise above that allowable for cell materials. This is accomplished by thermostatically controlling dampers in the blower system to divert cooling air flow to the modules. Temperature sensors within the modules activate the damper.

Other instrumentation and control devices expected to be incorporated in the engine system include a device analogous to the fuel gage. This instrumentation measures the state of charge of the modules. Also, automatic module isolation will be incorporated in the event of a malfunction to allow operation at partial power. In summary, the overall system is simple and self-regulating.

Performance Analysis

The conceptual electrochemical engine system that has been described in the preceding sections is sufficiently detailed to allow preliminary system performance analysis. Of particular interest are the system weight and volume and the electrical performance. Appendix 3 of this report describes the analytical techniques used to describe and predict cell performance. This section presents expected system performance data. Weight and volume data are furnished and a system energy balance for discharge over the ERDL duty cycle is given.

Electrical Characteristics

Based on experimental cell operating data for lithium-chlorine cells, performance characteristics are derived for the conceptual system design previously described. The performance analysis formulae given in Appendix 3 were the basis for estimating system performance.

Figure 1-3 in Appendix 1 describes the expected performance for a "D" cell in both the charge and discharge mode. The following cell characteristics were used to derive the curves presented:

- Cell pressure—5 atm
- Grooved electrode with 4 to 1 area ratio
- Excess Cl_2 flow—50%
- Equivalent electrolyte thickness—1 cm

These "D" cell characteristics were used to develop the electrical characteristics of the entire system, using resistances previously described for electrical contacts and leads. The power characteristics do not reflect intermittent power requirements for the following auxiliary loads of the system:

- Blower
- Chlorine valves
- Cooling air damper
- Instrumentation

Terminal voltage, current, and power characteristics are presented for the system in the discharge mode in Figure 28.

Single module charge characteristics are described in Figure 29. The upper curve is the power a module will draw as the applied terminal voltage is varied. The lower curve shows the current load as a function of applied voltage.

Figure 30 describes the charge and discharge efficiency of the entire system as a function of the terminal voltage. In the operating range of the ERDL duty cycle, discharge efficiencies of 75 to 90% are projected. The 6-hr discharge efficiency, excluding accessory loads over the duty cycle, would be approximately 85% as indicated in Table V.

Table V.

Average efficiency for the ERDL duty cycle.

Power (kw)	Time (hr)	Voltage (v)	Discharge efficiency (%)	Time × efficiency
10	2	241	87	174
25	1	231	89	89
45	2/3	216	85	57
50	2	213	84	168
75	1/3	192	76	25
			Total =	513
			6-hr average =	85%

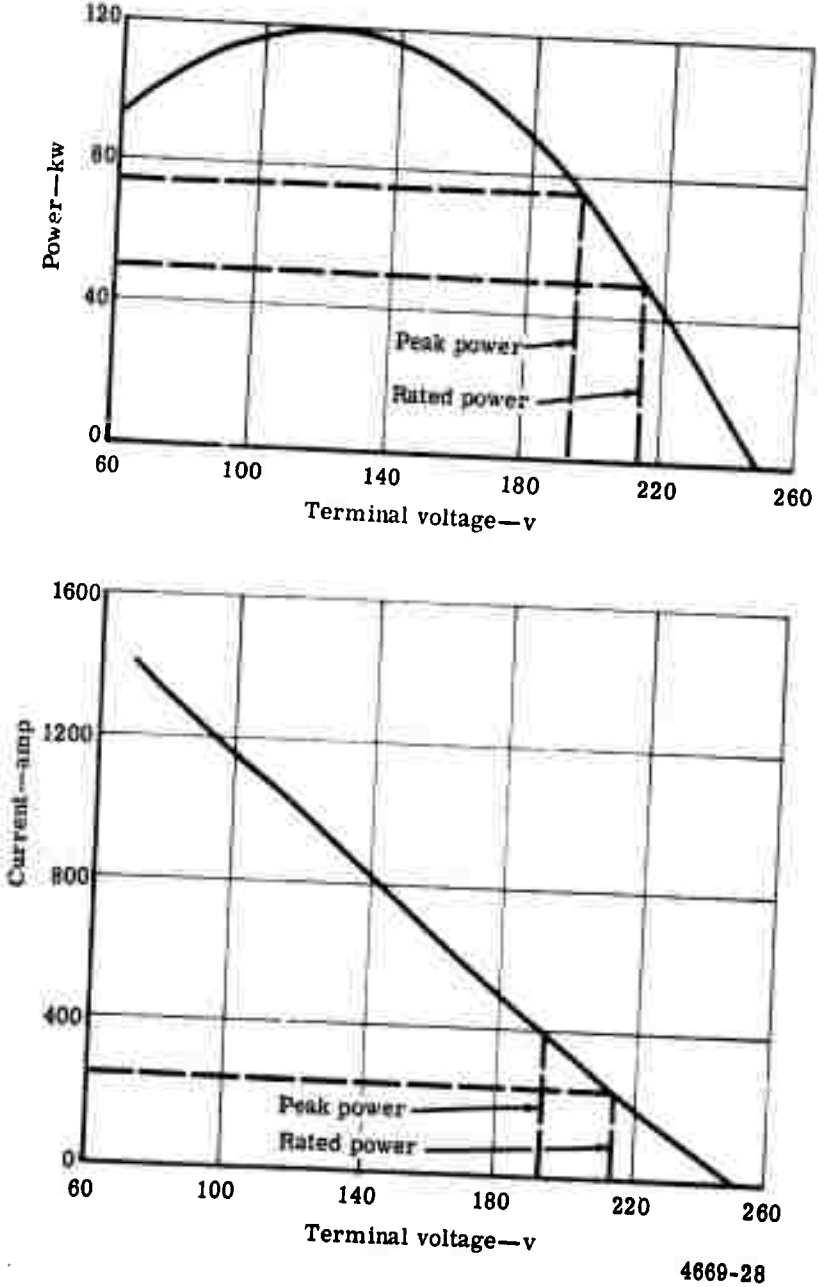

Figure 28. Electrochemical engine voltage and power characteristics (discharge mode).

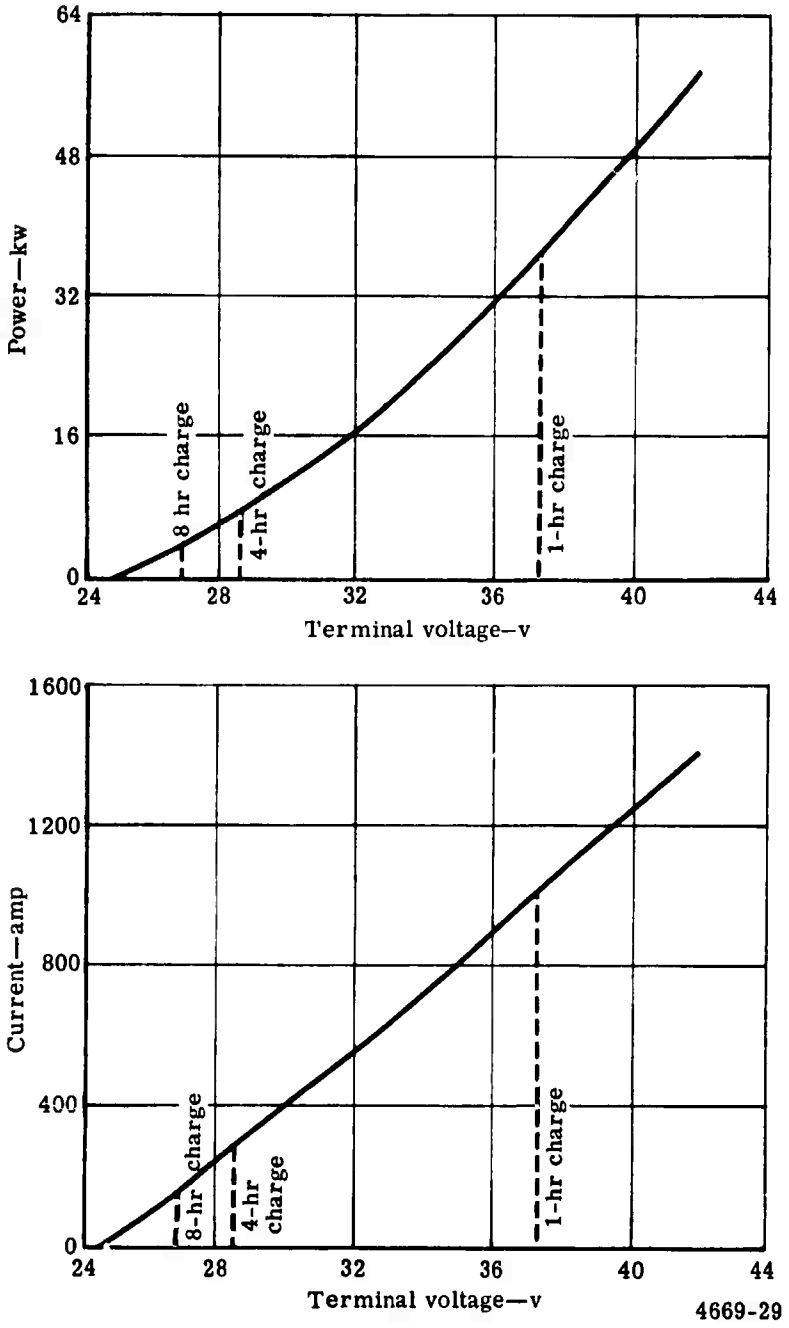

Figure 29. Electrochemical engine voltage and power characteristics (charge mode).

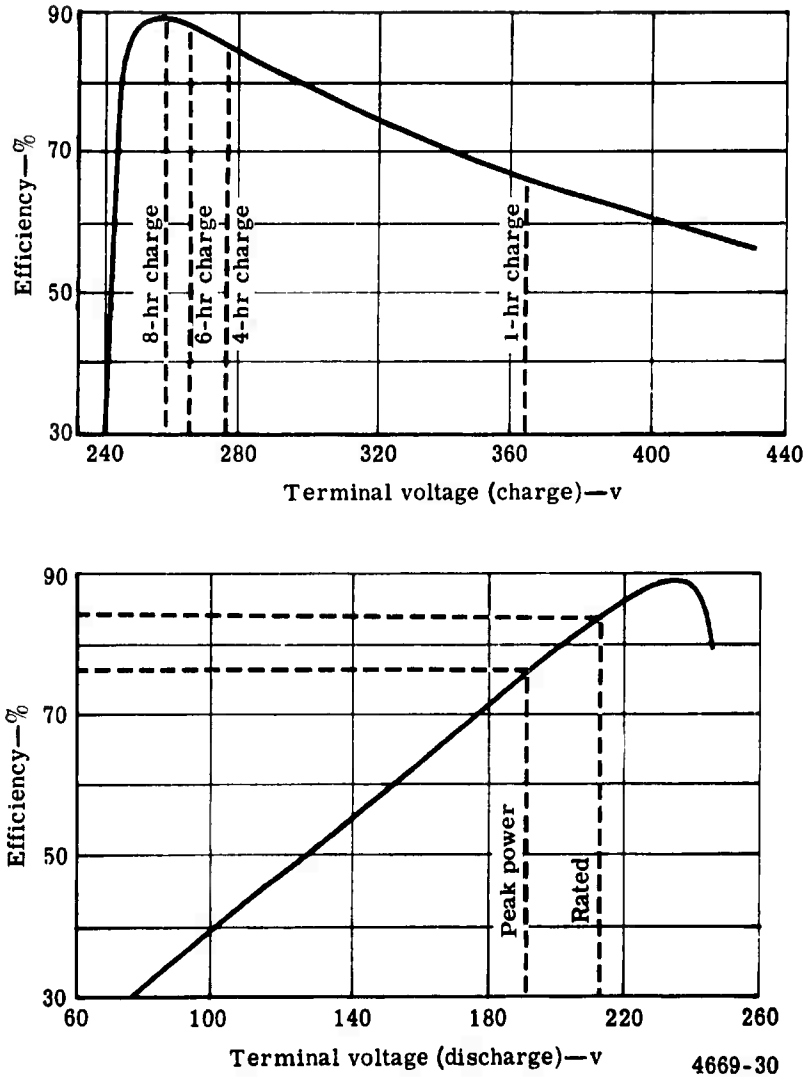

Figure 30. Electrochemical engine charge-discharge efficiency.

For the 8-hr discharge and including system accessory loads, the efficiency reduces to approximately 82%. Using a 6-hr charge efficiency of 88%, the overall charge-discharge cycle efficiency is expected to be approximately 75%.

Weight and Volume Data

Analysis of the weight and dimensions of the individual engine system components of the electrochemical engine was developed based on the conceptual design shown in Figure 24. This design incorporates the Cl_2 storage cylinders in the engine package. However, they could be more logically placed in some available space in the vehicle. Other accessories might also be better placed in other portions of the vehicle rather than integrally packaged. A weight and volume analysis of the engine system shown in Figure 24 predicted the following preliminary weight and dimensions:

- Weight—1246 lb
- Height—44 in.
- Width—25 in.
- Length—60 in.

The power section of the engine will contain the ten modules and require a volume 60 in. long, 25 in. wide, and 32 in. high. The accessories, plus plumbing and wiring connections, will require an additional overall package height of 12 in.

Table VI is a component weight breakdown of the conceptual engine design.

Table VI.

Component weight breakdown of the conceptual engine design.

Module		
Seven discharged cells (7.60 lb/cell)		53.2
Insulation (1/2 in. thick)		10.4
Inner pressure vessel		5.9
Outer pressure vessel		13.8
Leads, lines, etc		8.0
	Total (discharged)	91.3
	Total for 10 modules	913
Cooling system		
Manifold, lines, and fittings		26
Blower, motor, and filter		20
Air controller		5
	Total	51
Chlorine system		
Two cylinders		62
Supply lines		4
Fittings		4
Two manual cylinder valves		4
Two cylinder fill valves		4
Chlorine control system		20

Table VI. (Cont)

Tank heater and thermostat		1
Ten module solenoid valves		20
Cable, terminals, relays		10
Excess Cl_2		10
	Total	139
Electrical system		
Power cable and terminal box		7
Temperature sensors		5
Ten module circuit breakers and bypass		40
Temperature and voltage controls		76
Cables and terminals		15
	Total	143
	System total	1246

Energy Balance

Using the ERDL 8-hr duty cycle shown in Figure 23, an energy balance was calculated for the engine system described in the foregoing sections. This balance is presented in Table VII and describes the total energy available and where that energy is lost or utilized in the engine system. Overall discharge efficiency, based on available energy, is approximately 82% for this duty cycle.

Table VII.

Energy balance for ERDL 8-hr duty cycle.

Energy available	
Lithium chloride formed	240 lb
Total heat of reaction	276 kw-hr
Unavailable energy ($T\Delta S$)	33 kw-hr
Available energy	243 kw-hr
Energy losses	
Cell inefficiency during discharge	35.5 kw-hr
Instrumentation and controls	4.4 kw-hr
Contact and lead losses	1.6 kw-hr
Module heating during idle	1.5 kw-hr
Total	43.0 kw-hr
Engine system energy	
Gross engine energy	206 kw-hr
Net engine energy	200 kw-hr
Heat loads	
Total module heat load	70 kw-hr
Module heat leakage	5.9 kw-hr
Cooling system heat load	64.1 kw-hr

Table VII. (Cont)

Heat utilized	
Chlorine vaporization at 5 atm	6.6 kw-hr
Chlorine heating from 50 to 1200°F	7.6 kw-hr
	Total 14.2 kw-hr

FAST CHARGE MODE

The operational concept considered in this section is the fast charge mode of operation previously described. In this mode of operation, the engine consists of larger modules which are separable from the vehicle only by using lifting devices. The engine may be recharged by either returning the vehicle to a recharging station or by means of an electrical energy transporter analogous to a fuel truck. The major advantages of this mode of operation compared to module replacement are that total system weight is less and that no disconnecting of Cl_2 lines is required.

A conceptual illustration of this type electrochemical engine system is shown in Figure 31. The principal subsystems are:

- General purpose vehicle module consisting of five 24-v (nominal) basic units comprised of eight cells each
- Chlorine storage and supply subsystem
- Chlorine cooler and condenser subsystem
- Module cooling subsystem
- Electrical subsystem including instrumentation and control

In a practical engine system, these subsystems, or their components, could be packaged in available space in the vehicle. Even the multicell module has the capability of being sectionalized into a greater number of modules, however, with a resultant penalty of increased system weight.

Emphasis has been placed on investigating alternative cell designs which allow fast charging of an engine system. The basic vertical cell design described in Appendix 1 is restricted to a charge current limitation of 20 amp/cm^2 of Cl_2 electrode area. A system utilizing this "D" cell for power production was investigated during this report period. Alternative fast charge cells are currently being investigated and will be reported during the next report period. These cells will have greater electrode area to evaluate the weight penalty associated with obtaining highest efficiency.

Vertical "D" Cell System Description

In this system, the vertical "D" cell is used to build up the power section of the conceptual engine. The concept of the vertical "D" cell was described in the previous section; however, a detailed description is presented in Appendix 1. A preliminary laboratory investigation indicates that a charge rate of 20 amp/cm^2 of Cl_2 electrode surface area can be obtained when operating at 5 atm pressure. Using this charging current density and 20 min charge time as cell design criteria, an electrode area was determined for engine systems containing stored energies from 200 to 1600 kw-hr.

The engine system that was considered is conceptually shown in Figure 31. This illustration shows the entire engine integrally packaged; however, in any vehicular system, the

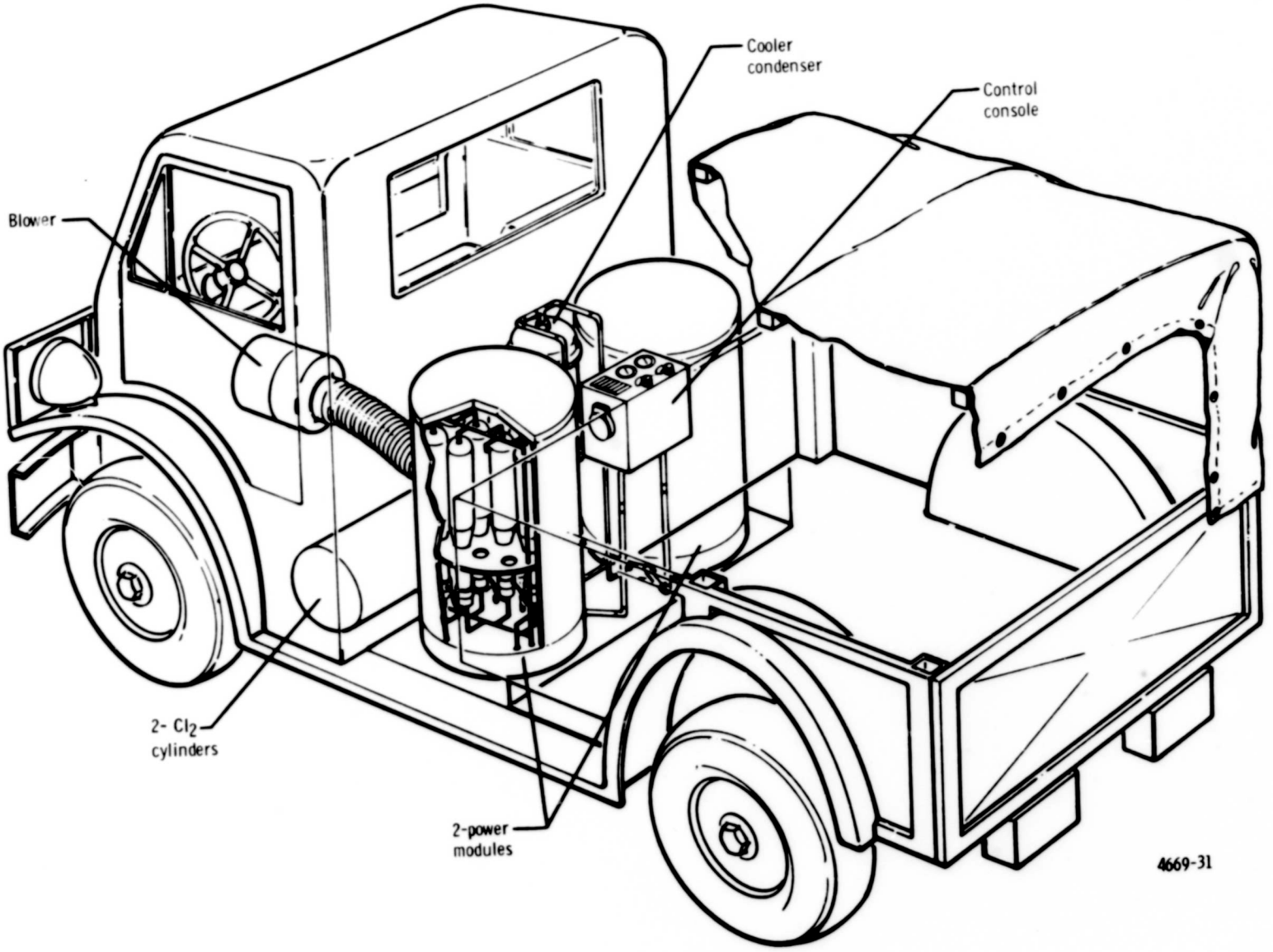

Figure 31. Lithium-chlorine electrochemical power system.

components would be rearranged to use available vehicle space to the best advantage. The fundamental engine building block is the vertical "D" cell with an output voltage, at rated power, of approximately 3.0 v/cell.* Eight of these cells form a basic unit. Grouping five of these basic units into a module was investigated to determine the potential system trade-offs.

Module Alternatives

Preliminary screening of the following three alternative module concepts was accomplished based on the containment of 40 cells with a power rating of 50 kw and a capability of furnishing 200 kw-hr over a 4-hr discharge cycle.

- Cylindrical module walls insulated with Superinsulation and elliptical domed top and bottom. The top and bottom use Min-K in areas requiring structural support and Superinsulation in other areas. (This module concept is described in detail in Appendix 1 for the module replacement mode.)
- Cylindrical module walls insulated with Superinsulation and circular slabs of Min-K for top and bottom.
- A rectangular box entirely constructed of Min-K.

These alternative design concepts were compared for a 15-day "hot time"—approximately 6 1/2% self-discharge rate of the cells. This summary evaluation indicated that on the basis of weight and size the first alternative was the most advantageous. Thus, a module concept similar to that described in Appendix 1 was used.

Chlorine Processing Alternatives

A number of alternative schemes were reviewed for reprocessing Cl_2. In the module replacement mode, chlorine reprocessing was accomplished by depot equipment. In the fast charge mode, chlorine is electrolytically separated from the LiCl, liquefied, and returned to the Cl_2 storage tanks on the vehicle.

The vapor pressure of Cl_2, shown in Figure 1-7 of Appendix 1, requires a system pressure of over 15 atm to maintain Cl_2 in the liquid phase over the Army design temperature range. If a pressure over 15 atm is maintained in the Cl_2 system, only ambient air or water cooling is required to reduce the Cl_2 gas from approximately 1200°F (the temperature at which it is generated) to 125°F. At this temperature, it will liquefy. If lower system pressures are employed, refrigeration is necessary to liquefy the gaseous Cl_2.

A number of alternative schemes were investigated employing air, water, and refrigeration for cooling and condensing of Cl_2. Based on considerations of on-vehicle weight and a desire not to disconnect the Cl_2 lines, the process shown in Figure 32 was selected. In this scheme, the refrigeration system and water chiller is employed only for low pressure systems, while the fan-cooled water circulation system is employed for high pressure systems.

The system is comprised of a cooler and condenser on the vehicle which are water cooled. Off the vehicle is a cooling water system which is attached by means of quick-disconnect couplings to cooling lines on the vehicle. Chlorine gas, evolved at approximately 1200°F, is cooled to a temperature somewhat above the boiling point of Cl_2 at system pressure. The cooled gas is then condensed to the liquid phase in the condenser. Both the cooler and condenser are cooled by the external water cooler.

*This cell voltage was determined for a 4-hr discharge by calculating the electrode area required for a 20-min charge.

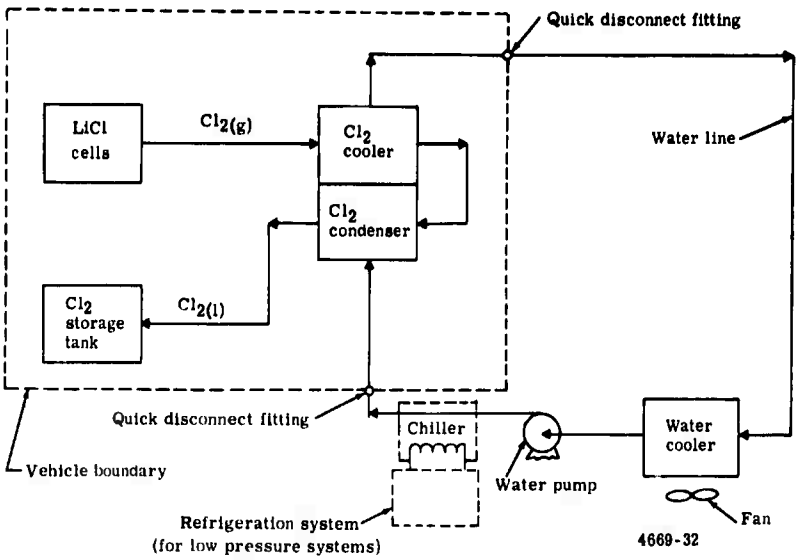

Figure 32. Fast charge mode process schematic.

Other System Auxiliaries

The other major subsystems comprising the engine are the electrical system, which includes the instrumentation and control, and the cooling system. These systems, for preliminary analysis, were considered to be identical to those used in the module replacement mode for a 200 kw-hr system (see Appendix 1).

System Parametrics

For the fast charge mode of operation, a parametric analysis was conducted to investigate a family of electrochemical engines. Using the previously described engine concept, energy storage capabilities from 200 to 1600 kw-hr were hypothesized at nominal power levels from 50 to 400 kw. System voltages of 120, 240, and 480 v were considered. The parametric analysis was carried out for the multicell power compartment and system auxiliaries.

Multicell Power Compartment

The thermal insulating power compartment or module contains five 8-cell basic units. To develop parametric data for analysis of this power package, a computer program was written. This program computes the cell and module design calculations based on the cell optimization described in Appendix 3.

A cell discharge voltage of approximately 3.2 v/cell is required to charge the cell in 20 min and is representative of the fast charge mode. A computer program subroutine, which optimizes the electrode design, was developed for obtaining weight and volume data on the

general purpose vehicle module over the required energy range. The data obtained during this report period was for an operating pressure of 5 atm. Higher pressures will be investigated to obtain optimum design during the next report period.

The results of the parametric analysis of the 40-cell vehicle module are presented in Figure 33. The curves allow selection of height, diameter, and weight trade-offs for any given energy required. The curves break rather sharply allowing for the selection of a minimum weight system which is very near minimum height. Figure 34 shows minimum module weight as a function of module energy.

All data are based on the extrapolation of an existing cell and module design. Although structural changes were included in the computer program for the larger cell and module designs, certain design considerations were considered as assumptions in the extrapolation. Such things as maximum Li wicking distance and electrode spacing required for bubble removal during fast charge are projections from limited laboratory experiments and require additional experimental verification. These parametric analyses were primarily conducted for general systems analysis by the Army.

System Auxiliaries

During this reporting period, the system auxiliaries for a 20-atm system were investigated. This system will be compared to a 5-atm system during the next report period. The energy densities of the two systems, including their respective power compartments, will be compared.

The system auxiliaries may be considered in two groups—components located on the vehicle and components located off of the vehicle. These two groups may be further broken down as:

- Components located on the vehicle:
  - Chlorine processing system
  - Electrical system
  - Module air cooling system
- Components located off of the vehicle:
  - Water system
  - Refrigeration unit and chiller (not required for high pressure systems)

The procedure used to derive auxiliary parametrics extrapolated weight data from a reference 200 kw-hr system. The reference system was designed for a 60-min charge time. The weight and volume of auxiliaries at different operating conditions were then estimated based on changes in charge efficiency, system energy, and charge time. Figures 35 through 38 present auxiliary weights and volumes* as a function of stored energy and charge time.

To arrive at these system weights and volumes, estimates were required for individual components. The estimated component weight breakdown on page 56 provides some indication of the relative component weights for a 1600-kw-hr system:

*Volume data is based on dimensional volumes and does not include any packaging efficiency considerations.

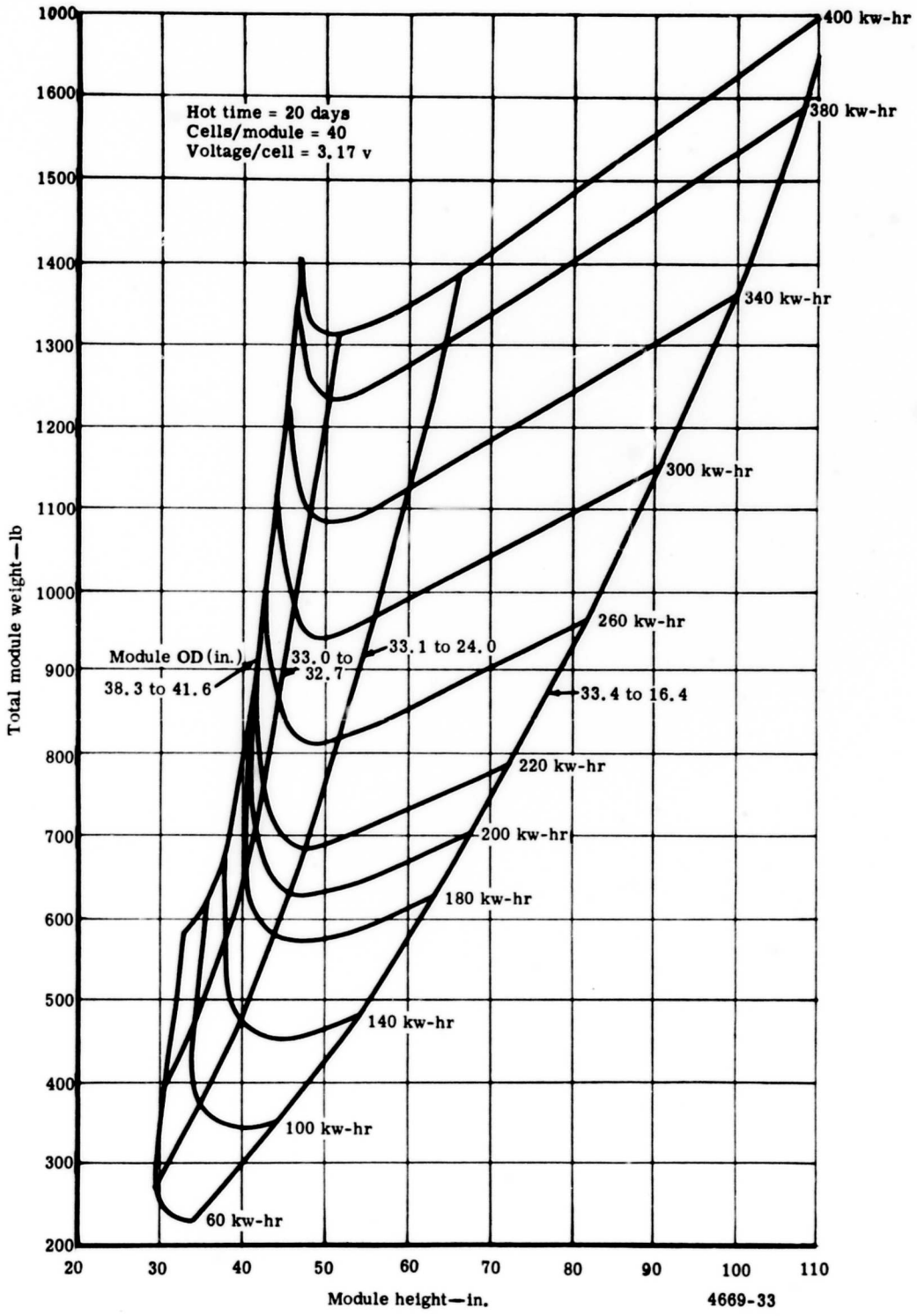

Figure 33. Total 40-cell vehicle module weight as a function of module height.

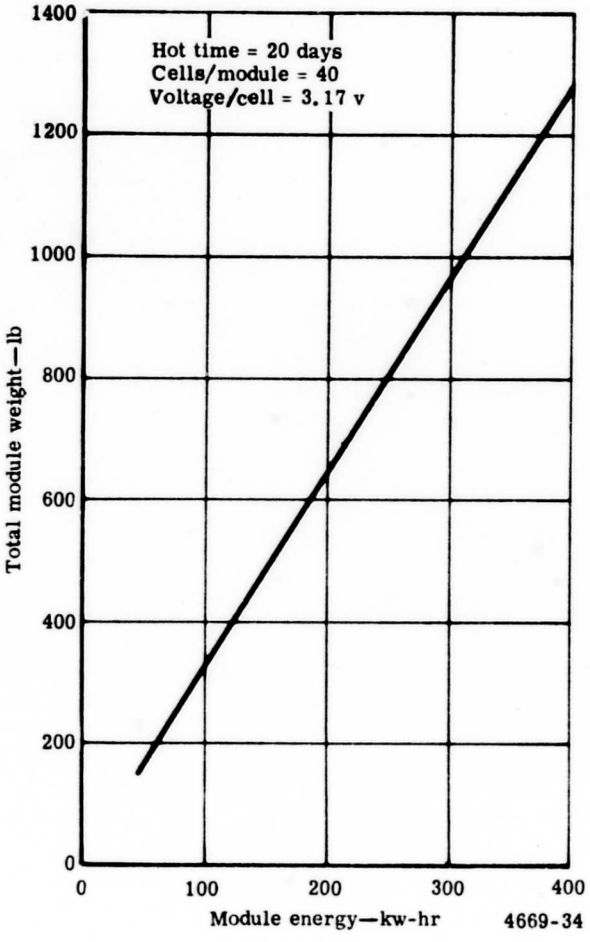

Figure 34. Minimum 40-cell vehicle module weight as a function of module energy.

	Weight estimate (lb) (1600 kw-hr and 20-min charge time)
On-vehicle components	
Electrical system	140
Cooling system	930
Chlorine system (less tanks and 5% excess)	290
Chlorine storage tanks	475
Excess chlorine* (5%)	85
	Total 1920
Off-vehicle components	
Water pump	610
Water cooler	1110
	Total 1720

*Only excess Cl_2 is considered in these weights because the weight of the cells is computed in the discharged condition, thereby including reactant Cl_2 weight.

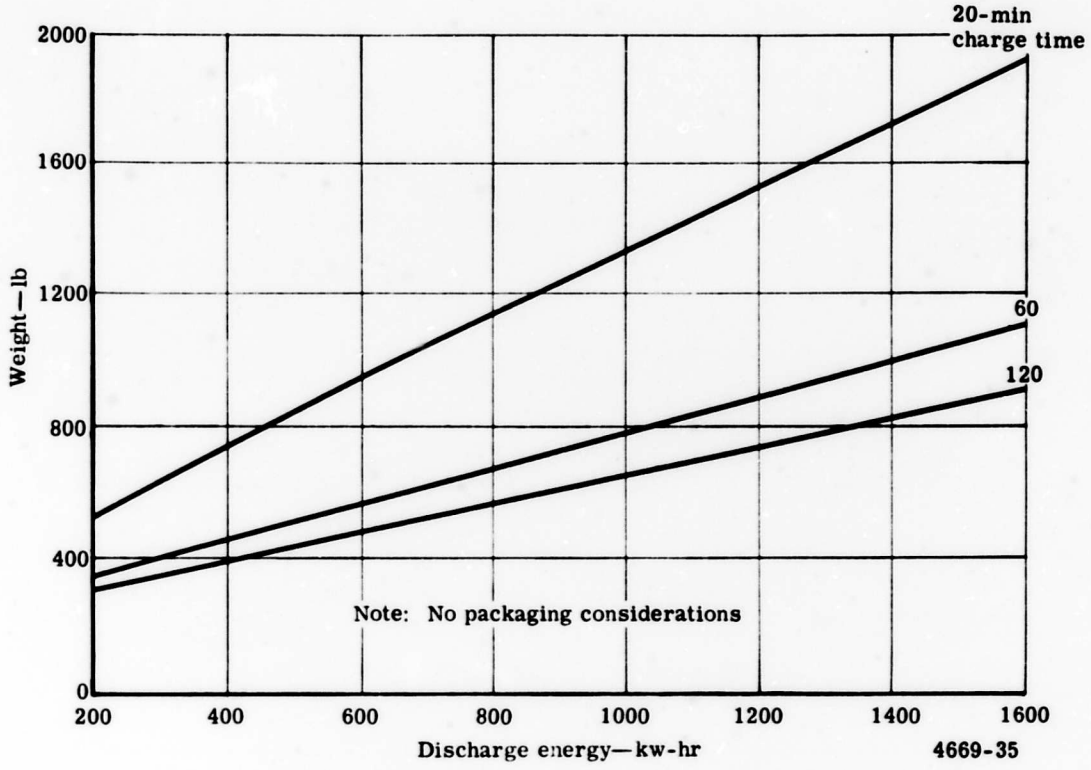

Figure 35. Weight of auxiliary components located on the vehicle versus discharge energy content.

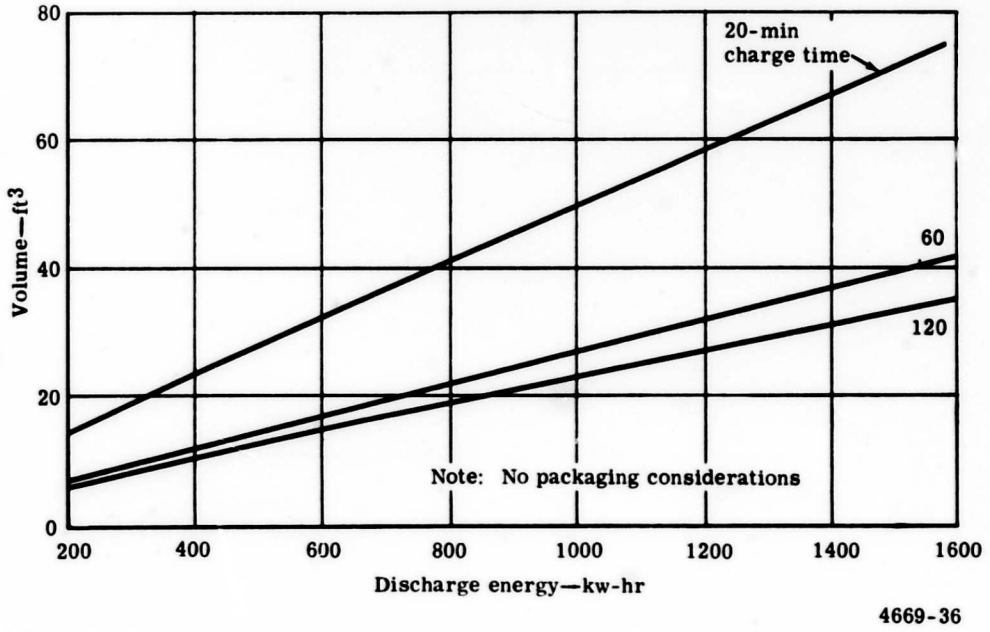

Figure 36. Volume of components located on the vehicle versus discharge energy content.

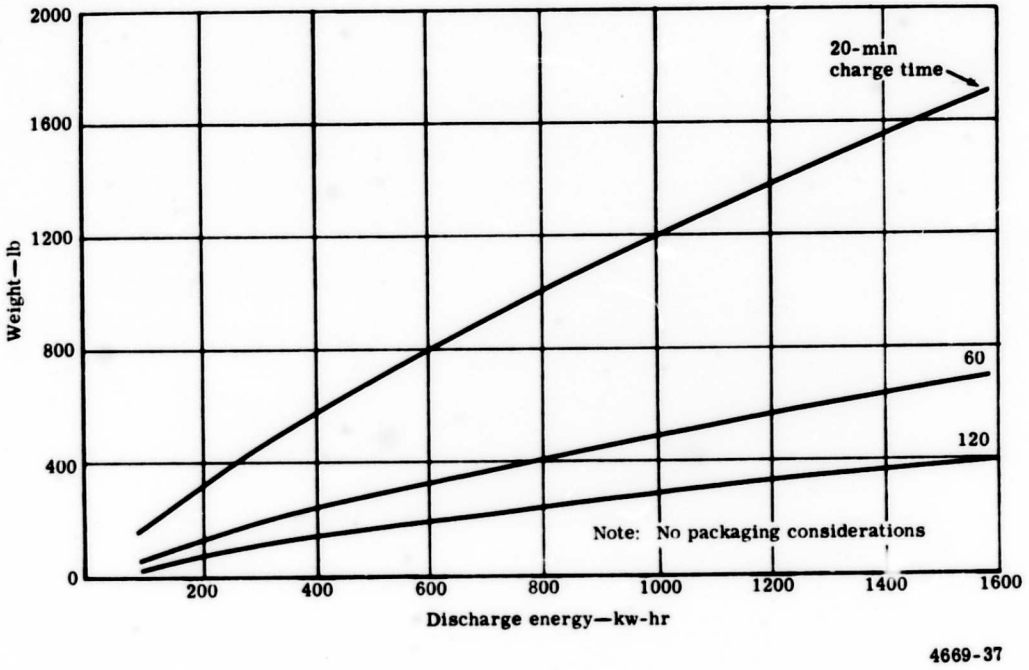

Figure 37. Weight of Cl_2 processing components located off of the vehicle versus discharge energy content.

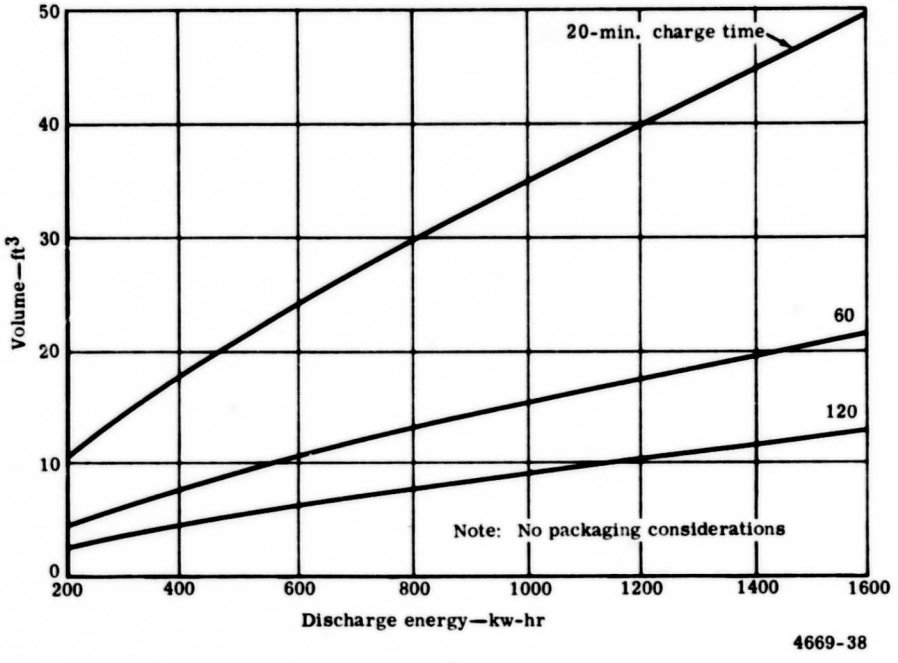

Figure 38. Volume of Cl_2 processing components located off of the vehicle versus discharge energy content.

Charge Efficiency

System charge efficiency for the lithium-chlorine cells using grooved Cl_2 electrodes was derived as a function of charge time using the analytical bases described in Appendix 3. Figure 39 describes the effect on charge efficiency of changes in charge time for those systems designed for a 20-min charge time. These data do not include the power losses in power leads or intercell leads which could be sized differently for a 20-min charge time.

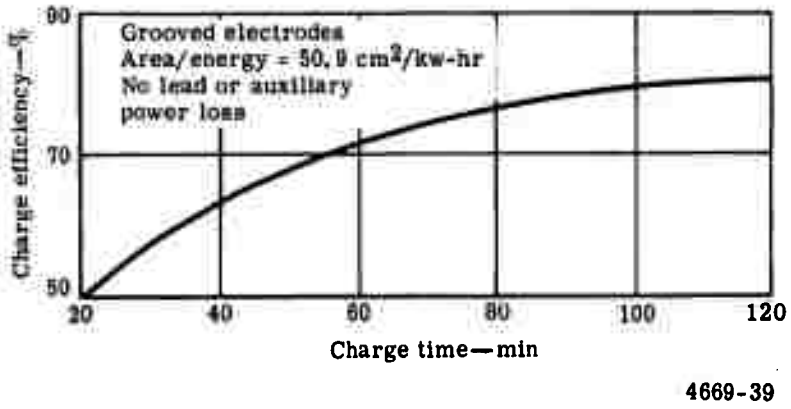

Figure 39. Electrochemical engine charge efficiency versus charge time.

VI. CHLORINE ADSORPTION INVESTIGATION (TASK V)

OBJECTIVE

The adsorption of Cl_2 on activated charcoal is being investigated as an alternate approach to storing Cl_2. This approach provides a margin of safety relative to liquid Cl_2 storage at the expense of additional weight and volume. The purpose of this task is to determine the feasibility of Cl_2 storage for fast charge lithium-chlorine systems by investigating the adsorption kinetics of Cl_2 on charcoal. Specific areas of work in this task are:

- To determine adsorption isotherm data for Cl_2 on charcoal between 1 and 20 atm and 25 and 200°C
- To determine adsorption rates for the previous conditions
- To determine heat of adsorption data for pressure, temperature, and Cl_2 flow rates consistent with the previous conditions
- To determine effects of recycling—i.e., hysteresis, structural integrity of the activated carbon, reproducibility from cycle-to-cycle, and physical and chemical characteristics (This was specified as additional information desired within the limits of allocated time and effort in this task.)

During the first three months of the program, effort was applied in determining adsorption isotherm data and Cl_2 adsorption recycle studies.

DETERMINATION OF ADSORPTION ISOTHERM DATA

During this report period, the amount of Cl_2 adsorbed on activated charcoal was determined at adsorption temperatures from 25 to 200°C and Cl_2 pressures from 1 to 5 atm gauge. The charcoal was contained in the adsorption vessel (Figure 40). The Cl_2 transport system (Figure 41) was fabricated using commercially available tubing, fittings, and valves. To reduce corrosion and contamination, the materials used in the apparatus were limited to Inconel, Teflon, and type SS 316 and 347. The adsorption vessel was maintained at temperatures of approximately 25, 50, 100, 150, and 200°C. The pressure of the Cl_2 gas was regulated at approximately 1 atm intervals between 1 and 5 atm gauge.

Operating Procedure

1. The charcoal was weighed in the adsorption vessel at ambient conditions. The fill tube was packed with Pyrex glass, and the cap was silver soldered to the tube. After leak checking the vessel, it was mounted on the apparatus, and then the apparatus was leak checked.

2. A flow of Ar was passed through the apparatus and atmospheric trap, and the adsorption vessel was heated to approximately 450°C. The charcoal was maintained approximately one day at these conditions for activation, determined by monitoring the vessel weight. The Ar flow was then stopped and the system was evacuated to approximately 50 microns, at which point the weight of the vessel of activated charcoal was determined.

3. Chlorine was admitted to the system and used to flush the charcoal at approximately 5 psig.

4. The weight of the adsorption vessel was then determined at various pressures and temperatures as the temperature of the adsorption vessel was gradually decreased to 200°C, maintaining the required pressures within the apparatus.

BLANK PAGE

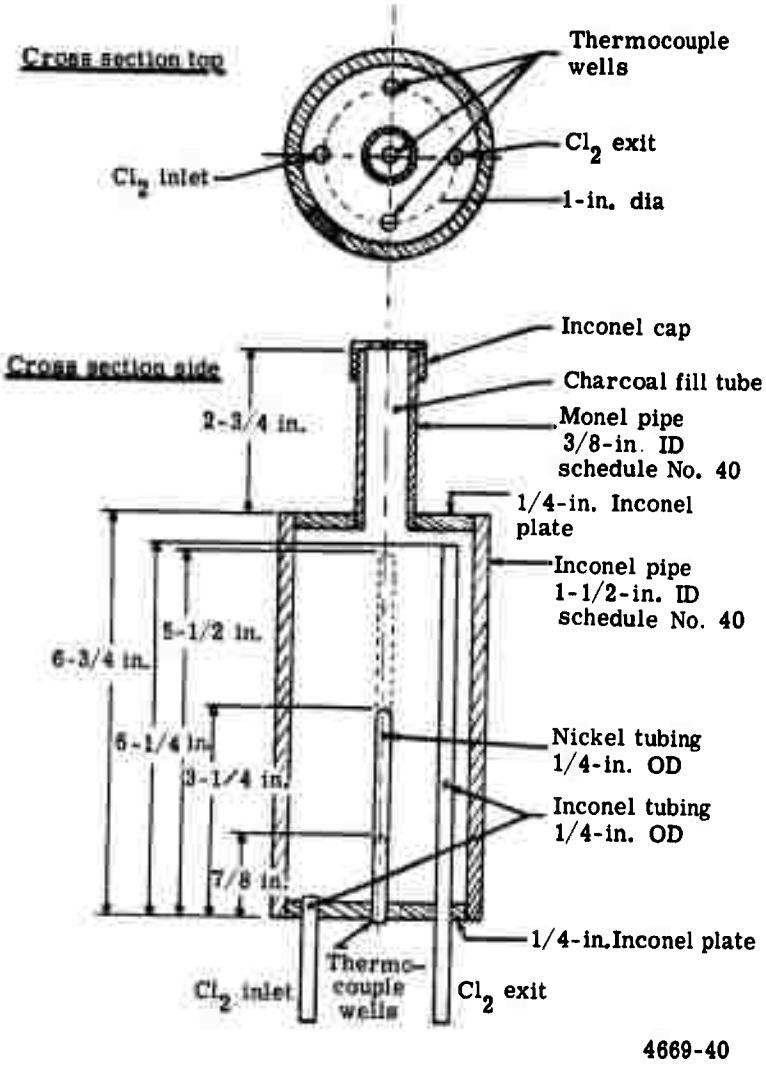

Figure 40. Adsorption vessel.

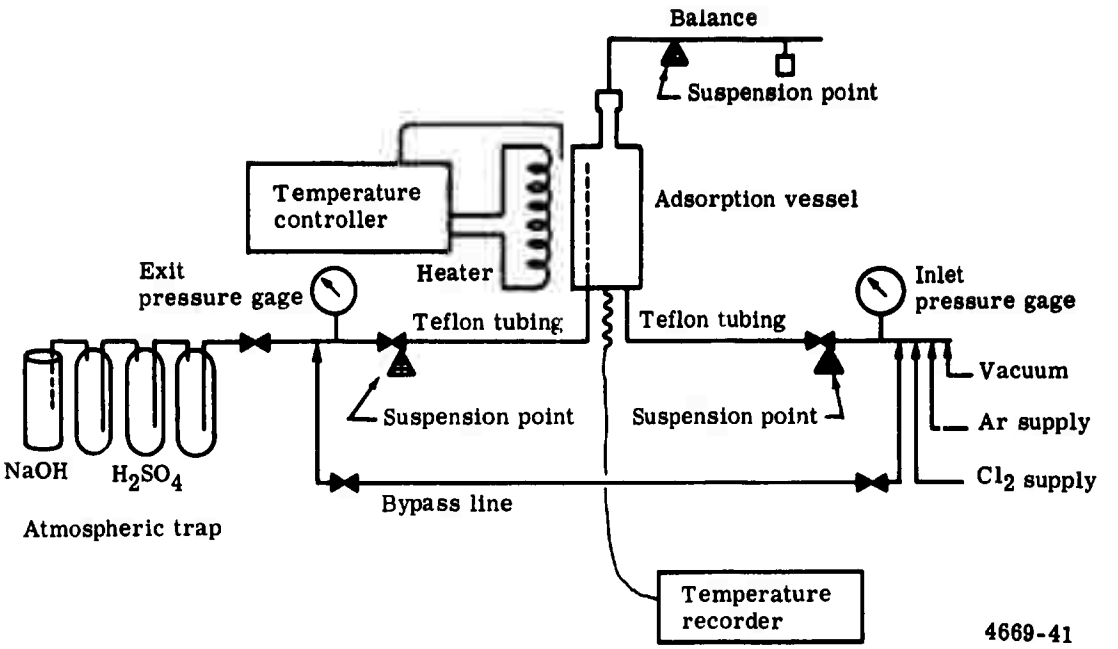

Figure 41. Adsorption system schematic.

5. With the vessel at 200°C, the pressure was adjusted at approximately 1-atm intervals starting at 3 psig up to a maximum of approximately 75 psig. Chlorine was permitted to flow through to the atmospheric trap.

6. At each pressure interval, the adsorption vessel was weighed and the pressure and temperature conditions were recorded.

7. After the maximum pressure was reached, the pressure was decreased at approximately 1-atm intervals and the weight, pressure, and temperature were determined and recorded at each interval.

8. The operations at 200°C were repeated at adsorption vessel temperatures of approximately 150, 100, 50, and 25°C.

Equipment and Materials for Adsorption Study

The following materials and equipment were used in this study:

- Sargent recorder (Model SR)
- Simplytrol temperature controller (Model 4532-PR-1)
- Welch duo-seal pump (Model 1405)
- Taylor barometer
- Ohaus triple-beam balance (capacity 2610 gm)
- Grade Cal 12 x 40 charcoal (Pittsburgh Chemical Company)
- Chlorine (Matheson Company, Inc)

Test Results

Adsorption isotherm data obtained from the experiments is presented in Figure 42. These data show the combined effects of temperature and pressure on Cl_2 adsorption and were obtained from Cal 12 x 40 activated charcoal.

After evaluating the test apparatus, it was found that during connection the Teflon lines were placed in distortion which was reflected on the balance. However, heating these lines with a heat-gun appeared to minimize the effect of this distortion on the balance. The true weight was calculated by correcting for the weight transferred. The amount of correction was determined by calibrating the balance at different pressures and temperatures within the adsorption vessel.

While making these isotherm measurements, it became apparent that the method of controlling the adsorption vessel temperature was not adequate. This was evident in the data obtained at 100°C where the temperature gradient between the top and bottom thermocouples was approximately 25°C due to the chimney effect inherent with this type of apparatus. During the 50 and 25°C measurements, a preheater was used below the vessel enabling a gradient of less than 3°C to be maintained.

After making these adsorption measurements, an effort was made to reproduce the initial isotherm at 200°C. It was found that the vessel weight had increased by 3.1 gm. This weight increase was probably due to contamination of the charcoal by corrosion products formed within the vessel. To reduce this contamination during future measurements, the vessel temperature will be held as low as possible when Cl_2 is in the system.

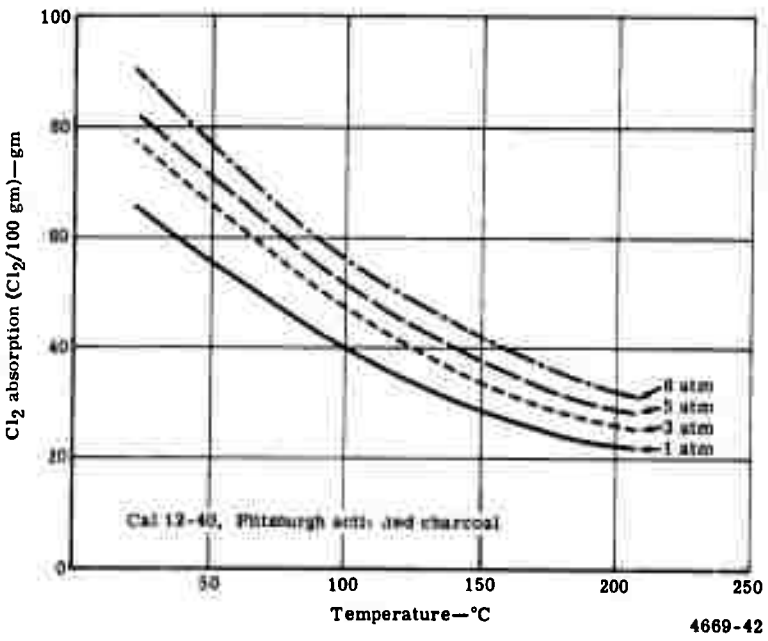

Figure 42. Adsorption isotherms of Cl_2 on charcoal—adsorption at constant pressure.

Previous Cl_2 adsorption on charcoal data at below atmospheric pressures is presented in Appendix 5. Although essentially the same method was used for this work, the two families of curves do not have the same slopes and intercepts. The reasons for these differences are that the adsorption vessel and lines were glass in the below atmospheric pressure work. By using glass instead of metal, the charcoal was exposed to less contamination and was maintained at a more uniform temperature.

CHLORINE ADSORPTION RECYCLE STUDIES

Work was initiated in this area prior to completion of the other items of work because of the importance of impurity build-up on the performance of the charcoal storage concept. The apparatus used in the chlorine adsorption recycle studies is shown in Figure 43. This system was designed to study multiple adsorption and desorption cycles in a closed system and to simulate the Cl_2 system for a secondary battery operation. With the design of this system, a Cl_2 material balance can be made at any time during the recycle experiment. The apparatus was constructed of glass, Teflon tubing, and Monel valves.

Operating Procedure

1. Apparatus was assembled as shown in Figure 43.
2. The adsorption cylinders were loaded with known weights of charcoal.
3. The scales were adjusted and the total weight of apparatus plus charcoal was recorded.
4. An Ar sweep was started across both samples of charcoal and vented through the H_2SO_4 atmospheric seal.
5. The temperature of the charcoal was then raised from 25 to 450°C. The impurities liberated during activation were removed with the Ar sweep.
6. A continuous record of weight loss was kept.
7. As soon as the sample weights of charcoal stabilized, the Ar sweep was stopped and the whole system was evacuated. The system was generally evacuated overnight at temperature.
8. After the charcoal was activated, the activated weight was recorded.
9. The initial Cl_2 adsorption was started with a programmed cooling of the charcoal.
10. As soon as the initial loading was completed, the vent valves were opened and the impurities in the Cl_2 were removed by flushing Cl_2 through the charcoal.
11. The final Cl_2 adsorption was completed in this manner.
12. The No. 1 cylinder and/or Cl_2 storage cylinder was isolated and Cl_2 in the No. 2 cylinder (secondary battery) was desorbed by heating. The Cl_2 was vented through the atmospheric seal.
13. Chlorine desorption of charcoal in cylinder No. 2 was completed at atmospheric pressure and 450°C.

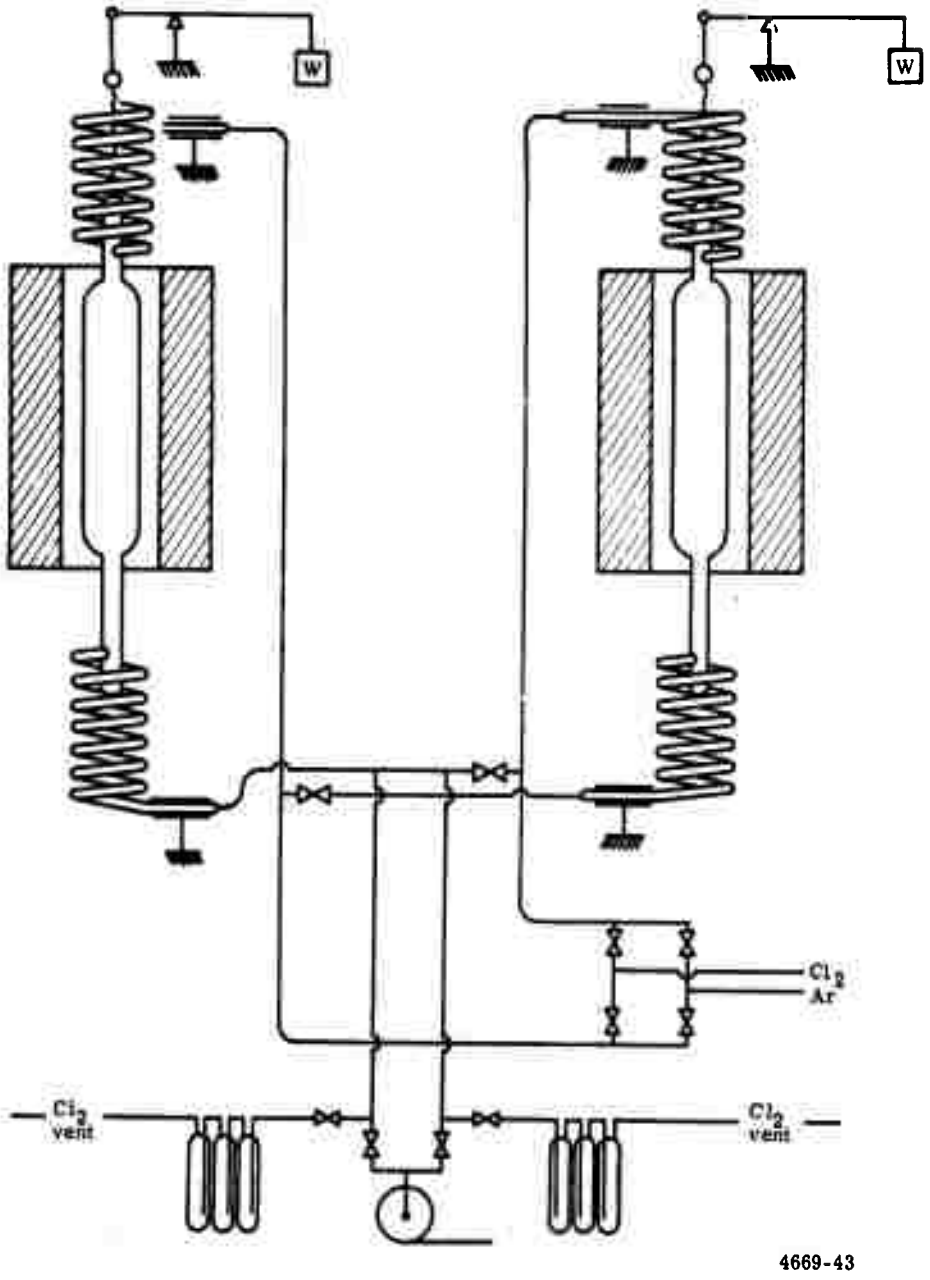

Figure 43. Chlorine recycle system.

14. The atmospheric sealed vents to cylinder No. 2 were closed and the recycle adsorption-desorption was started.

15. The recycle of Cl_2 was conducted at pressures slightly above atmospheric by programming the cooling of adsorbing charcoal and the heating of the desorbing charcoal. The transfer rate of Cl_2 now became a heat problem which will be improved by proper heat exchange design of the adsorbing chamber.

Equipment and Materials for Recycle Studies

The following equipment was used in the recycle studies:

- Pyrex Cl_2 adsorption cylinder (2 required)
- Simplytrol temperature controller (Model No. 4532-PR-1 with heavy duty relay—2 required)
- Honeywell potentiometer (Model No. 2730)
- Heavy duty furnaces—580 w at 115 v (2 required)
- Welch duo-seal pump (Model No. 1435)
- Valves (Whitey series) monel (10 required)
- Ohaus triple-beam balance—2610 gm capacity (2 required)
- Glass and Teflon transfer lines

Activated charcoal is the most unique of all the surface active materials that adsorb Cl_2. It ranks very high in its adsorptive capacity and is essentially nonreactive with Cl_2—i.e., the carbon is nonreactive, however, the ash contained in the activated carbon can be reactive. This can be better understood by comparing activated carbons produced from bituminous coal with that from coconut shells. The ash content of activated bituminous charcoal is 8 to 8.5%, while the ash content of coconut charcoal is 4.0%. The ash of the bituminous charcoal is considered nonreactive with Cl_2, while it has been demonstrated that the ash in coconut charcoal is very reactive and produces chlorides which block the adsorption sites and lower the adsorptive capacity of the charcoal.

Of the bituminous charcoals, Grades SGL 8 x 30 and Cal 12 x 40 appear to have the highest Cl_2 storage as recycle capacity. These charcoals are produced by Pittsburgh Chemical Company.

Test Conditions

The following test conditions cover the temperature and pressure range at which charcoal activation and Cl_2 adsorption-desorption are conducted:

- Activation
  - Argon sweep at atmospheric pressure with the temperature programmed from 25 to 450°C
  - Evacuation of charcoal at 450°C for 16 hr
- Adsorption
  - Initial temperature and pressure are 450°C and 14.7 psia
  - Final temperature and pressure are 25°C and 14.7 psia
- Desorption
  - Initial temperature and pressure are 25°C and 14.7 psia
  - Final temperature and pressure are 450°C and 14.7 psia

Test Results

The preliminary test results were satisfactory; however, the experiment did not continue long enough to predict any impurity build up.

Very little information on adsorption and storage capacity of Cl_2 on charcoal was found in the literature. Consequently, some preliminary laboratory experiments were made to determine adsorptive capacities of known adsorbents.*

Table VIII presents a tabulation of the adsorptive capacities of the adsorbents studied.

Table VIII.
Tabulation of the adsorptive capacities of the adsorbents studied.

Material	Total adsorption (gm Cl_2/100 gm adsorbent)	Storage capacity (gm Cl_2/100 gm adsorbent)
Molecular Sieves Type AW 500	19.6	—
Silica Gel (Type FM-1044-C)	23.5	—
Charcoal (activated)		
BPL (4 x 40)	72.2	61.8
Cal (12 x 40)	74	65.1
N x C 6/8	72	57
SGL (8 x 30)	69.5	59.5

*R. H. Perry, editor, Chemical Engineers' Handbook, New York: McGraw-Hill, 1963, Section 16, pp. 2-40.

VII. CONCLUSIONS AND RECOMMENDATIONS

TASK I—CHLORINE ELECTRODE CHARGE PERFORMANCE

The highest current densities over a given period of time were observed with the dense graphite (886). Although current densities of 20 amp/cm^2 were sustained for 25 min without occurrence of anode effect and without use of current reversal, this material is not suitable in the discharge mode. Fairly high current densities were attained with both FC-11 and FC-13 porous graphite using current reversal. The results, however, are not final since the maximum duration of these high current densities was not fully investigated. Also, the effect of reversal frequency on limiting current density was not fully investigated for FC-11. It was not possible to completely optimize this reversal frequency for the FC-13 due to the limitations of the current reversal unit. The 30 sec to 0.3 sec forward time-to-reverse time, however, was found to improve the cell performance at a given current density relative to the ratio of 30 sec to 5 sec.

The use of a pulse generator utilizing rapid electronic switching would solve problems inherent in the present current reversal unit, which utilizes mechanical switching by relays.

Since the dense graphite works best in the charge mode and the porous graphite in the discharge mode, a compromise must be made. The use of FC-11 appears promising. The limiting current density sustained by FC-11 was several times greater than that observed with FC-13 over a similar period of time, with or without the use of current reversal. With the optimization of current reversal, perhaps the large current densities (>15 amp /cm^2) can be maintained for a longer period of time (>30 min).

If all the Cl_2 were consumed at the anode during current reversal, lithium attack of the graphite would take place with the formation of Li_2C_2. After reacting with Cl_2 over a period of time, LiCl and amorphous carbon would be formed. Since no significant amount of amorphous carbon was found in the LiCl after the runs where current reversal was employed, lithium attack of the anode during the reverse mode must not have occurred to a very high degree. Also, examination of the anode surface after the runs did not reveal any excessive pitting, tending to support this hypothesis.

It is thought that the Li_2C_2 enhances the wetting of LiCl on graphite. This could be investigated easily by use of a sacrificial electrode in the cell to produce known amounts of Li_2C_2 *in situ* and observing the effect on the limiting current densities over a period of time. The long-term effects on cell performance should also be studies, since accumulation of amorphous carbon could be detrimental during operation of the cell during charge and/or discharge.

The use of pressure reduction behind the anode as an attempt to improve limiting current densities over a period of time cannot be completely ruled out since experiments to date are only of a preliminary nature. Although there was no significant improvement noticed in cell performance, the wetting of the graphite was enhanced, as noted by increased ease in initiating current flow, at the start of the first run. However, if the pressure differential across the porous graphite becomes too large, there is the danger of the LiCl flooding the pores. With a larger porous anode area available for potential Cl_2 flow and a suitable experimental cell design, perhaps pressure reduction would be of more significance.

The results of the aqueous anode-effect study indicated that the configuration of the anode had an effect on the limiting current densities that could be attained. Although the aqueous LiCl solution wets graphite completely, while the molten LiCl does not wet the graphite to a large extent, an anode-configuration study in molten LiCl appears warrented.

Preliminary temperature studies at the anode surface during passage of large currents suggests that the anode temperature may be an important factor in maintaining large current densities over a long period of time, since anode effect is temperature dependent. The temperature at the anode during passage of current densities over 20 amp/cm^2 , if successfully maintained, may cause excessive local heating over a prolonged period of time (30 min or more), resulting in a decrease of the current density. If the appearance of anode effect depends significantly on the temperature in the LiCl system, use of a KCl-LiCl should be helpful, since its melting point is over 250°C less than that of LiCl. Also, the KCl will not be removed chemically or electrochemically under proper conditions. Various other suitable fluoride-chloride eutectic combinations of LiCl could also be studies if the KCl-LiCl eutectic should prove beneficial.

An Inconel tank was constructed for future use during the limiting current densities investigation of porous graphite anodes using high Cl_2 pressures (up to 10 atm).

TASK II—CONSTRUCTION OF CELL MODEL

The Mark IV cell has progressed to a point where it is an operating device. Design modifications were required to eliminate short circuits in the flange area of the cell.

A pertinent design modification of the cell cooling system was completed to allow for higher charge currents. This should allow the cell to be charged in approximately 1.6 hr.

Task III—EXPERIMENTAL EVALUATION OF ENERGY EFFICIENCY

One test was run on the Mark IV cell during this report period. The test was terminated before meaningful efficiency data could be obtained due to an electrical short circuit in the flange area of the cell. However, sufficient information was obtained to prove specific design features of the cell and to pin point areas where design improvements are required. Appropriate design improvements will be made so that performance data can be obtained.

TASK IV—SYSTEM ANALYTICAL STUDIES

The systems design and analysis effort of the lithium-chlorine electrochemical engine resulted in a definition of two system concepts which appear attractive for vehicle propulsion—the module replacement concept and the rapid charge concept. Both systems incorporate an advanced cell concept characterized by vertical electrodes and a cylindrical cell geometry. This geometry is amenable to higher pressure operation and good heat transfer from the power section of the cell. An additional feature of the cell is that the Li and LiCl storage is in the cell eliminating plumbing of the liquid metal and molten salt at high temperature.

The module replacement mode concept is an engine system comprised of ten replaceable modules weighing approximately 90 lb each. This system will provide 200 kw-hr over a specified ERDL duty cycle requiring a peak power of 75 kw. The complete system is estimated to weigh approximately 1250 lb and will require a total vehicle space of 60 in. × 25 in. × 32 in. An overall discharge efficiency of 82 to 85% is estimated based on projections of laboratory data on electrode performance.

Work is in progress on the fast charge mode of operation. This work has not progressed sufficiently to project engine system data. Preliminary comparisons, however, can be made between power compartments. The module replacement system weighs approximately 900 lb while a comparable fast charge 40-cell module is estimated to weigh 600 lb. This indicates that considerable weight saving can be achieved in the engine system.

TASK V—CHLORINE ADSORPTION INVESTIGATION

The experimental program established the adsorptive capability of several charcoals under specific test conditions.

The present status of isotherm experiments indicates a lack of capability to reproduce isotherm data. Several causes and effects were suggested in the test results for these variations. Further testing with improved cycle control should improve isotherm data and minimize deviations in the results from future tests. Adsorptive capacities are increased by the combined effects of temperature and pressure.

The program in the recycle studies has not progressed far enough to be conclusive. The design of the required appartus, however, was completed.

APPENDIX 1

DESCRIPTION OF SYSTEM COMPONENTS FOR THE MODULE REPLACEMENT MODE

INTRODUCTION

This appendix describes in detail the ERDL system design for the module replacement mode of operation. The investigation and analysis leading to the design selection are also described.

Lithium and Cl_2 can be reacted in a cell to produce LiCl and electrical energy. The reaction is reversible; by supplying energy, the LiCl can be dissociated electrolytically to reform the original reactants. A conceptual design of a vertical lithium-chlorine cell system is described in this section. Seven vertical cells, packaged inside a thermally insulated container, constitute a power module. A series of these modules used in conjunction with certain auxiliary equipment makes up an electrochemical engine system. This appendix describes in greater detail the components of the conceptual electrochemical engine system shown in Figure 24.

CELL CONCEPT

The primary function of the lithium-chlorine cell is to provide a means of obtaining electrical power from the free energy of the reactants—Li and Cl_2. In addition, the cell performs a second function of providing the required storage volume for the retention of the Li reactant and the LiCl produced. This is done to facilitate electrical separation of succeeding cells and to eliminate Li and LiCl plumbing. Lithium, a liquid metal at the cell operating temperature, is an excellent electrical conductor. Flowing liquid Li into the cells from a common storage supply would either place the cells in parallel electrically or require electrical separation devices in the supply line to each cell. Application requirements require a higher voltage than can be obtained if the cells are placed in parallel, and electrical separators represent a complication of design that is not attractive. These considerations indicate separate, internal Li storage. But the same difficulty does not exist with Cl_2 because it is not an electrical conductor. Consequently, a common Cl_2 storage may be utilized, provided electrical isolation of the tubing is accomplished.

The cell design concept that was originated employs concentric vertical cylindrical electrode surfaces. Figure 1-1 illustrates this design. This cell design was designated the "D" cell to differentiate it from alternative Allison design concepts.

In the "D" cell design, chlorine is supplied to a porous carbon electrode. This is done by means of an inlet tube from the bottom of the cell. Any excess Cl_2 is channeled up to an annular flow channel by a gas separator screen and collected in a storage plenum at the top of the cell where it exits through the Cl_2 outlet.

One of the distinct advantages of this design concept is the ability to have a "flow through" Cl_2 electrode. Circulating excess Cl_2 (approximately 1.5 times stoichiometric amount) through the porous carbon electrode allows the following advantages.

- Impurities in the gaseous Cl_2 can be circulated rather than accumulating in the pores where they would polarize the Cl_2 electrode.
- The bubbling action on the surface of the Cl_2 electrode provides a mixing action enhancing the transport of Cl_2 to the electrode-electrolyte interface.

Lithium has a density approximately one-third that of LiCl; the Li reservoir is thus contained below an inverted cup by the buoyant force. Lithium reaches the electrode zone by capillary action in a porous metal wick.

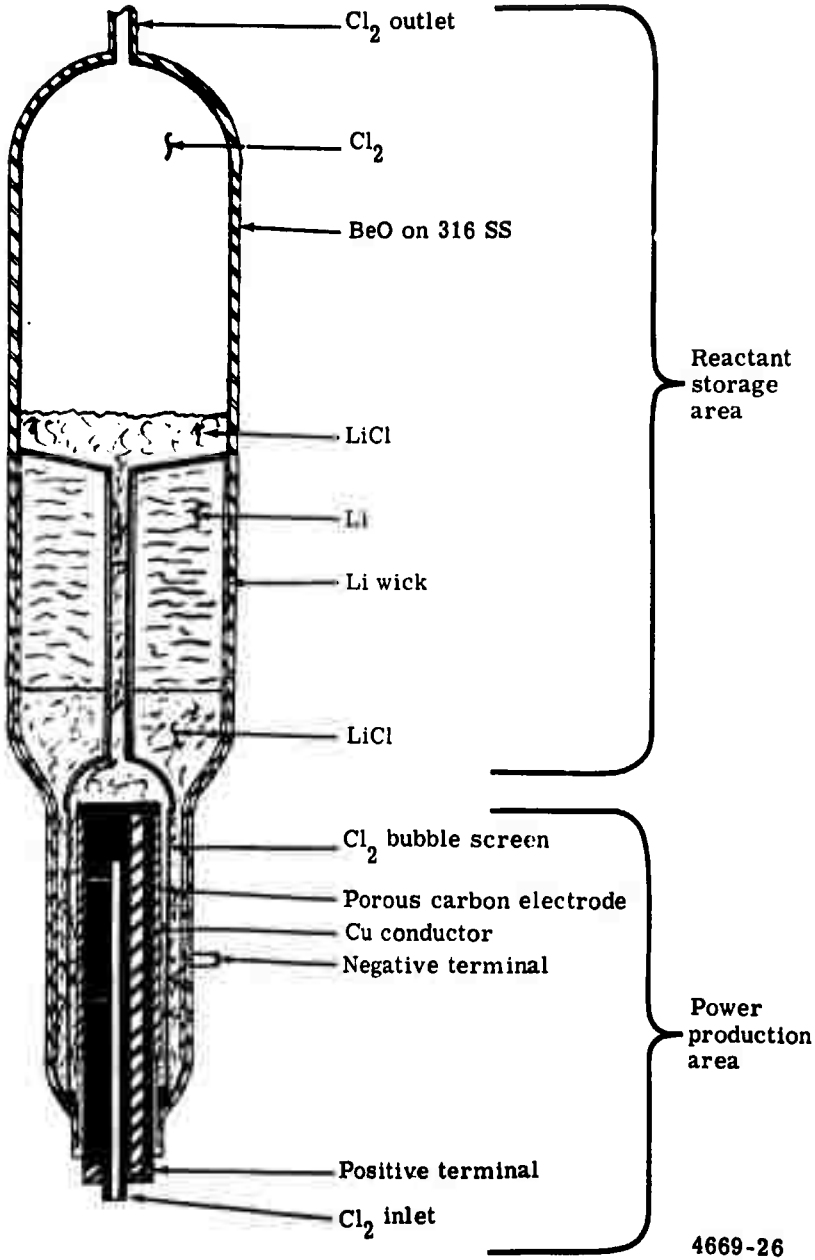

Figure 1-1. Vertical "D" cell design.

The cell stores LiCl in the space given up as the Li is used. The surplus LiCl then fills the plenum at the top of the cell. A corrosion resistant coating is used on the metal walls which are exposed to hot Cl_2.

Electrical insulation between the Cl_2 electrode terminal and the cell walls, which are at Li electrode potential, is accomplished with a beryllia brazed seal in this concept.

The Cl_2 which is generated during a charge cycle will exit as did the previous excess Cl_2. The Li that is formed will return to the storage cavity via the wick. However, if any were to break free from the surface, it would return to its storage compartment by its own buoyant force.

The Cl_2 electrode consists of porous carbon bonded to a dense graphite structure. Metallic conductors are imbedded in the graphite to reduce the internal voltage drop and resultant power loss. The metal chosen should have low electrical resistivity and a thermal expansion coefficient as close as possible to that of the graphite in which it is imbedded. The metal which best satisfies these criteria is molybdenum. However, the inclusion of the necessary cross section for the required length adds weight and expense to the design. An alternate approach is to use braided copper strands which provides excellent conductivity and deforms sufficiently to meet variations in thermal expansion compared to graphite.

It is noted that reasonable advances in technology were assumed in the cell design. This applies primarily to materials of construction and certain fabrication processes. Research and development programs are in progress with the objective of advancing the state of the art in these areas.

CELL DESIGN

The optimization of the total cell weight and efficiency, using the "D" cell conceptual design, over the ERDL duty cycle allowed cell design parameters to be selected (see Appendix 3). This cell design is shown in Figure 1-2. The following are the design conditions:

- Cell pressure—5 atm
- Excess Cl_2 flow—50%
- Temperature—650°C
- Electrolyte thickness—0.75 cm (1 cm equivalent)*
- Lithium storage—981 amp-hr (535 cm^3)
- Lithium chloride storage—1041 cm^3
- Chlorine electrode area—115 cm^2

The cell in the charged condition would have the Li storage annulus filled with Li to the point where the Li shield domes above the Cl_2 electrode. This Li would be floating on LiCl which would occupy the remainder of the cell outside the Cl_2 electrode and up to the bottom of the upper pressure vessel. The upper pressure vessel will contain gaseous Cl_2 at 5 atm pressure.

The purpose of the LiCl storage chamber is to provide storage for the LiCl generated during cell discharge. Approximately half of the generated LiCl will fill the Li storage cavity as

*The additional 0.25 cm is added as an artificiality in computer programming to account for other resistances between the electrodes—i.e., bubbles and the Cl_2 separator.

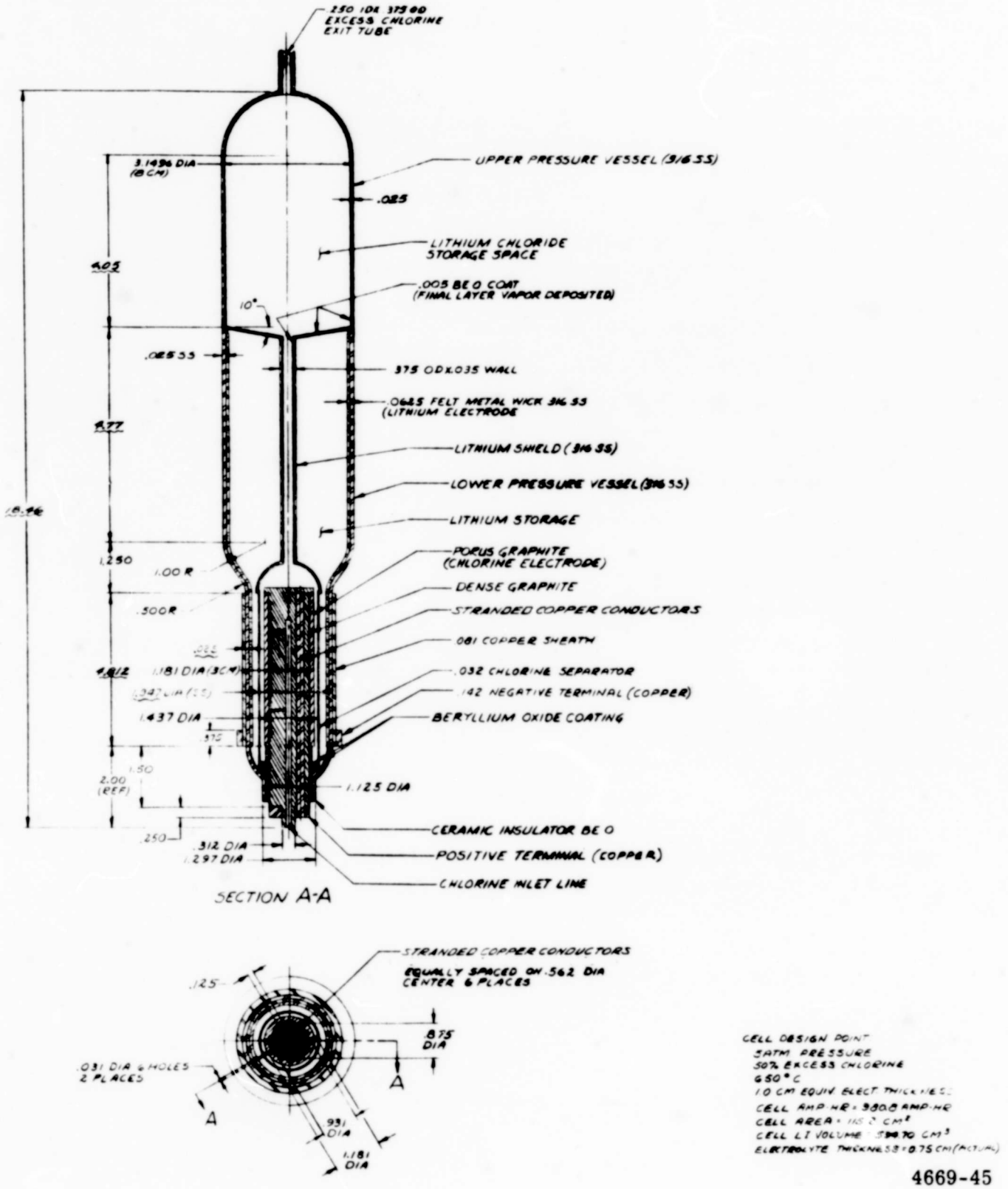

Figure 1-2. "D" cell design.

the Li is consumed, and the remainder will fill the upper pressure vessel. When the cell is completely discharged, the LiCl will reach the bottom of the hemispherical dome.

Table 1-I is a weight summary of the "D" cell for the ERDL application.

Table 1-I.

Weight summary of the "D" cell.

Component	Material	Weight (lb)
Stranded conductors	Copper	0.194
Dense graphite	Graphite 6	0.225
Porous graphite	FC 11	0.071
Pressure vessel	316 SS	1.070
Chlorine separator support	316 SS	0.008
BeO coatings	BeO	0.040
Felt metal wick	316 SS	0.752
Chlorine separator	BeO	0.039
Lithium storage shield	316 SS	0.164
Ceramic insulator	BeO	0.038
Positive terminal	Copper	0.039
Copper sheath	Copper	0.801
Conducting ring	Copper	0.121
		3.562
Reactants		
Lithium (charged)		0.560
Lithium chloride (charged)		0.648
Lithium (discharged)		0
Lithium chloride (discharged)		4.037
Total charged weight		4.770
Total discharged weight		7.599

A grooved Cl_2 electrode was incorporated into this design. Grooving of the graphite electrode increases the effective surface area in contact with the electrolyte without increasing the electrode weight. This effective increase in surface area provides an electrode that demonstrates improved performance and will allow an increased current density compared with a smooth electrode surface.

Figure 1-3 shows the expected charge and discharge voltages of the cell as a function of the Cl_2 electrode current density. Normal operation of the cell to meet the ERDL duty cycle with 6-hr charge will be in the range of the current densities indicated.

The cell, as previously described, was designed to meet minimum weight and maximum efficiency for the ERDL duty cycle. Table 1-II describes the cell performance for certain power levels. Power and current densities are referenced to the surface area of the Cl_2 electrode.

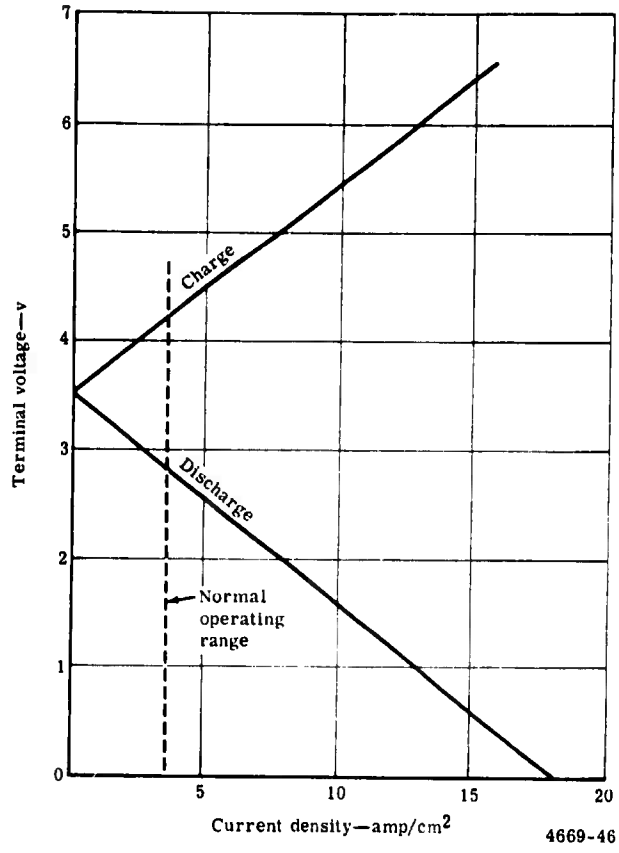

Figure 1-3. "D" cell operating characteristics.

Table 1-II.

ERDL cell operating characteristics (excludes external lead losses).

	Power level			
	Maximum possible	Design peak	Rated	Average*
Power (kw)	120	75	50	25
Power density (w/cm^{-2})	15.36	9.30	6.20	3.10
Current density (amp/cm^{-2})	9.30	3.36	2.19	0.90
Voltage	1.65	2.77	2.84	3.44
Discharge efficiency	46%	77%	83%	88%

*For operation at 25 kw; average power for ERDL duty cycle.

MODULE DESIGN

The engine module, shown schematically in Figure 27, provides structural containment and thermal insulation for a series of cells. In the module replacement mode of operation, it represents that package which is removed on discharge and replaced with a charged module.

The method of describing module insulation is by its "hot time". This represents that period of time at operating temperature (1200°F) before its energy storage would be completely dissipated if the energy storage would be used only in generating heat to maintain the module at temperature. The significance of the "hot time" value is that it is a quantitative measure of the length of time a fully charged engine will remain on standby ready for instant use. The most significant factor in the determination of the "hot time" is the heat leakage rate which is a function of insulation quality and thickness. The "hot time" can be directly correlated with the self-discharge rate—a 20-day hot time corresponds to 5% self-discharge per day while a 10-day hot time corresponds to 10%.

The design criteria used for the module were based on the optimized ERDL cell design and on those other specifications described in Section V of this report. Figure 1-4 illustrates a preliminary design for the module.

Insulation Material

Two types of insulation have been utilized in this conceptual design—Superinsulation produced by Linde Division of Union Carbide Corporation and Min-K produced by Johns-Manville Corporation. A system incorporating these two different types rather than only one is conceived because of their very distinct properties.

Linde Superinsulation is a unidirectional, multiple layer foil with fibrous separators, giving high performance insulation. Its construction consists of a number of highly reflective shields of copper, stainless steel, or nickel for high temperature applications which are separated by fibrous quartz mats. The metal shields are as thin as mechanically practical (foil) to permit minimum weight and maximum flexibility. Fibrous mats of quartz separate the shields. Thin filaments in the mats are used to reduce the area of contact points, increasing the length of conduction paths through the fibers. Small voids in the separator minimize gaseous conduction. To further reduce the gaseous conduction, a vacuum of 10^{-3} to 10^{-4} mm Hg is utilized. The thermal conductivity value, as reported by the manufacturer at 10^{-3} mm Hg, nonload bearing with a source temperature of 1200°F, is 5×10^{-4} BTU-ft/hr-ft^2-°F. A value of 1.5 times this, or 7.5×10^{-4} BTU-ft/hr-ft^2-°F was used in this design for the side insulation where no loading exist. A value of 3.0 times, or 1.5×10^{-3} BTU-ft/hr-ft^2-°F, was used for that insulation located in the module top. These values are considered to be conservative.

Min-K is a bonded structure of opacified powders with fibrous media and containing appreciable quantities of particulate matter, the ultimate structure of which is exceedingly small. This creates pores in the structure so minute that the gaseous conduction is greatly minimized. The opacifying medium reduces the radiation component of the heat transmission. The manufacturers reported value for thermal conductivity at 1 mm Hg is 7.5×10^{-3} BTU-ft/hr-ft^2-°F. This value was used in the heat transfer analysis for this module design. The most significant characteristic of Min-K applicable to this design is its excellent strength and handleability and that it may be fabricated to close dimensional tolerances. Min-K is used in this design primarily because of its strength and load carrying ability.

Structural Design

As previously described, the low heat leakage requirement makes desirable use of the advanced thermal barriers—i.e., Linde Superinsulation. This insulation requires the provision of an evacuated jacket for the structure. This is accomplished by providing an inner pressure vessel and an outer case with an evacuated chamber between the two. The inner can contains the cells, the cooling air distribution lines, the Cl_2 supply and excess distribution lines, a jet pump for recirculation of excess Cl_2, and the power cable connections. The atmosphere inside the inner pressure vessel is slightly above ambient pressure at a maximum temperature of 1200°F.

The inner vessel is a welded structure fabricated of austenitic type SS 316 with cylindrical sides and elliptical dome ends. Seven cells are assembled inside this inner vessel, as shown in Figure 1-4, supported by the perforated disk which is held by snap rings on the inner pressure vessel. All air, Cl_2, and electrical lines and leads are fed through the bottom of the module so that all plumbing lines and manifolds are under the engine box to permit easy module removal from the top.

A two-piece outer module case of aluminum and stainless steel will be fabricated with cylindrical sides and dome ends. A bolted or riveted circumferential flanged seal joint connects the aluminum top and stainless steel bottom sections to form the complete case. The bottom section is stainless steel to permit welding of the module inlet and outlet air and Cl_2 line feed-through joints to obtain a tight vacuum seal of least complexity.

The dimensions of this outer case are basically an 11-in. OD and 30-in. overall length as shown in Figure 1-4. A 1/2-in. vacuum chamber (approximately 10^{-4} mm Hg) between the inner and outer cases is provided in the sides and upper dome for the thermal insulation. A combination of thermal insulation types is used in the module. For the sides and portions of the top where no load is carried, a 1/2-in. layer of Superinsulation is used. Min-K is used for the structural load-carrying areas—i.e., the bottom and small portions of the top.

The basic structural concept transfers the loads of the inner pressure vessel to the outer case by utilizing the compressive strength of the molded Min-K insulation. The primary vertical and bottom lateral loads are supported by the bottom cavity insulation which is molded to conform to the bottom of the inner vessel and outer case. A vertical reaction load is provided by a small piece, 2-in. in dia by 1-in. thick, of molded Min-K located on the top center between the inner and outer case. Upper lateral loads are carried by a ring of molded Min-K placed at the upper dome to the cylindrical section transition plane. By utilizing the good compressive loading characteristic of the molded insulation, structural connections between the inner and outer case are eliminated. This eliminates a major source of heat leakage. This design concept provides an increased "hot time" for a given insulation thickness and module weight, or reduces the insulation required and module weight for a given "hot time".

MODULE PLUMBING AND ELECTRICAL LEADS

During the cell operation, cooling air is required to remove heat resulting from cell inefficiencies. Maximum heat removal of approximately 126,000 BTU/hr total, or 1800 BTU/hr/cell, is required at the 75 kw maximum engine operating power point. The cooling air system was designed for this condition. This heat rejection can be obtained with 12.15 lb/hr air flow/cell or 846 lb/hr total air flow (305 cfm). To minimize the system pressure drop and the blower motor size, air velocities of 50 to 100 ft/sec in the air distribution

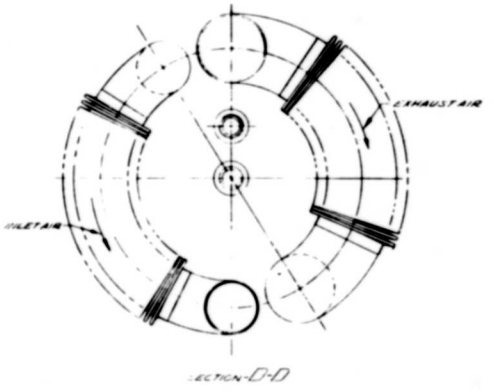
EXHAUST AIR
INLET AIR
SECTION-D-D

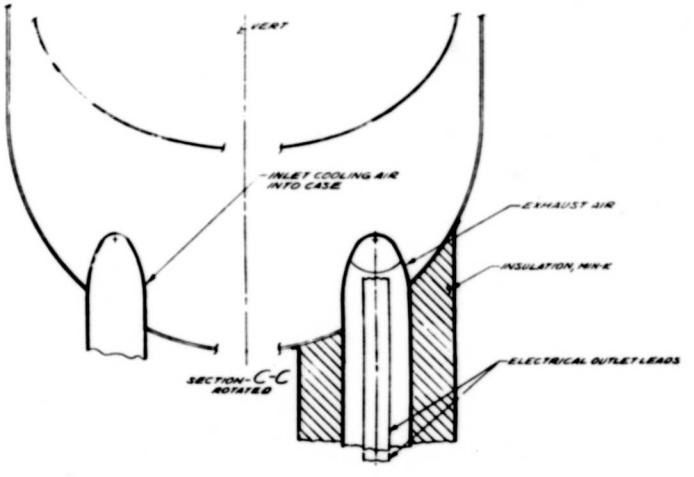
VERT.
INLET COOLING AIR INTO CASE
EXHAUST AIR
INSULATION, MIN-K
ELECTRICAL OUTLET LEADS
SECTION-C-C ROTATED

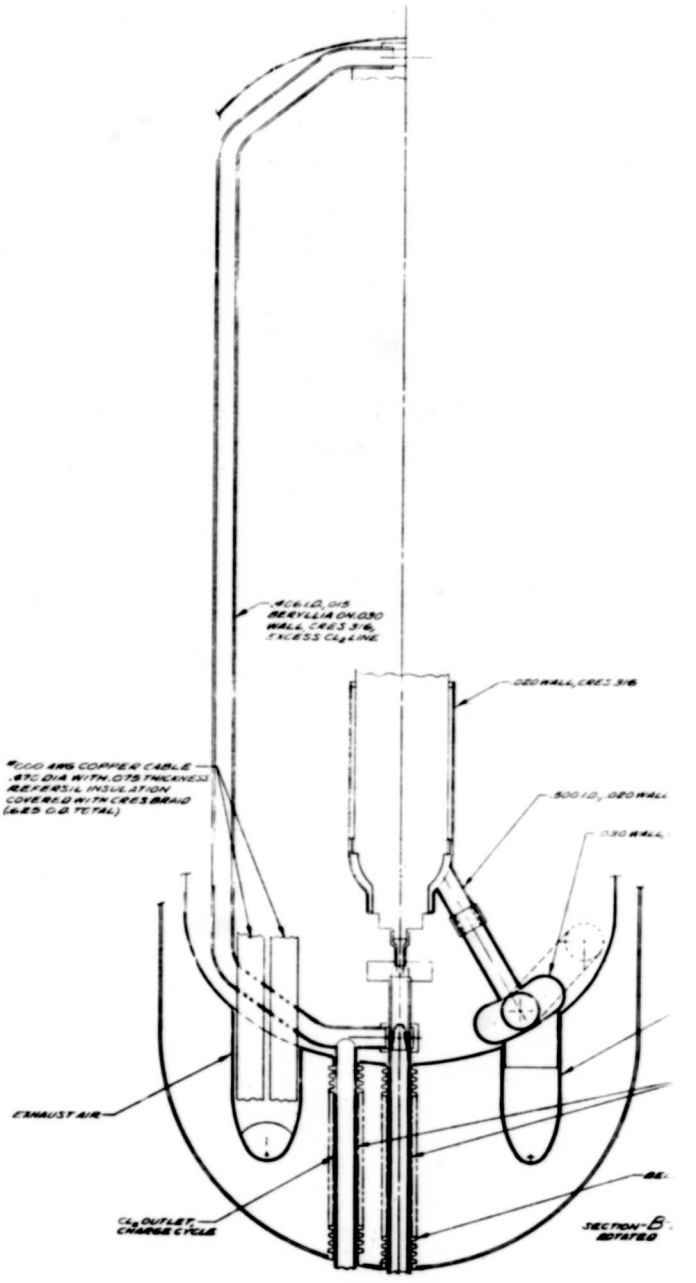
EXHAUST AIR
SECTION-B ROTATED

A

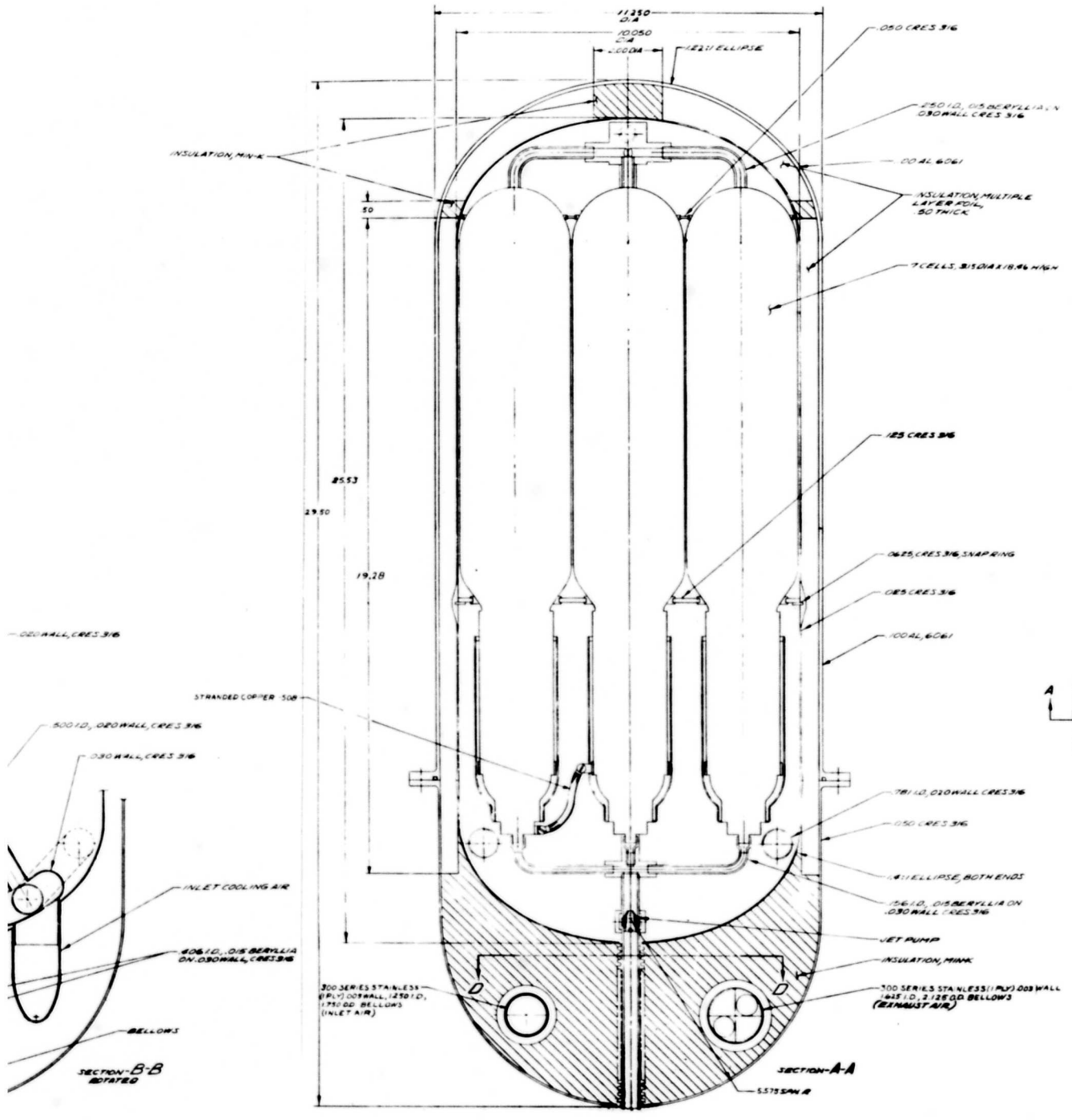

B

Figure 1-4. Seven-cell module assembly for lithium-chlorine electroc

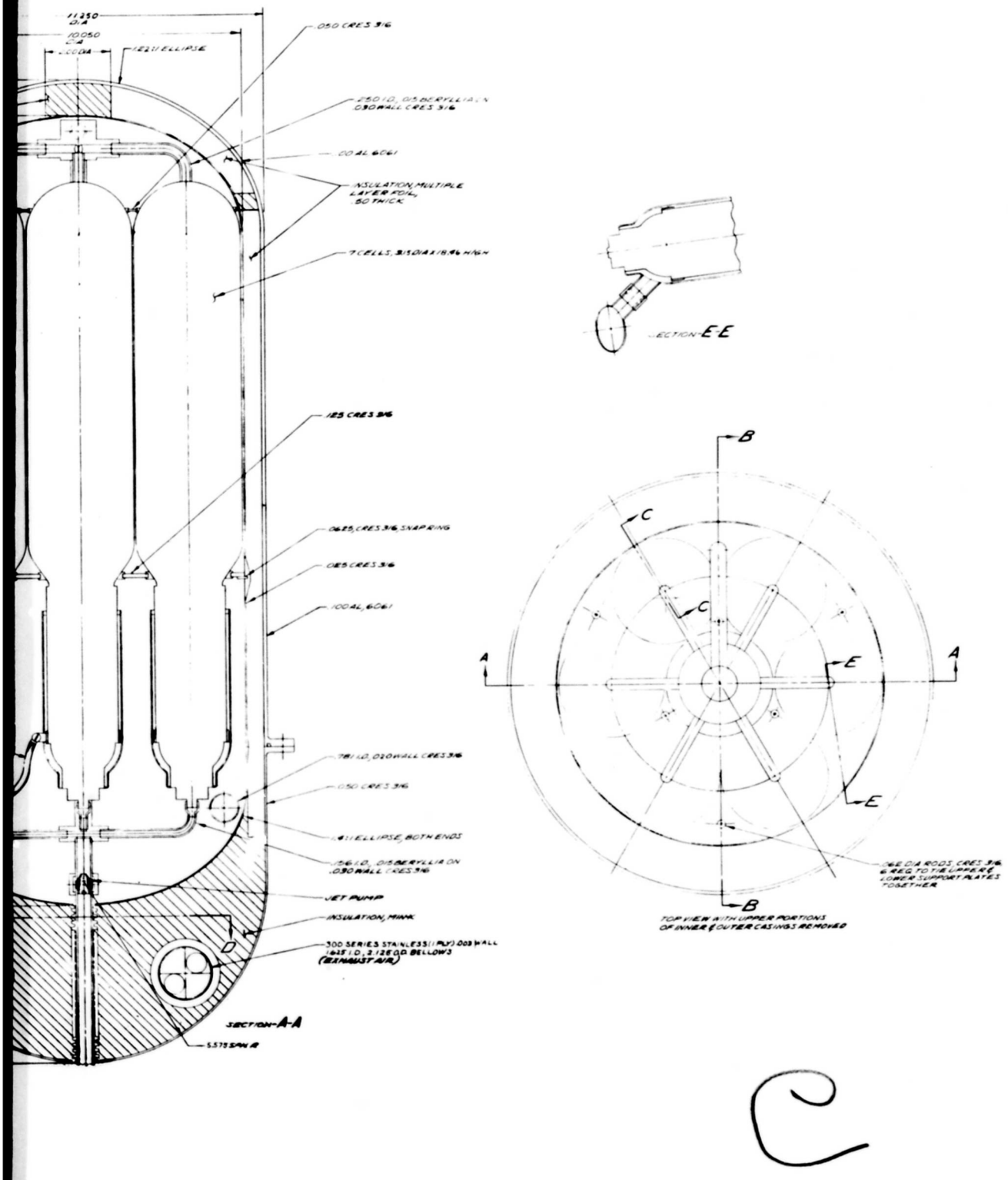

C

ven-cell module assembly for lithium-chlorine electrochemical power system.

system is desirable. The air distribution lines are stainless steel. Cooling air is brought into the bottom of the module from the external distribution manifold through a bellows tube to reduce module heat loss. It is then manifolded past the power section of each cell and discharged into the inner pressure vessel cavity. Exhaust air is ducted out of the inner vessel and module through a bellows tube attached flush to the inner vessel wall at the bottom. This opening is also used to feed the electrical power and instrumentation leads out of the module.

The module Cl_2 system functions as follows: chlorine vapor is piped under pressure through a line entering at the bottom of the module, the Cl_2 passes through the primary side of a jet pump and through the cell inlet manifold to the cells. An excess amount of Cl_2 will enter the cell. This excess will be discharged through individual lines into the excess Cl_2 manifold. The excess Cl_2 manifold passes this Cl_2 to the secondary side of the jet pump and back into the primary inlet flow. During the charge cycle, chlorine is generated within the cell and is removed via an excess Cl_2 system and piped from the module through a line connected to the excess manifold ahead of the jet pump. This line is only opened during the charge cycle and, like all other lines, pipes, and leads, is located at the bottom of the module.

Sealing of the evacuated chamber between the inner vessel and outer case at the module inlet and outlet Cl_2 lines is accomplished by use of a bellows tube surrounding the Cl_2 lines. The ends of the bellows tube is welded or brazed to the inner and outer contained walls, sealing the openings. The ID of the bellows tubes is sized to provide a flush fit around the Cl_2 line OD for minimum heat leakage.

Two electrical power and several instrumentation leads are required for each module. These leads enter the module through the exhaust cooling air line. The power leads are connected to terminals at the bottom of the cells completing a series electrical connection of the seven cells. The electrical power leads are sized for the 1200°F environment. As a result, power cables of the standard size AWG No. 000 (168,000 circular mils) was selected. These cables have a resistance of 0.000228 ohm/ft. Due to the size of the power leads, the use of stranded cable is contemplated. The diameter of AWG No. 000 stranded cable is 0.470 in. The leads are insulated with a high temperature quartz fiber or fiberglass type electrical insulation with an overall stainless steel wire braided sheath. A coating to reduce oxidation of the copper in a 1200°F environment is required in addition to the electrical insulation.

MODULE HEAT LOSS ANALYSIS

The heat loss from each module was calculated to be as:

Component	Heat loss (BTU/hr)
Sides (Superinsulation, 1/2-in. thick)	107
Top (Superinsulation and Min-K, 1/2- and 1-in. thick)	42
Bottom (Min-K, 6-in. maximum thickness)	22
Air lines	2
Chlorine lines and bellows	28
Electrical leads	50
Total	251

BLANK PAGE

These calculations are based on a hot source temperature of 1200°F and a cold receiver temperature of 0°F. Convective heat transfer coefficients for the thin wall inner and outer case were considered to be infinite. The heat loss through the module walls is based only on resistance of the insulation-to-thermal conduction, a conservative calculation.

The heat loss values are based on the following thermal conductivity values:

Materials	Heat loss (BTU-ft/hr-ft^2-°F)
Linde Superinsulation	
Sides	7.5×10^{-4}
Top	1.5×10^{-3}
Min-K	7.5×10^{-3}
Stainless Steel	12
Alumina Al_2O_3	8
Copper	200

Certain simplifying assumptions were made on module geometry for ease of calculation, and electrical lead thermal losses were estimated at 10% of the calculated uninsulated valve, based on their being insulated in the design.

The hot time value is a function of the insulation used, but is limited by solubility and diffusion of the Li in LiCl. It is possible to significantly increase "hot time" by adding additional insulation weight to the design. Figure 1-5 gives a measure of how insulation weight varies as increased or decreased "hot time" is desired. If a 30-day hot time is required, the module weight will approximately double, adding 420 lb to the system weight.

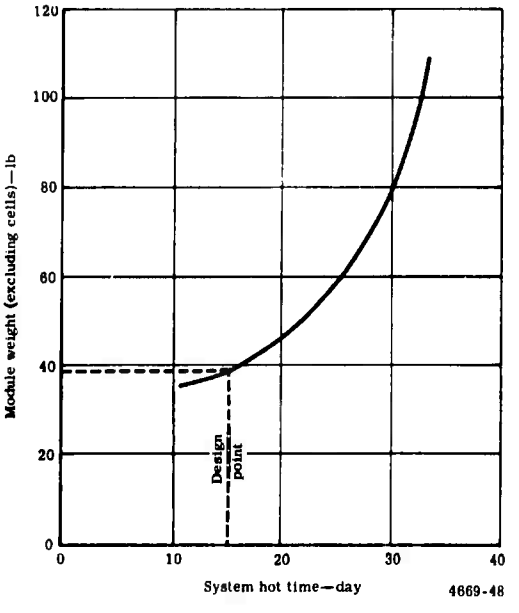

Figure 1-5. Module weight versus hot time.

For the design configuration considered herein, the total energy for 70 cells converted to heat is 943,000 BTU.* The total heat leakage from ten modules is 2516 BTU/hr. This results in a "hot time" of 375 hr or 15.6 days.

COOLING SYSTEM

A cooling system is required in the electrochemical engine so that reasonable temperature limits can be maintained in the lithium-chlorine cell. During cell discharge, excess heat is generated in the cell and power leads above that amount that the module will reject. The amount of excess heat generated is shown as a function of power level in Figure 1-6. To maintain a 1200°F temperature, this heat is rejected by a forced air cooling system. This same blower system is used to supply atmospheric or heated air to the Cl_2 tank for vaporization of Cl_2 during discharge operation and standby.

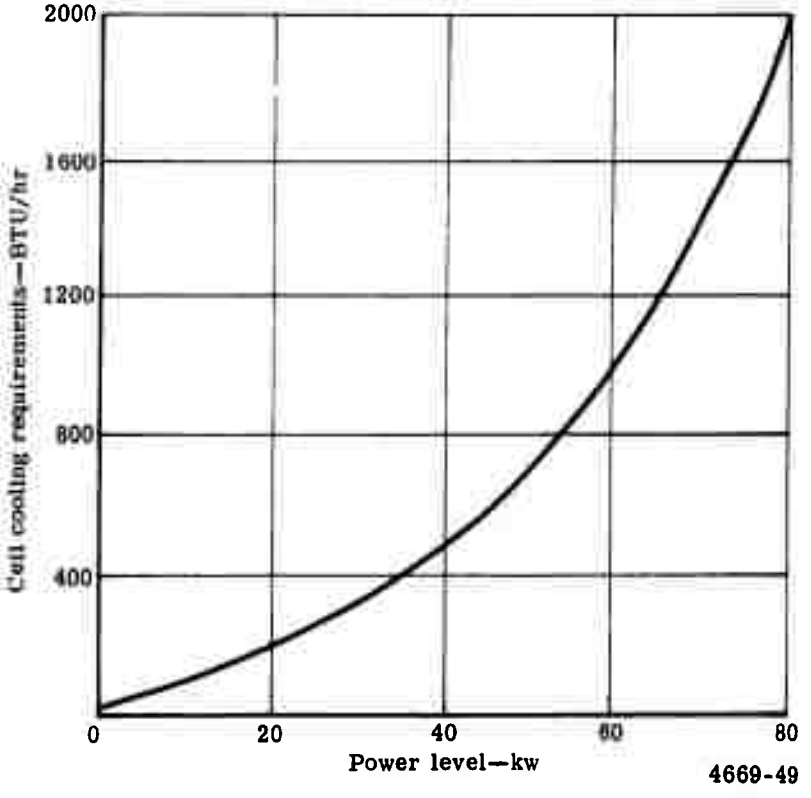

Figure 1-6. Heat load versus power for ERDL cells.

*The total heat available as a result of conversion of the total energy is determined from the heat of formation (ΔH_f) of LiCl at 1200°F, which is 92.214 kilocalorie/gm mole or 392 BTU/lb. This engine when fully charged will have 39 lb of Li, forming 240 lb of LiCl.

The cooling system, external to the module is comprised of the following components:

- Blower, motor, and filter
- Ducting
- Controls
- Chlorine tank heater

Cell cooling is necessary to remove waste heat during both the charge and discharge conditions of operation. It is assumed that depot equipment will provide cooling during charging. To provide cooling during discharge, the blower is on at all times and only as required for the standby mode. The air flow leaves the blower and enters a manifold for distribution to the individual modules. An air control damper is used to either direct the cooling air flow into the modules for cooling or through a cell bypass duct to the exit manifold.

After entering the exit manifold, the air is either dumped overboard or is passed through a controller to the Cl_2 tank heat exchanger to provide the heat necessary to maintain Cl_2 tank pressure. This air allows the heat of vaporization of the Cl_2 to be supplied with engine waste heat.

An integrated blower, motor, filter package is used, requiring a 1/3-hp motor to furnish approximately 300 cfm at 4 in. of H_2O.* This size will handle the cell heat rejection requirements for engine operation at 75 kw, removing approximately 126,000 BTU/hr for the 70-cell engine.

Air ducting is required to furnish air to the modules for cooling and for venting the hot exhaust air or diverting it to the Cl_2 tank heater as necessary. The ducting consists of inlet and exhaust manifolds with individual module inlet and outlet supply lines from the manifolds. The cooling air from the blower is carried by a 3-in. dia flexible hose similar to that used by an automotive defroster. The individual module lines consist of 1-in. dia hose.

The exhaust air ducting is designed to handle air at 700 to 800°F in metal pipe. The exhaust air ducting is 4 in. in dia for the manifold and 1.5 in. in dia per individual module lines. This ducting is larger than the inlet due to the increased temperature and the desire to keep air velocities below 100 ft/sec to minimize the pressure drop and the blower motor size.

Cooling air control requirements are relatively simple. During discharge operation, the blower operates continuously. Inlet butterfly valves on each module adjust the cooling air supply. These inlet valves are thermostatically controlled by a sensor in the module to maintain a reasonably constant cell temperature. A Cl_2 tank heater butterfly valve is controlled by the Cl_2 tank temperature to duct the hot exhaust air from the modules into the tank heater or to the atmosphere ahead of the heater as necessary. An additional control in the air ducting is required to duct the blower outlet to Cl_2 heater inlet for starting on cold days.

To obtain the desired Cl_2 inlet pressure, the tank temperature is maintained above the saturation temperature for the given pressure—5 atm requires a temperature of 51°F. Also during engine operation, heat is added to the Cl_2 tank to replace the heat of vaporization. Rather than use electric energy from the cells, which would decrease the overall

*The 4 in. of H_2O pressure was determined from a requirement for differential pressure in the module air lines and the external air supply and exhaust ducting.

engine efficiency, the waste heat of the engine is utilized. The Cl_2 tank heater, as conceived, is of the gas-to-liquid tube type installed inside on the bottom of the Cl_2 tank.

CHLORINE SYSTEM

The Cl_2 supplies gaseous Cl_2 to the lithium-chlorine cells on a demand basis, according to engine power requirements.

For the engine system under consideration, two cylindrical tanks (12 in. in dia, 29 in. long, and fabricated 0.100-in. thick stainless steel wall) are required to store liquid Cl_2. Tank protection features depend on the location on the vehicle, but heavy vehicle members (i.e., frame components) would be used to protect the tanks. In general, the design of the Cl_2 tankage is based on 125°F hot day conditions and sized for 5% excess Cl_2 and 25% excess volume. The design of these tanks is governed by the ASME Boiler and Pressure Vessel Code. An allowable stress of 14,450 psi has been used for the design. This is based on the value given in the Code for a seam welded stainless steel.

In addition to the Cl_2 actually required for power production, an extra 5% Cl_2 is provided to allow pressure to be maintained when the last of the required supply is withdrawn. Also, a minimum of 25% excess volume is provided in the tanks to prevent over-pressurization. This is similar to a requirement of the Interstate Commerce Commission for Cl_2 shipping containers.

The Cl_2 tank will not require insulation or standby electrical heaters. At -25°F (-4°C), which is the standard cold day for Army design, the vapor pressure of Cl_2 is greater than one atmosphere as shown in Figure 1-7. This ambient temperature provides sufficient Cl_2 pressure and flow to start the lithium-chlorine cells. After initiation of operation, the waste heat from the cells is ducted to the tank heaters to provide the necessary heat to raise tank temperature and pressure to normal operating level.

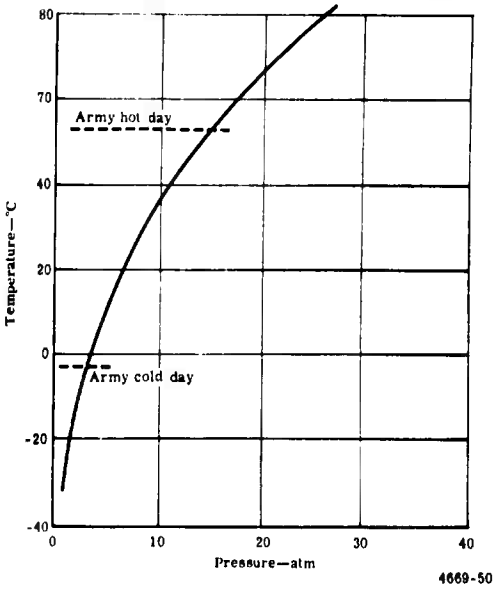

Figure 1-7. Vapor pressure of Cl_2.

The Cl_2 distribution control system regulates the flow of gaseous Cl_2 from the storage tank by means of an on-off valve. A quick disconnect coupling is also provided for tank removal. Chlorine then enters the manifold distribution system to each module. In each module line, a pressure regulator and on-off solenoid valve are necessary along with a quick disconnect coupling. The Cl_2 in this system is nominally at a cell pressure of 5 atm and is maintained by means of a pressure regulator. In the module, the Cl_2 is distributed to the individual cells. The cell system requires a 50% excess Cl_2 flow to maintain electrode performance. The excess flow is recirculated to the mainstream by a jet pump. Chlorine flow within the module was discussed previously.

Distribution piping consists of an inlet Cl_2 manifold with individual module inlet lines. The Cl_2 line from the manifold to the tanks requires a diameter of approximately 0.600 in. Individual module inlet lines are approximately 0.250 in. in dia. The module inlet connections utilize a power disconnect type valve with self-purging characteristics. All Cl_2 supply lines external to the module are fabricated of stainless steel for handling Cl_2 at a maximum temperature of about 125°F. Since this engine consists of replacement modules, a hot Cl_2 system for the charge cycle is not included on the engine. This will be provided at the charging depot.

Because Cl_2 is a hazardous gas, other storage concepts are being investigated to obtain maximum safety. Four methods are being considered. The first of these, which has been used in this design concept, is to store the Cl_2 as a liquid, protected mechanically from damage. On the basis of preliminary investigation, this method is the lightest and least expensive of the alternatives. Experimental studies are being planned to test the reliability of this method.

Three alternative storage systems that are being considered are:

- Storage as a chlorine-rich compound which could be decomposed when needed
- Storage as a gas absorbed on activated carbon
- Liquid storage surrounded by reactant (caustic)

The first possibility is to store Cl_2 as a chlorine-rich compound. This compound is then decomposed to supply the Cl_2 as it is needed. The feasibility of this method, especially with respect to the ability to separate the compound and recycle the Cl_2, has yet to be investigated.

The second alternative is to adsorb the Cl_2 on activated carbon. The gaseous Cl_2 is obtained by heating the carbon or possibly by evolving the gas by a low pressure. This method has an associated weight penalty because of the weight of carbon required to store a given amount of Cl_2. As the carbon is reused, it is probable that less Cl_2 can be adsorbed each time. The recycle efficiency and carbon activation lifetime have not been evaluated.

The third alternative, which is an extension of protected storage, considers Cl_2 stored as a liquid. In this system, the tank is surrounded with a caustic solution with which the Cl_2 would react in case of an unexpected leak. This technique requires a large weight of caustic and a very good design to ensure complete reaction of the Cl_2 and appears to be the least desirable of the alternatives.

The best method of storing Cl_2 for a given application must be determined after all of the schemes have been thoroughly investigated and system analysis completed. The liquid storage system is the one used for commercial transportation of Cl_2 at the present time.

Although millions of tons of liquid Cl_2 are safely transported yearly, the vehicle application represents a safety problem of new dimensions, and other schemes will have to be considered.

INTEGRAL CHLORINE STORAGE ALTERNATIVE

An alternative that was investigated utilizes separate Cl_2 storage vessels in each module. Figure 1-8 illustrates this alternate storage method. By placing the necessary Cl_2 supply on each module, the module becomes more nearly a complete system in itself. A module could be used singly or in any sized group more easily, providing valuable versatility.

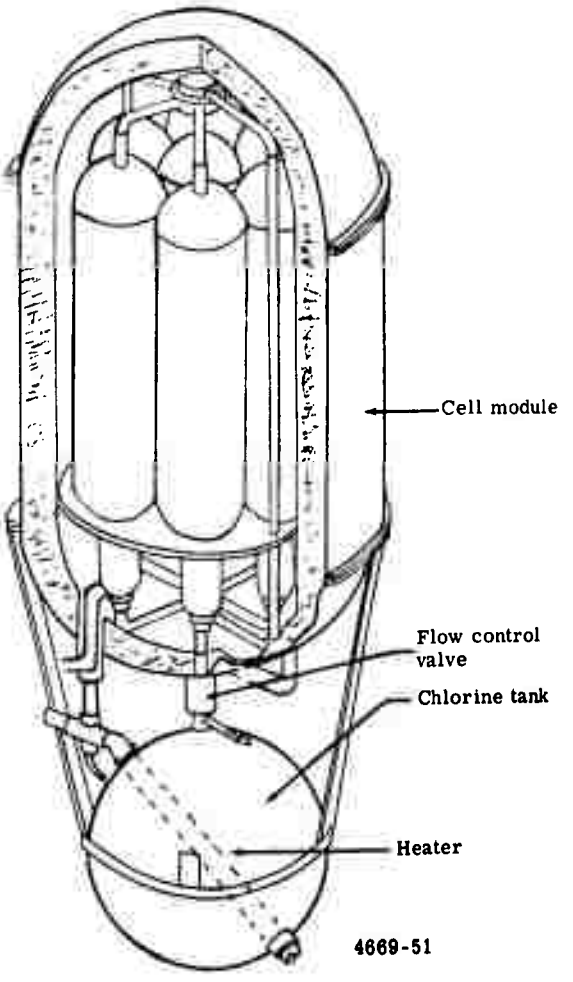

Figure 1-8. Integrated Cl_2 storage concept.

Preliminary weight and system studies have been completed for incorporation of the chlorine tank and system on each module rather than a single engine system. It is estimated that the discharged module weight would be increased by approximately 21 to 112 lb. The engine weight would have a net increase of approximately 72 lb for a total engine weight of 1318 lb.

The integrated chlorine system module would incorporate:

- A 10.5-in. dia spherical tank with heater and attachment brackets
- Chlorine pressure regulator, shut-off, and fill valves
- Chlorine piping
- Air piping with heater bypass valve

The engine cooling air supply and electrical systems would remain essentially unchanged.

ELECTRICAL SYSTEM

The electrical system consists of interconnecting copper leads and a terminal box. The leads provide the current for all external loads during discharge and are the current path during charge. The leads used are No. 19 wire stranded copper cable 0.470 in. in dia. The main electrical system consists of the necessary leads between modules and to the engine terminal box. The leads are housed in insulated conduits to decrease module heat leakage. Quick disconnects with low contactor resistance are provided at each module. The contact modules are also used to bypass disabled modules in case of component failure.

The internal wiring within the modules was designed with copper. Copper is normally considered to be the most practical conductor for electrical hookup; however, it oxidizes readily in air at high temperatures. Plated copper, copper alloys, and possibly hermetically sealed aluminum or liquid metal (sodium, potassium, or NaK) are alternatives to be investigated for interconnecting wiring within modules and in the high temperature zones external to the modules.

Contact and lead resistance plays an important role in the overall performance of the engine system. At least 20 contacts, or electrical connections, are required in the wiring circuit; most of these are at a temperature of 1000°F or higher. Twenty of these at 1000°F, having a resistance which is common in current contacts of 20 milliohms each, represent a voltage drop of 16 v at 400 amp from the nominal 200 v generated, or 8% of the electrochemical engine power would be lost in the contacts. Advances in technology* indicate that contact resistances of the order of 50 to 100 microhms are possible. The 100-microhm contacts were used in system design calculations for this system. For lead resistance, a total length of cable of 20 ft was assumed at 228 microhms/ft. The total resistance of leads and contacts was calculated at 6.56 milliohms.

INSTRUMENTATION AND CONTROL

General Description

The conceptual electrochemical engine previously described consists of ten 7-cell modules. The ten modules are connected in series electrically and are mechanically identical to each

*P. Karkan and E. J. Tuchy, "Hemispherical Contact Resistance Theory," IEEE Transactions on Power Apparatus and Systems, Vol. PAS-84, No. 12 (December 1965) pp. 1132 to 1143.

other. Each cell contains sufficient Li for one complete discharge cycle; the other reactant, Cl_2, is supplied under pressure to all modules in parallel. The Cl_2 lines for all seven cells within a module are in parallel. The plant is load-following—the electrical power demand directly regulates the Cl_2 flow (see Appendix 4). Module temperature is controlled at 1200°F to maintain the LiCl electrolyte in a molten state.

To minimize buildup of contamination at the Cl_2 electrode-electrolyte interface, prevent plugging of the Cl_2 electrode by electrolyte, and significantly increase the output of the cell, excess Cl_2 (nominally 50%) is passed through the cells. This excess Cl_2 is recycled from the cell outlets to the inlet manifold through a jet pump utilizing the makeup flow through the jet to educe the excess from the cell outlets. The manifolds are constructed so that the cells are electrically isolated from each other.

As previously noted, the powerplant is load-following. Chlorine flow varies directly with load from a constant pressure source. Variable pressure control can be employed if found necessary during testing programs.

Provision is made in the control scheme to permit operation at partial power if warranted by some malfunction within a cell or module which necessitates its isolation from the network. During operation, heat is removed to maintain cell temperatures at approximately 1200°F. During standby, heat must be added to the module to make up for the heat losses either by self-discharge of the cells or by other means—i.e., electrical resistance heating from the main bank or from the depot supply.

Chlorine Flow Control

The chlorine system, as previously described, consists of the liquid Cl_2 storage, piping, pressure reducing valves, solenoid operated shut-off valves, manual valves, and tank heater. Standby and low power is achieved at 15 psia at -25°F if heat is added to the tank to make up for the heat of vaporization. Chlorine pressure is maintained at the inlet valve to each module, while the flow is regulated by the load requirements. Instrumentation is provided to sense and control the module temperatures, sense and indicate the module state of charge, and annunciate the need for module isolation.

The lithium-chlorine electrochemical engine during discharge is a load-following, self-regulating type prime mover. It will supply power to the using components in magnitudes required by these components as long as the engine power capability is not exceeded. A simplified schematic diagram of the cell Cl_2 system is shown in Figure 1-9 to illustrate the operation of the system.

For the standby mode, approximately 0.6 lb/hr of Cl_2 will be used, requiring approximately 20 w of heat to maintain a temperature of -25°F at an ambient temperature of -25°F. Ambient air flow from the blower is used to supply the heat needed to vaporize the Cl_2. Module discharge is waste heat which is passed through coils in the Cl_2 storage tank to maintain the tank pressure at approximately 75 psia for power generation.

Figure 1-10 schematically illustrates the Cl_2 control valves for the conceptual engine. Pressure regulating valves PRV-1 and PRV-2 are used to regulate the Cl_2 heater pressure for power generation and standby conditions, respectively (5 atm for PRV-1 and 1 atm for PRV-2). In the standby mode, solenoid valve S-1 is closed and valve S-2 is open providing Cl_2 pressure at 15 psia to the module Cl_2 valves (S-3 X).

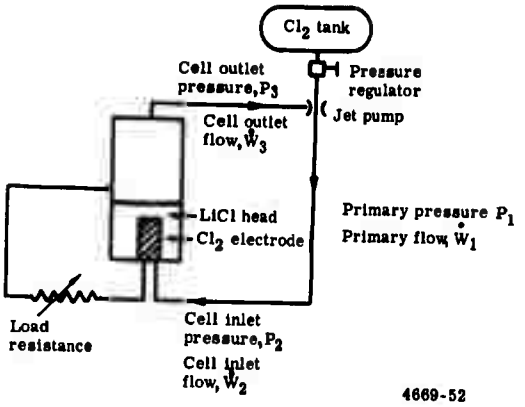

Figure 1-9. Chlorine system schematic.

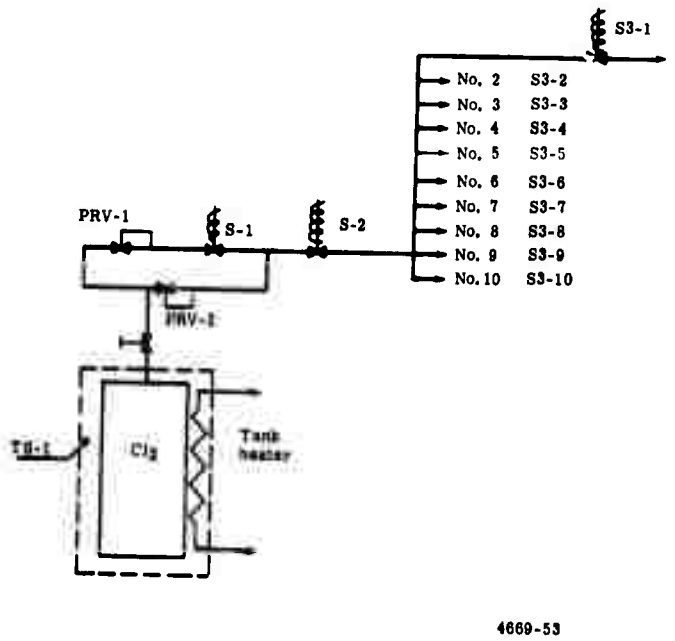

Figure 1-10. Chlorine control system discharge mode.

In a power generation mode, solenoid valves S-1, S-2, and all module Cl_2 valves are open, except for any module Cl_2 valve which has been closed by the module isolation control. This provides Cl_2 gas at design operating pressure, less line losses, to the cells for consumption as demanded by the load.

A combination pressure gage and pressure switch is provided for periodically checking the settings of the regulating valves and tripping valve S-2 shut. This is required in the event of a regulating valve failure which could expose the modules to unsafe pressures.

Module Failure and Isolation

Preliminary analysis of the various abnormalities that could result during cell operation would manifest themselves as an open circuit, a reduction in voltage output, or a change in temperature. These conditions can be easily detected by a complete loss of power to the load, voltmeter indications, and thermocouple indications.

Cell voltage will vary with power level; however, individual cell voltages, or module voltages, within a cell stack will all vary similarly. Therefore, comparing voltages of two, or three cells or groups of cells with each other, will pinpoint an abnormally operating cell because its output voltage will be lower than those with which it is compared. Electronic comparator circuits of this type are very common.

An open circuit condition would probably be due to some wiring or cable failure external to the individual cells. The cell power level control could function to transfer the power pack to the standby mode of power generation for an open circuit condition.

As a result of cell or module malfunction, it would be desirable to isolate one or more of the modules from the rest of the engine. The minimum perturbation to the plant would result if Cl_2 could be shut off from only the module being isolated and its electrical terminals could be shorted together. Shutting off the Cl_2 to the module is necessary to prevent the further generation of power in the cell and waste of fuel. This could be easily accomplished by closing the Cl_2 feed valve. Electrically bypassing a module is somewhat more difficult.

Opening the leads to the module would, of course, break the power circuit. Electrical shorting of the terminals provides electrical isolation of the cell. If the cell were allowed to continue to conduct without generating power, it would add significantly to the electrical load on the cell stack and the cell could overheat due to high I^2R heating. In addition, lithium would be plated on the Cl_2 electrode which would form Li_2C_2 and destroy the Cl_2 electrode.

A concept of an electrical connector device to electrically brake the module connector, and, at the same time, short the cable to complete the circuit for reduced power operation is shown in Figure 1-11. In normal operation, the primary contacts are spring-loaded to minimize contact resistance. On demand, the explosive charge in the shunt support bolt is fired, causing the shunt to be driven against the cable connector and causing the cable contacts to be driven away (breaking the circuit) from the module contacts.

The specific design of a connector may vary considerably from that shown schematically in Figure 54. Relatively larger contact areas incorporating a sliding arrangement, together with a special plating of the contacts and provision for lubricating the surfaces may be required. To prevent oxidation of the contacts, especially at the high operating temperatures, special lead materials may be required.

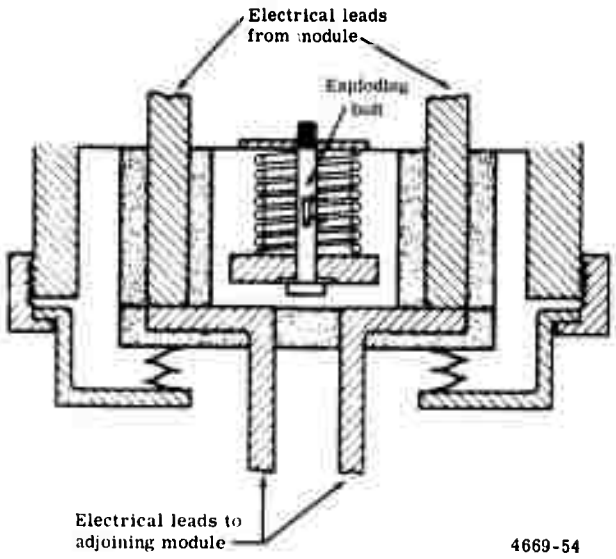

Figure 1-11. Module electrical disconnect.

Figure 1-12 shows ten 7-cell modules wired in series. An alternative concept is shown in Figure 1-13. Figure 1-12 is identical to Figure 1-13 except that jumpers are shown external to the modules which may be either manually or automatically closed to electrically isolate a module. (When closing the contacts, the chlorine valve to the module, which is isolated, would also be closed.)

Start-up

Start-up from a frozen condition requires an external source of electrical energy for resistance heaters. System heating to 1200°F will be done electrically at a rate consistent with the allowable heating rate limitations of the cells and power available. It is necessary to design a cell heating capability into the module which is not incorporated into the existing design if this capability is required.

Standby

Standby mode of operation consists of maintaining the cells at operating temperature and corresponds to the no-load condition for the powerplant. Heat will be needed at the no-load condition to make up for the thermal losses from the individual modules. This heat is either supplied by chemical reaction of dissolved Li and Cl_2 in LiCl or by individual electrical resistance heaters in each module powered from external power sources. The preferred system will probably be a combination of the two systems.

Power Generation

The power generation condition covers only that portion of the plant operation where electrical power is delivered to the external load. Since the Cl_2 flow is a function only of the electrical demand, maintaining a constant Cl_2 pressure at the Cl_2 electrode would provide the system control required.

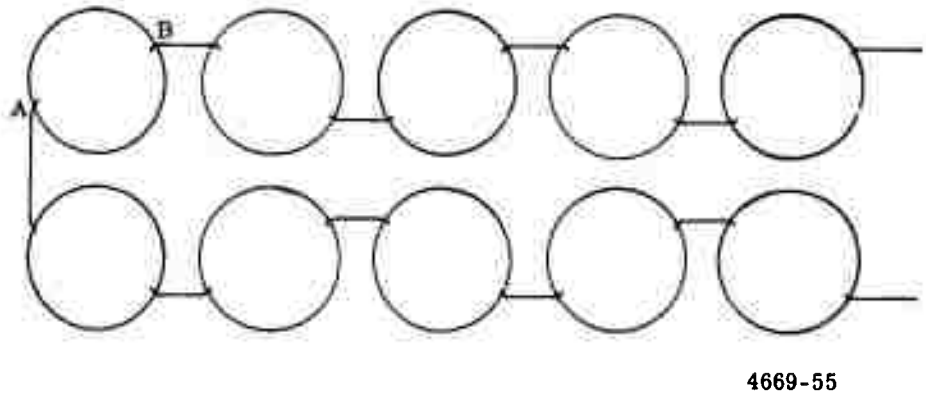

Figure 1-12. Ten module engine—series wired.

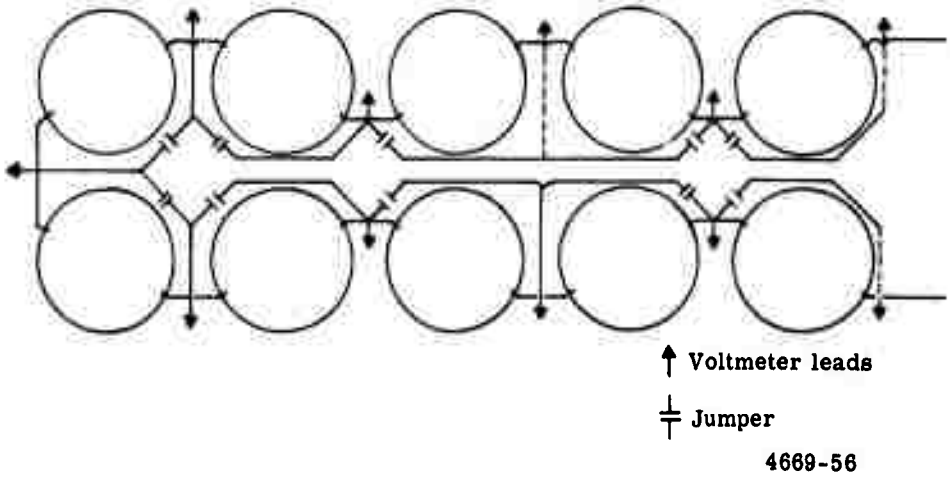

Figure 1-13. Ten module engine with module isolation connectors.

As indicated previously, cell operation is improved with approximately 50% excess Cl_2 flow over that required to follow the load. The excess Cl_2 bubbles through the electrolyte to the cell gas space. By tapping this gas space and recycling the Cl_2 gas directly to the cell inlet, this excess flow is maintained through the cell without cooling and with no increase of flow from the Cl_2 supply. In the system, this is accomplished on a modular (7 cell) basis by manifolding the outlets of all seven cells to the vacuum inlet of an eductor, or jet pump.

Ideally, each of the ten modules in the powerplant will deliver 10% of the electrical load, have the same heat losses, and use the same quantity of Cl_2.

Deviations from this ideal condition assumed the following.

- Modules are individually temperature controlled
- State of charge indications were incorporated on each module in the concept
- Voltage detectors are utilized on a per-module basis
- Actuators were incorporated to effectively isolate a module in the event of a detectable malfunction in the individual module (These actuators shut off the Cl_2 valve to the module and electrically shunt the load current around the module.)

Depending on the particular application in which the powerplant is used, the heat generated may be 15 to 30% of the total power generated. This heat will be used to the maximum extent possible within the plant for Cl_2 vaporization, cab heating, etc, and only the excess will be dumped overboard. In any event, cooling of the modules is required. Since the modules may not be perfectly matched so that each contributes 10% of the total heat, a modular air cooling system is provided, as described in an earlier section. This system consists of a blower, piping manifold, and temperature controlled inlet and outlet air valves. The air valves of any module are opened when the individual module temperature reaches its high temperature limit. Conversely, all valves are closed when the respective modules are below their upper temperatures.

Shutdown

The normal shutdown operation will be, in reality, a transfer to the standby mode previously discussed. To minimize the required energy and time for start-up, all cells should be recharged prior to a complete shutdown where the cells are permitted to cool. After charging, all manual Cl_2 valves would be closed and sealed (to prevent inadvertent opening) and all external cabling removed from the modules to minimize heat losses. If power actuated connectors are used, these could be energized from an external source.

Charging

The modules will be recharged from depot power. Power controlling devices will be incorporated in the charging units. Instrumentation will be active to indicate the state of charge and to control the module temperatures below their temperature limits. (Cell design should preclude overcharging any of the cells during charge of the plant.) Instrumentation will actuate alarms if the heat generated during recharging exceeds the capability of the cooling system. This might be the case when some of the cells reach their full-charge state because of the heat of reaction of the dissociated reactants.

The open circuit voltage for an individual lithium-chlorine cell is approximately 3.5 v; a 7-cell stack has an open circuit voltage of approximately 24.5 v. To recharge a module at a 160 amp rate (~6-hr charge) approximately 27 to 28 v will be required (approximately 4.5 kw/module).

APPENDIX 2

HORIZONTAL CELL SYSTEM

INTRODUCTION

An alternative engine system was investigated incorporating a horizontal cell design. The general system concept is shown in Figure 2-1. It is similar in most respects to the previously described vertical cell system concept. The major variation is the use of a horizontal cell design in the seven-cell module. This revision causes dimensional changes in module design and power section packaging.

This engine system was also designed for the ERDL duty cycle shown in Figure 23. Rated power is 50 kw with a 75 kw capability. Stored energy is sufficient to deliver 200 kw-hr over the ERDL duty cycle. Operating modes and system description are the same as those presented for the vertical cell system.

The horizontal cell is adapted from the type cell currently undergoing research testing by Allison. The most recent of the laboratory horizontal cells is the Mark IV cell shown in Figure 2-2. This cell, employing horizontal electrodes, is designed to supply data for pressures up to 20 atm. It is approximately 10 in. in dia and 18 in. high. The dry weight of the cell is 85 lb, while the weight of the fully charged cell is 100 lb.

This laboratory type cell requires redesign for a practical system. Using the Mark IV cell design concept, an extrapolated design was developed for a practical engine system. This advanced design concept is referred to as the extrapolated Mark IV cell. Figure 2-3 is a representation of the cell.

During discharge operation, chlorine is supplied to the electrode surface through the carbon electrode. The Cl_2 gas diffuses through the portion of the electrode that is porous carbon and reaches the electrolyte interface. However, the LiCl does not wet carbon well and cannot wet through the pores of the carbon and into the Cl_2 plenum chamber within the electrode. A Cl_2 flow rate larger than the actual requirement is used to promote the transport of Cl_2 gas bubbles from the pore openings in the electrolyte region to the surrounding electrode surface where the Cl_2 ions must be formed. The electrical performance was highly dependent on the excess Cl_2 flow rate. The excess gas makes its way up through the vertical holes in the electrode to the cavity above the electrode. A porous carbon splash plate is provided which removes any LiCl which might cling to the Cl_2 gas bubbles before they reach the exit tube.

Lithium covers a porous metal screen which is the top of the Li reservoir. Lithium chloride is 3.2 times as dense as Li and, if the Li were to break free from the screen, it would float up to the carbon portion of the Cl_2 electrode. It is held to the screen because of the preferential wetting of the screen by Li rather than the LiCl. The Li below the screen is kept in contact with the screen by the buoyant force imposed by a layer of LiCl at the bottom of the cell. As the Li is consumed as the cell discharges, a portion of the LiCl which is formed is allowed to fill the otherwise evacuated space below the Li. However, 1.00 volume of Li yields 1.93 volumes of LiCl. The additional storage volume for LiCl is the cavity provided above the Cl_2 electrode. The LiCl will be forced up through the same holes utilized to remove the excess Cl_2 gas from the interelectrode zone.

The walls of both the Li storage cavity and the surplus LiCl cavity are to be type SS 316. Since the upper compartment walls will be exposed to Cl_2 during part of the cycle, they must be protected by a coating. A ceramic coating applied by flame spraying, plasma spraying, or vapor deposition was tentatively selected, similar to the vertical cell design.

BLANK PAGE

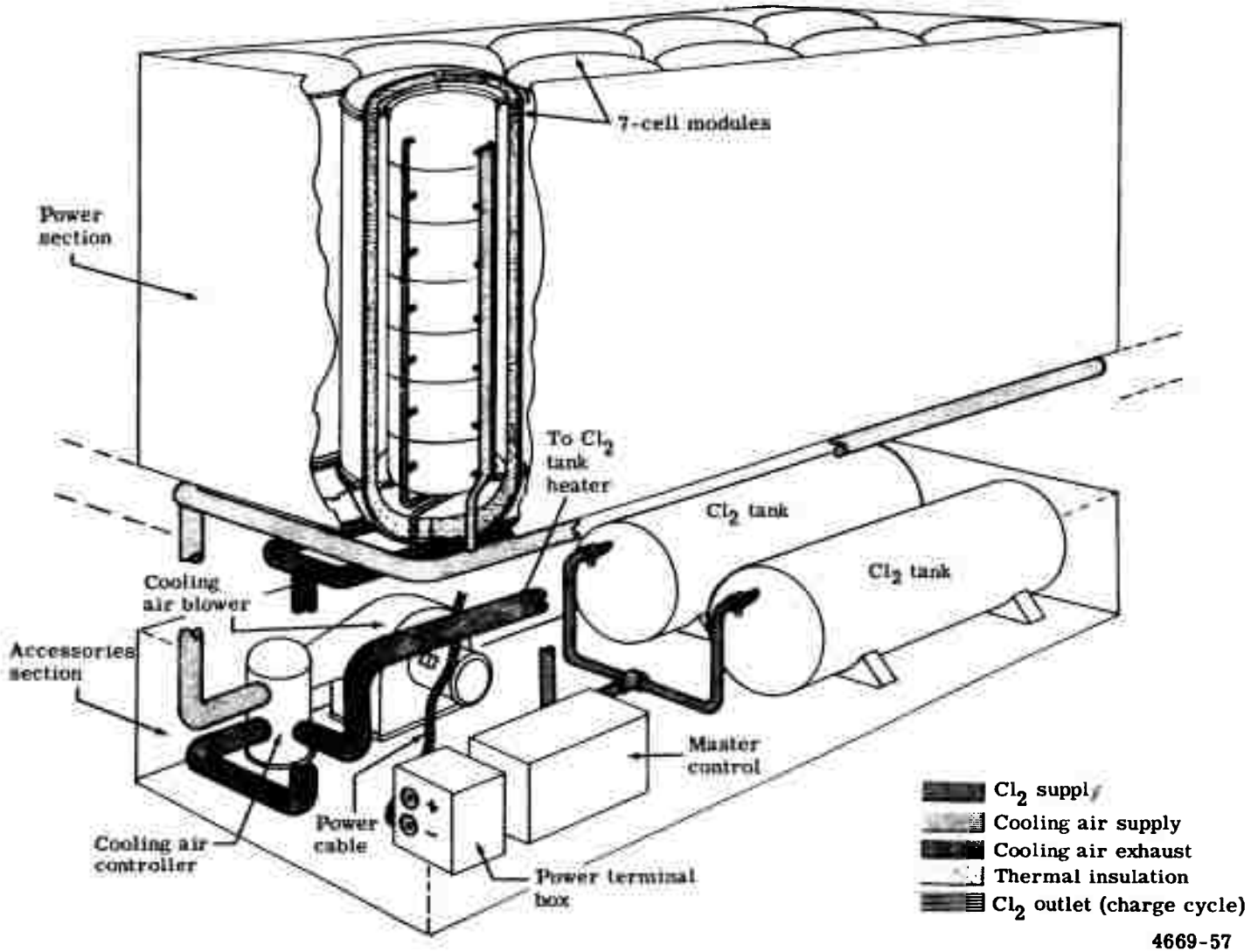

Figure 2-1. Horizontal cell system design (extrapolated Mark IV cell design).

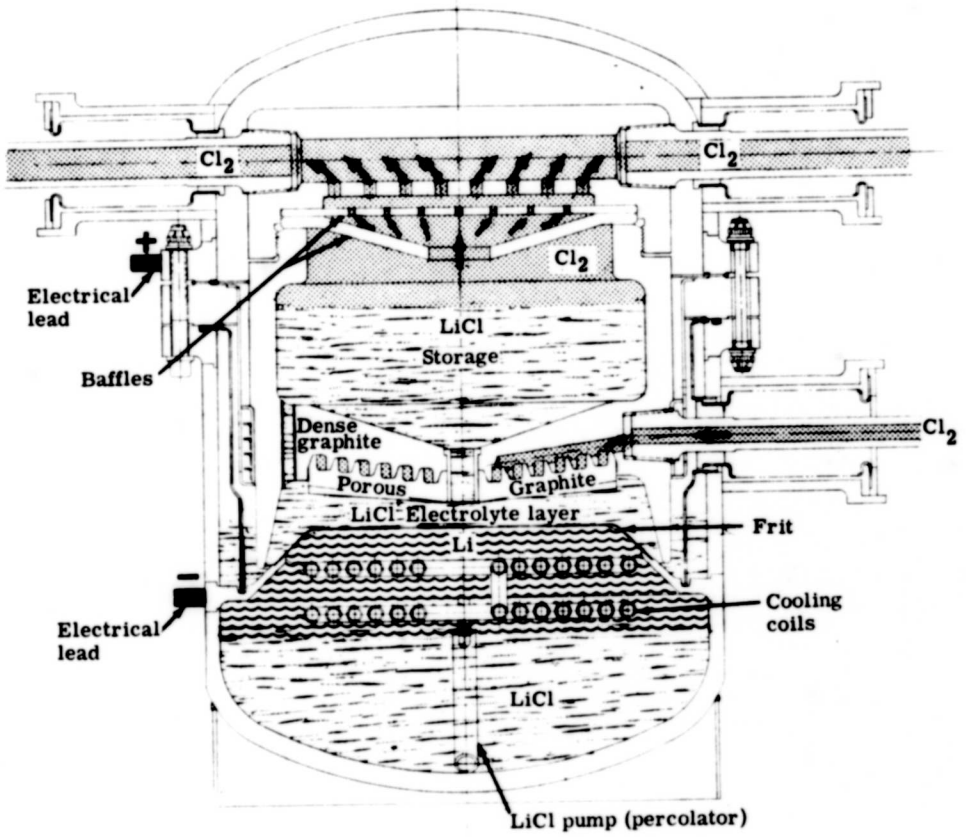

Figure 2-2. Laboratory Mark IV cell design.

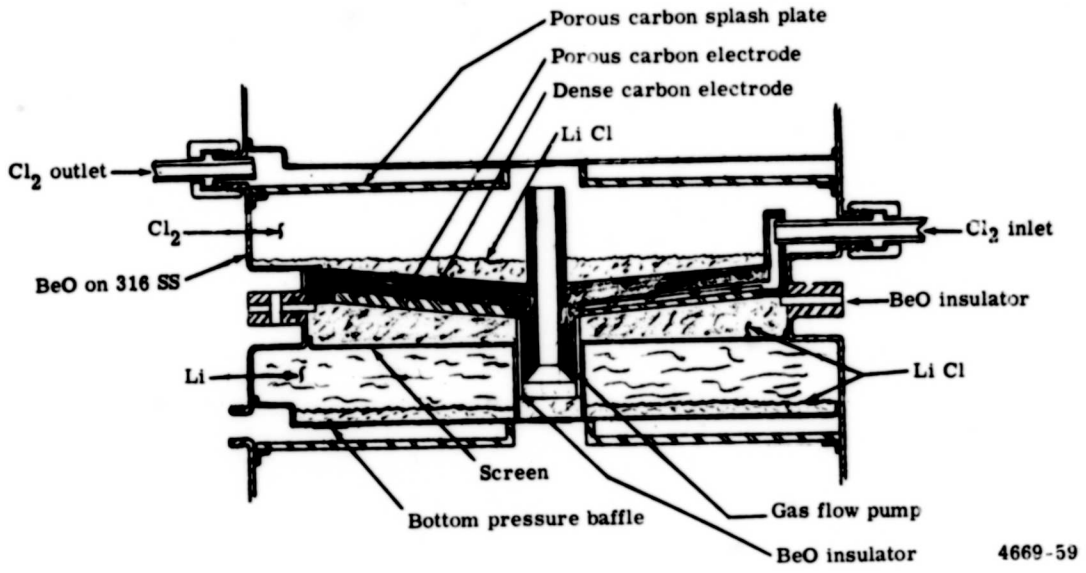

Figure 2-3. Extrapolated Mark IV cell.

Electrical separation of the electrodes is accomplished with a beryllia ring. This ring, however, requires development effort. Sealing at this split line is accomplished by compressing two type SS 316 O-rings. The Cl_2 inlet and exit tubes are alumina to prevent shorting the cells through the Cl_2 manifold. Compressed O-ring seals are also utilized. The higher strength alumina may be used at this location instead of beryllia because no LiCl will be present.

During the charge cycle, the Cl_2 that is generated on the carbon electrode will make its way to the exit tube in the same manner as the excess Cl_2 did. However, difficulties are incurred at the Li electrode, the Li is generated on top of the screen and wetting is not now sufficient to prevent the Li from escaping and reaching the other electrode. To suck the Li below the screen, a favorable differential pressure must be applied. A percolator has been invented by Allison to do this. Chlorine is generated at the bottom of a dense graphite tube connected to the Cl_2 electrode. As the gas is collected and rises through the tube, it will trap LiCl taken from beneath the Li screen and raise it above the upper LiCl level. This action will impress a pressure gradient across the screen which will pull the Li below it.

The cell was also designed to facilitate stacking. The top of one cell becomes the bottom of the succeeding cell. The cell wall from one cell to the next is continuous, providing the desired series electrical connection.

SELECTION OF CELL DESIGN AND OPERATING POINTS

To determine optimum cell design and performance, the horizontal cell concept was mathematically modeled and a program written for computer analysis. The investigation carried out was similar to that described in Appendix 3 for the vertical cell. Figures 2-4 and 2-5 are representative of the analytical curves derived from this model.

Weight variations for a 50-kw, 200-kw-hr system with changes in numbers of cells and modules were analyzed for several module designs. Figure 2-4 shows how variations in numbers of cells and modules affects weight. This illustration indicates that a minimum number of cells and modules should be used. To meet the nominal voltage requirement of 200 v for the system, however, a lower limit to the number of cells exists. With a single cell voltage of a little less than 3.0 v at the 50-kw power step of the duty cycle, approximately 70 cells are required to obtain a 200-v system.

Three criteria must be considered in selecting the number of modules.

- The number of modules should be kept as low as possible, as shown in Figure 2-4.
- The module weight should be kept below 100 lb.
- The height of the module should not exceed 36 in.

To investigate the height criteria, a model for the cell was programmed which showed the effect of placing a height restriction on the individual cell. Figure 2-5 shows the effect of cell height on weight.

As a result of cell and system analysis, a design point was selected for the horizontal cell system. The system was designed with the following parameters:

- Cell pressure—5 atm
- 50% excess Cl_2 flow
- Cell discharge efficiency (ERDL duty cycle)—81.8%

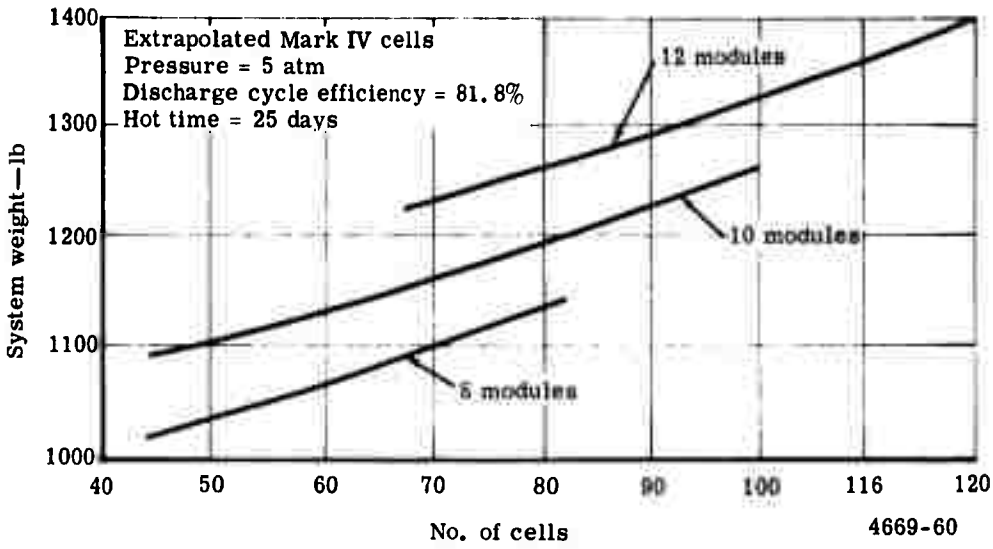

Figure 2-4. System weight versus number of cells.

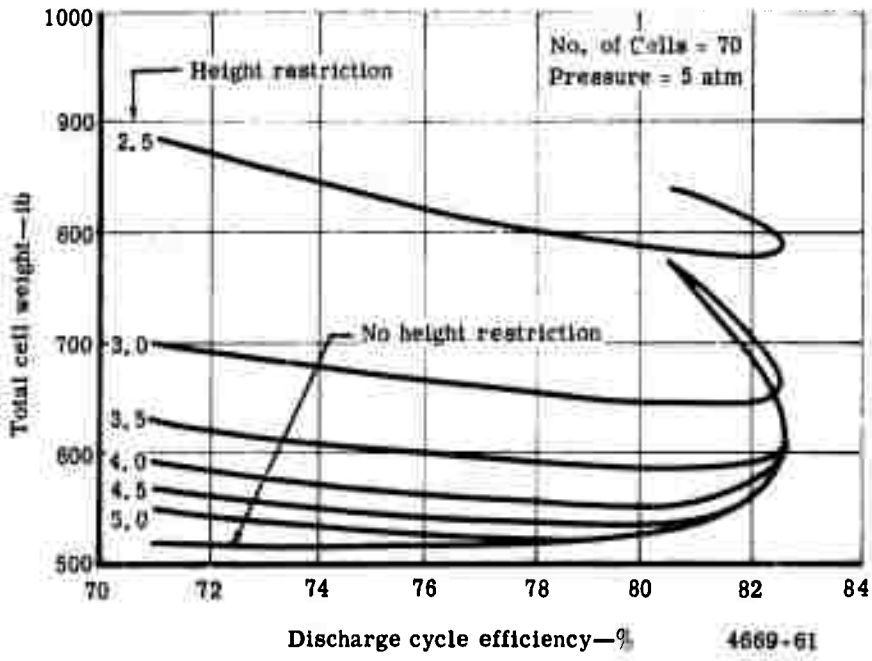

Figure 2-5. Extrapolated Mark IV cell weight versus height restriction.

- Electrode area—8750 cm^2
- Number of cells—70
- Number of modules—10
- Cell height—3.5 in.
- Cell diameter—7.3 in.

PERFORMANCE ANALYSIS

The conceptual engine design, using the horizontal cell which resulted from the foregoing analysis, allowed a performance analysis to be conducted. Comparisons were then made with the vertical cell system.

Weight and Volume Data

Engine weight and volume analysis was conducted on the conceptual system shown in Figure 2-1. Module weight was estimated to be approximately 98 lb in the discharged condition. The remainder of the engine system apart from the Cl_2 tanks and modules is truck mounted. The total weight of the system was estimated to be 1389 lb. A weight breakdown of the major components is:

	Weight (lb)
Modules	979
Cooling system	45
Chlorine system	139
Electrical system	141
Total	1304

The power section of this engine will require a space measuring 60 in. wide, 24 in. deep, and 36 in. high plus an additional clearance height under this section of 6 in. for plumbing. The accessories section, including the Cl_2 tanks, if integrated into a single package with the power section, will require an additional 12-in. height if placed under the power section, or an additional 12 in. in depth if placed to the rear. However, in all probability the accessories will be located as space is available in any particular vehicle installation.

Energy Balance

Using the ERDL duty cycle, an energy balance for discharge was calculated. This energy balance is presented in Table 2-I. Net cell discharge efficiency using an integrated net efficiency over the duty cycle is 78.8%. To establish the system performance, the following characteristics were used:

- Electrolyte thickness
  - Actual 0.75 cm
  - Performance 1.00 cm
- Auxiliary power 0.55 kw
- External electrical lead resistance 0.0114 ohm
- Electrical contactor resistance 0.0022 ohm

Table 2-I.

Energy balance.

Discharge	Integrated ERDL 8-hr duty cycle
LiCl formed	251 lb
Energy available (free energy of LiCl)	254 kw-hr
Heat of formation	288.5 kw-hr
Gross energy out of engine	204.4 kw-hr
Net energy out of engine	200.0 kw-hr
Energy to T Δ S	34.5 kw-hr
Cell efficiency, gross	80.4%
Cell efficiency, net	78.8% (discharge)
Energy lost to inefficiency and auxiliaries	54.0 kw-hr
Summary	
Total energy lost	88.5 kw-hr
Total energy to external circuit	200.0 kw-hr
Grand total	288.5 kw-hr
Heat of formation	288.5 kw-hr
Chlorine heat requirements	
Vaporize Cl_2 at 5 atm	6.90 kw-hr
Heat Cl_2 50 to 1200°F	7.95 kw-hr
Heat lost through insulation	6.39 kw-hr
Total heat consumed	21.24 kw-hr
Electrical energy to auxiliaries	4.4 kw-hr
Net heat rejected	62.86 kw-hr
Auxiliaries	
Electrical requirement	
Blower	250 w
Control and instrumentation	300 w

APPENDIX 3

LITHIUM-CHLORINE SYSTEM PERFORMANCE ANALYSIS AND TRADE-OFF STUDIES

INTRODUCTION

Having arrived at a conceptual engine system, sizing of components for the ERDL application was required. Each component of the system should be selected and sized based on optimization of the entire system. System optimization effort was based on engine weight being of primary importance, and preliminary analysis indicated that the individual cells would comprise approximately one-half the total system weight. Thus, the weight optimization of the cells was initially approached to meet the ERDL requirements. It is planned in the future to develop a total electrochemical engine system optimization capability. System optimization will be conducted in future programs for those concepts investigated and found attractive for further development by ERDL.

PERFORMANCE ANALYSIS

An analysis was made of the expected performance of the conceptual electrochemical engine using the "D-type" cell. The lithium-chlorine electrochemical power system is a storage system for electrical energy, and the electrical performance of the cells is of great importance in the system analysis.

The electrical performance of an electrochemical cell is dependent on the reactants and electrolyte, cell temperature and pressure, and current density. Figure 3-1 shows a typical cell voltage versus current density characteristic. This characteristic exhibits four distinct phenomena: an open-circuit voltage, activation polarization, ohmic polarization, and concentration polarization.

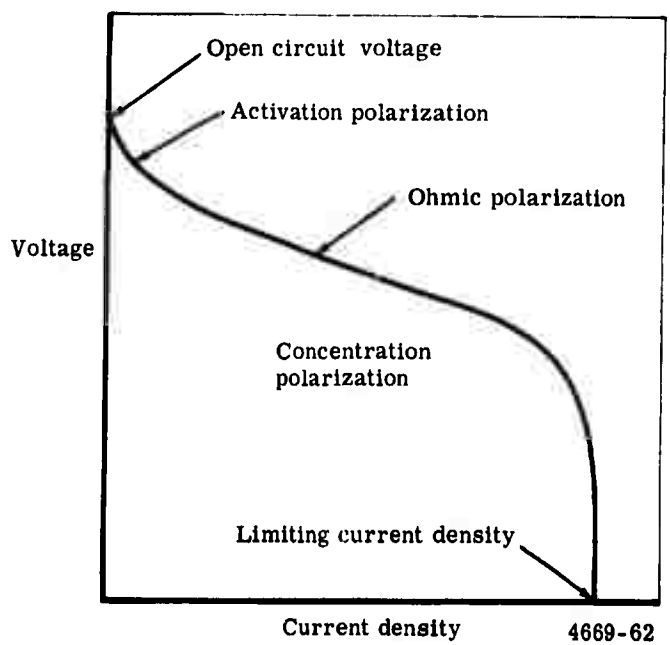

Figure 3-1. Typical voltage-current density characteristics.

The open circuit voltage is dependent on the reactants, electrolyte, temperature, and pressure. At 1.0 atm, the open circuit voltage is

$$V_{oc} = \Delta G/nF \tag{1}$$

where

ΔG = Gibbs' free energy change of the reactants, joule/gm mol
n = oxidation number, equivalents/gm mol
F = Faraday constant, coulomb/equivalent

For a given chemical couple, the free energy change is a function of temperature and pressure. The open circuit voltage of the lithium-chlorine couple, if the temperature is assumed constant at 650°C, is

$$V_{oc} = 3.4669 + (RT/nF) \ln (P)_{atm}$$
$$= 3.4669 + 0.03975 \ln P \tag{2}$$

where

V_{oc} = open circuit voltage at 1.0 atm, v
R = gas constant, 8.314 joules/gm mol-°K
T = temperature, 923°K
n = no. of equivalents/mol of the gaseous reactant Cl_2, 2 equivalents/gm mol
F = Faraday constant, 96,500 coulombs/equivalent
P = pressure, atm absolute
3.4669 = the increase in V_{oc} attributable to an increase in pressure above 1 atm

The activation polarization is due to various irreversible effects at the electrodes. It is believed to represent the "motive force" that must be applied to the atoms to make them overcome an energy barrier in becoming solvated ions. A complete understanding of the mechanics of this polarization phenomenon is not available, but data which was obtained in the laboratory correlates well with the expression

$$i = i_o \left\{ \exp\left[\frac{(1-\beta)\eta_A}{RT/nF}\right] - \exp\left[\frac{-\beta\eta_A}{RT/nF}\right] \right\} \tag{3}$$

or, when algebraically reduced, to

$$\eta_A = 0.0795 \ln \left[(5/3)\, i + \sqrt{(25/9)\, i^2 + 1} \right] \tag{4}$$

where

i = current density, amp/cm^2
i_o = constant exchange current density, ≈ 0.3 amp/cm^2
β = constant, ≈ 0.5
η_A = activation polarization, v

The ohmic polarization is the voltage loss attributable to electrical resistance. For the electrolyte alone, the resistance is

$$R = \rho t/A \tag{5}$$

where

ρ = electrical resistivity of the electrolyte, ohm-cm
t = electrolyte thickness, cm
A = cell electrode surface area, cm^2

The electrical conductivity, K, of pure LiCl is given as a function of temperature by*

$$K = 0.5282 + 1.125 \times 10^{-2}\ T - 4.554 \times 10^{-6}\ T^2 \quad (6)$$

At 650°C, the electrical resistivity of the LiCl is

$$\rho = 1/K = 0.16902 \text{ ohm - cm} \approx 0.17 \text{ ohm - cm} \quad (7)$$

Other internal resistances (i.e., as in the electrodes or a gas separator) may be treated in the electrical analysis by obtaining an equivalent thickness of electrolyte, t_e.

One possible limitation to the validity of this analysis is the use of the resistivity of pure LiCl. The electrolyte in the cell will have lithium in solution, and ionic concentration gradients will exist at the electrode interfaces. The effect that these factors will have on the resistivity is still undetermined. In addition, the presence of Cl_2 gas bubbles in the electrolyte will raise the resistivity according to the Bruggeman equation for dispersions of nonconducting occlusions.

$$\rho_x = \rho_o\ (1-f_x)^{-3/2} \quad (8)$$

where

ρ_x = local effect resistivity of a dispersion, ohm-cm
ρ_o = gas free resistivity, ohm-cm
f_x = void fraction of occlusion

However, studies of the void fraction which occurs were not made. Temporarily, the resistivity of the pure electrolyte has been used.

The concentration polarization is due to concentration gradients which are established within the cell. The primary source of this in the lithium-chlorine cell occurs at the gaseous-porous carbon electrode. Again, laboratory studies have formulated the expression

$$\eta_c = (RT/nF) \ln i_L/(i_L-i) \quad (9)$$

where

η_c = concentration polarization, v
i_L = limiting current density, amp/cm^2
i = current density, amp/cm^2

With an (RT/nF) value of 0.03975, Equation 9 becomes

$$\eta_c = 0.03975 \ln i_L/(i_L-i) \quad (10)$$

---

*Van Artsdalen and Yaffe, Journal of Physical Chemistry, Vol 59 (1955), pp. 118 to 127.

The limiting current density is the maximum current density that can be obtained because some diffusion limited processes are occurring. In this case, the combination of flow of the Cl_2 gas through the porous carbon electrode and diffusion of the Cl_2 in the electrolyte determines the limiting current density. In addition, it is a function of pressure and specific properties of carbon (i.e., porosity and pore size distribution) and to some extent by electrode geometry and excess Cl_2 flow.

Therefore, during discharge operation, the terminal voltage is

$$V = V_{oc} - \eta_A - \eta_c - i\rho t_e \tag{11}$$

On the charge cycle, these polarizations must be added to the open circuit voltage rather than subtracted from it. Except for the concentration polarization, this phenomenon does not occur during charge, but is

$$V = V_{oc} + \eta_A + i\rho t_e \tag{12}$$

This does not mean that charging can be accomplished at an unlimited rate. A phenomenon known as the anode effect will occur which will limit the charging current. Preliminary investigations of the anode effect have led to a restriction of 20 amp/cm^2 as the maximum charge current density to be used.

The voltage efficiency for discharge may be defined as

$$\eta_v = V/V_{oc} \tag{13}$$

and for charge as

$$\eta_v = V_{oc}/V \tag{14}$$

This represents the ratio of energy obtained to the ideal free energy available, assuming a current efficiency of 100%.

However, the current efficiency is not 100%. Because Li has a natural solubility in LiCl, a loss of energy storage occurs as long as Cl_2 is supplied at the one electrode. This may be represented by a loss current proportional to the area and inversely proportional to the electrolyte thickness. In terms of a loss current density, this is

$$i_c = K/t$$

where

K = constant obtained from laboratory data, amp/cm
t = electrolyte thickness, cm

A value 0.05 for K was used in the following studies. However, this value may be changed when more data become available. The current efficiency is

$$\eta_i = i/(i + i_c) \tag{15}$$

The overall efficiency is the product of the voltage efficiency and the current efficiency ($\eta = \eta_v \eta_i$).

The expressions which have been presented here are being used to predict the performance of the lithium-chlorine cell. Many of them were based on laboratory data taken primarily at 1.0 atm pressure and extrapolated for higher pressures. As additional information becomes available, the expressions may be altered.

CELL TRADE-OFF STUDIES

The cell concept, described previously in Appendix 1, was developed into a computer program to allow optimization of the design using the foregoing analytical methods. The mathematical model for the cell is basically straightforward using the following independent parameters:

- Cell electrode area
- Lithium volume storage requirement
- Pressure
- Electrolyte thickness
- Reactant storage zone dia

The first two parameters were used to establish the interior dimensions in the cell. The pressure determines the necessary wall thicknesses. The electrolyte thickness has a minor effect on cell weight and volume, but it is an important variable in cell electrical performance.

The vertical "D" cell consists of two zones that may be almost independently sized—the power production zone and the reactant storage zone, as shown in Figure 3-2. The power production zone is the lower portion of the cell which includes the electrode. For a given electrode area and current density, the internal voltage loss is reduced as the electrode diameter is increased, but the electrode weight is increased. Consequently, a trade-off between the voltage loss and weight exists. For cells having electrode areas and current densities in the area of interest, it was found that a reasonable selection for the electrode diameter is 1.125 in. With this diameter set, the required electrode area is obtained by simply calculating the proper length.

The heights in the storage zone are functions of the required Li storage and the diameter of the storage chamber. The wall thickness is determined from the cell diameter and cell pressure, using an allowable stress of 5500 psi for type SS 316 at 1200°F. This corresponds to a safety factor of 2 over the rupture stress of type SS 316 for 25,000 hr at 1200°F. A minimum wall thickness, regardless of stress requirements, of 0.025 in. was selected to permit ease of fabrication and to minimize possible damage in handling.

The electrolyte thickness will have only a minor effect on the cell weight. In the present designs, an electrolyte thickness of 0.75 cm is used. In performance calculations, an equivalent electrolyte thickness of 1.00 cm was used. This is to allow for the resistance of the screen separator and for tolerances in assembly. The reasons for selection of 0.75 cm actual thickness are as follows.

- Reducing the electrolyte thickness to a minimum reduces the internal voltage loss, thereby improving the power density and efficiency.
- The 0.75 cm thickness is currently considered to be the minimum spacing that can be achieved because of physical design problems.

The weight of the cell was shown to be a function of the diameter of the reactant storage zone in addition to the other independent parameters noted. As an example, Figure 3-3

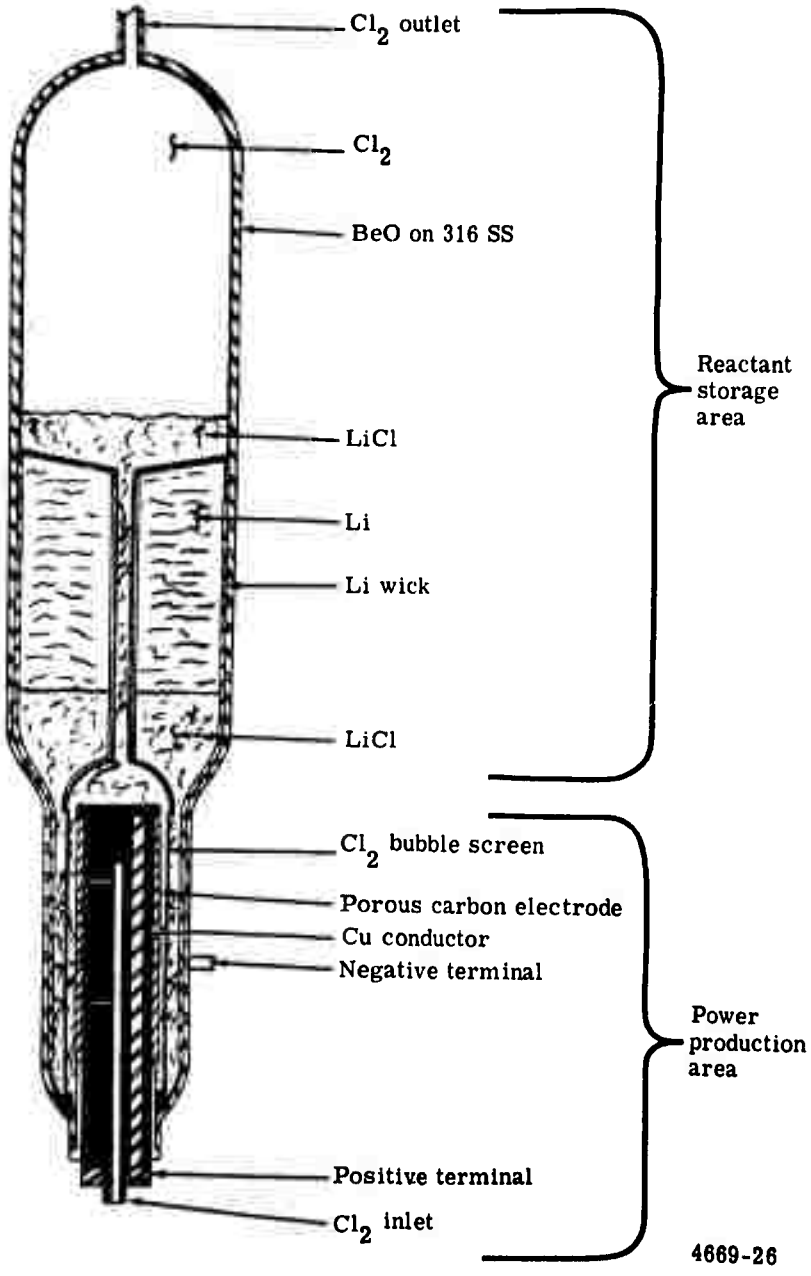

Figure 3-2. Vertical "D" cell.

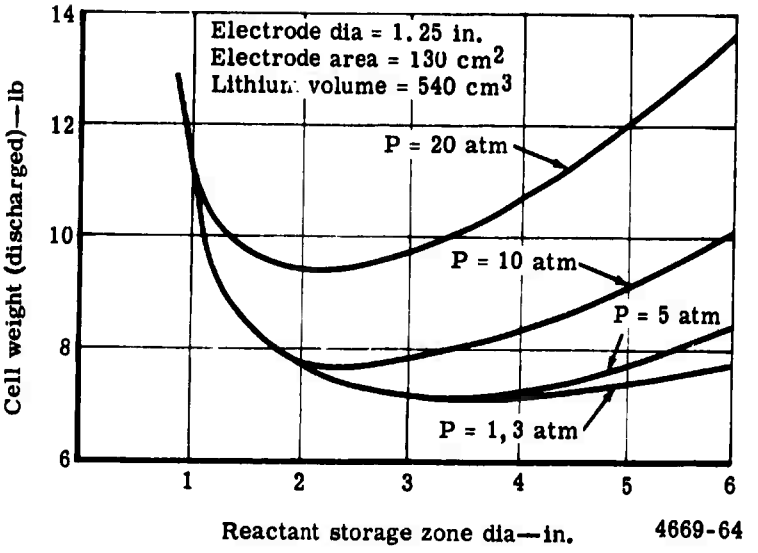

Figure 3-3. "D" cell weight versus diameter.

shows the weight of one cell versus this diameter as a function of pressure for a cell electrode area of 130 cm^2 and a Li storage volume requirement of 540 cm^3. As can be seen, a diameter exists which produces a minimum weight cell. The value of the optimum diameter decreases as the pressure increases. The word optimum is used here to denote the value of reactant zone diameter that corresponds to the minimum cell weight subject to the other variables. A computer routine that selected the weight optimum diameter was used to produce the data shown in Figure 3-4. This plot shows the optimum value of reactant zone diameter for different cell pressures and storage volume requirements. It is independent of the cell electrode area.

Figure 3-3 demonstrates that an optimum storage zone diameter exists that will yield a minimum weight cell. It also shows that a weight penalty over the minimum point occurs if the diameter is selected at a value other than the optimum. This penalty increases as the diameter is selected further from the optimum value. The rate at which the weight penalty increases with diameter also increases as the pressure is increased.

An examination of plots similar to Figure 3-3 also revealed that the optimum diameter is a function of cell pressure and the storage volume. Figure 3-4 summarizes results of studies directed toward defining the optimum diameter. At low storage volumes, the optimum diameter is the same for all pressures. As the storage volume is increased, the

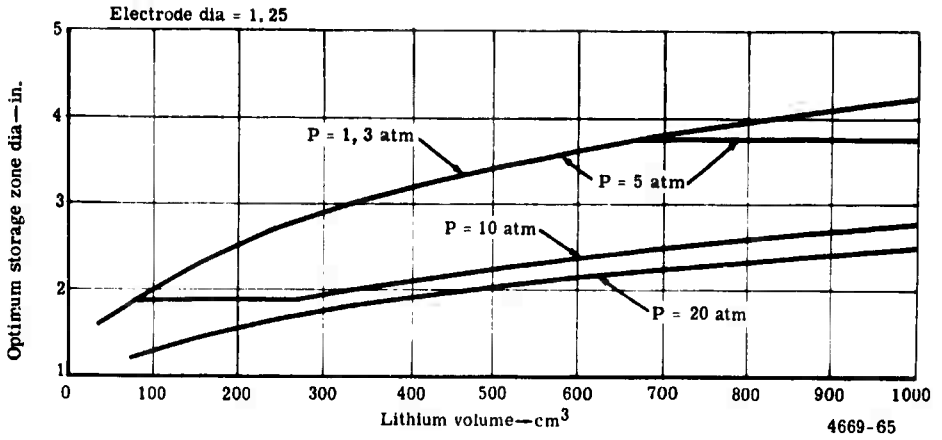

Figure 3-4. Optimum cell diameter.

optimum diameter for a given pressure reaches a constant value and separates from the original curve. Further analysis reveals that the constant diameter value assumed for a given pressure corresponds to the diameter which cannot be exceeded without increasing the minimum value of 0.025 in. But as the storage volume is increased still further, the optimum diameter will again begin increasing. The 10-atm line is the only one shown on Figure 3-4 that exhibits this complete cycle of behavior in the range of storage volumes portrayed.

Figure 3-5 shows cell weight versus pressure and efficiency for 70 cells operating over the ERDL duty cycle. The illustration indicates that minimum weights with respect to efficiency occur at about an efficiency of 78 to 82%. The minimum weight with respect to pressure for the vertical cell is obtained with a cell pressure close to 5 atm.

The final design point for the system was selected based on weight and efficiency optimization. Figure 3-6 shows the total cell weight as a function of pressure and number of cells for a constant efficiency of 82%. This plot indicates that a minimum number of cells should be used and that a system pressure between 4 and 5 atm should be used. As a result of these studies, the design parameters selected were 8 cm for the reactant storage vessel diameter and 5 atm pressure.

The studies of the effect of the numbers of cells indicated that the fewest possible cells should be used. However, because the system voltage is required to be at least 200 v with one cell producing approximately 3.0 v*, a minimum of about 70 cells can be used.

*Open circuit voltage is 3.53 v. Preliminary studies indicate an operating voltage of approximately 3 v offers the best balance of maximum efficiency and minimum weight.

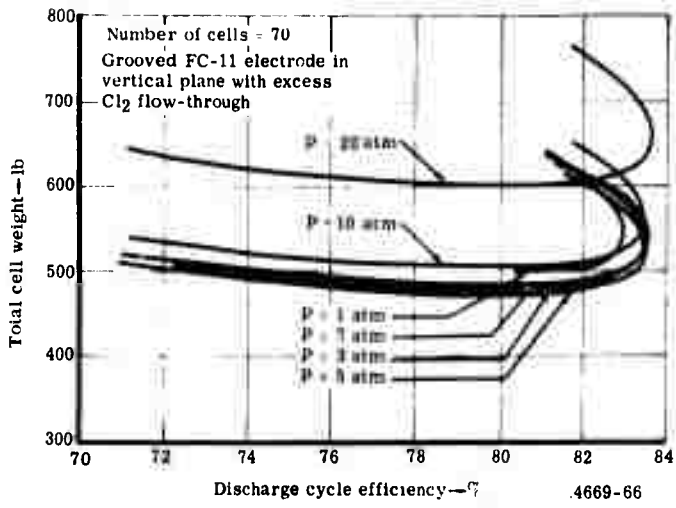

Figure 3-5. Vertical weight.

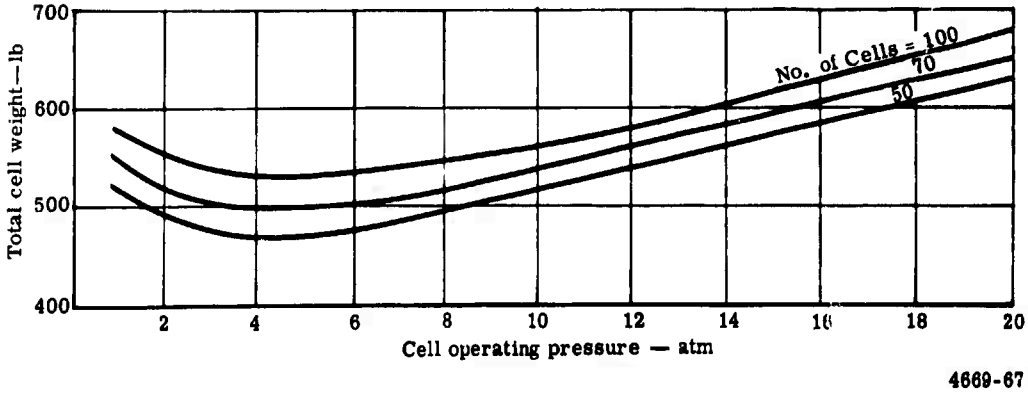

Figure 3-6. Pressure effect on vertical cell weight (discharge cycle efficiency equals 82%).

It is also desirable to have the fewest possible modules. But if fewer than ten modules are used with 70 cells, the module height and weight exceed the limits of 36.0 in. and 100 lb set in the requirements. Therefore, the best selection within the constraints would be a 70-cell, ten module system. Based on the operation of these 70 cells over the ERDL duty cycle, the design conditions selected were 115.2 cm^2 for the cell Cl_2 electrode area and 534.7 cm^3 for the cell Li storage volume.

MODULE WEIGHT ANALYSIS

Having arrived at a cell design to meet the ERDL criteria, as previously described and shown in Figure 1-2, an insulated module was devised. This module concept is described in Appendix 1 and is illustrated in Figure 1-4. This module must satisfy two ERDL criteria.

- It must weigh less than 100 lb to allow ease in handling during replacement.
- It must thermally insulate the cells so that they will not freeze and will have reasonable self-discharge rates.

The criteria of 15-day "hot time" was selected as a reasonable self-discharge rate (see Appendix 1 for discussion). Using a module design computer program, alternatives were considered where a larger number of ERDL cells would be contained in a module. Based on maintaining the 15-day "hot time", total module weights were computed as shown in Figure 3-7. As indicated, seven cells were the maximum number that would allow the module to weigh less than 100 lb.

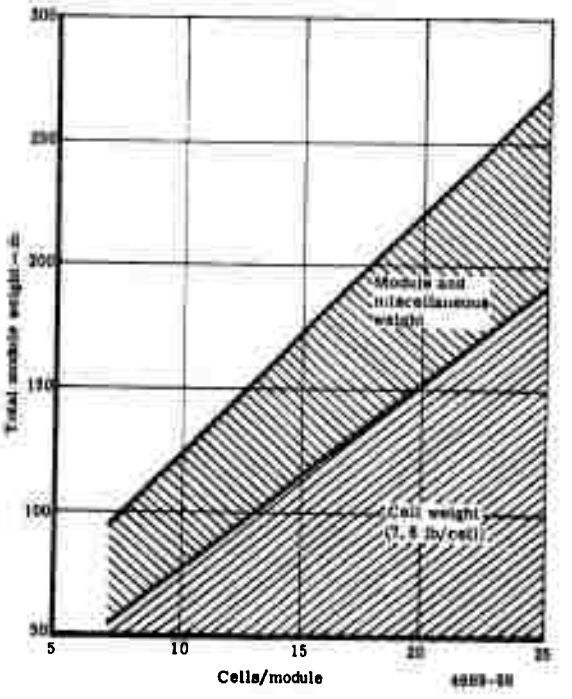

Figure 3-7. Weight of module for ERDL system.

CHLORINE SYSTEM TRADE-OFFS

Alternative schemes for containment of Cl_2 were considered, as discussed in Appendix 1. The one selected as most attractive for the ERDL application was protected liquid storage. Further studies of alternative techniques may suggest other methods to be considered.

Having selected liquid Cl_2 storage as the means to be used, packaging and weight considerations entered into the storage vessel design. Figure 3-8 illustrates several alternatives that were investigated. To facilitate placement, two 12-in. cylinders were selected for use. It can be seen, however, that if vehicle space allowed placement of a single spherical vessel (approximately 21-in. dia) in a protected location, a system weight savings of approximately 20 lb would result.

SYSTEM OPTIMIZATION

Based on a review of weight and efficiency data in the cell parametric analyses, a cell design was established to meet the ERDL specifications. This cell design was selected based on total cell weight optimization and was used in conjunction with other component parametrics to develop an engine system.

A further refinement to system optimization would be desirable if the concept is deemed attractive. This would be to optimize the entire system weight and efficiency. A computer program is currently being developed at Allison for this purpose. This program will give consideration to the module structure and insulation enclosing the cells and to other system components, and it will allow optimization on a total system weight basis. A preliminary curve showing how results may be changed is shown in Figures 3-9 and 3-10. These curves show system weight as a function of discharge efficiency and pressure, considering the following system components:

- Cells and reactants
- Module structure
- Chlorine storage (spherical tank)

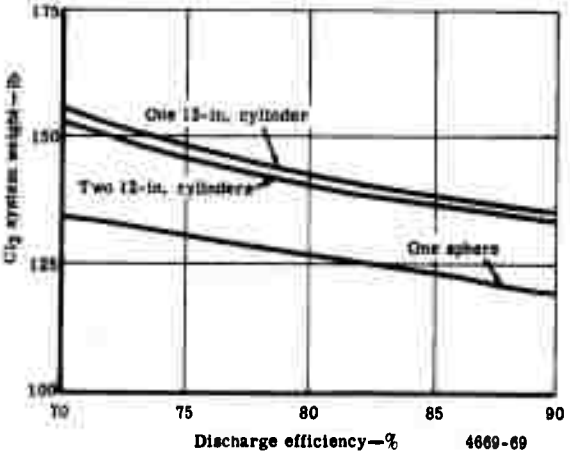

Figure 3-8. Chlorine system weight.

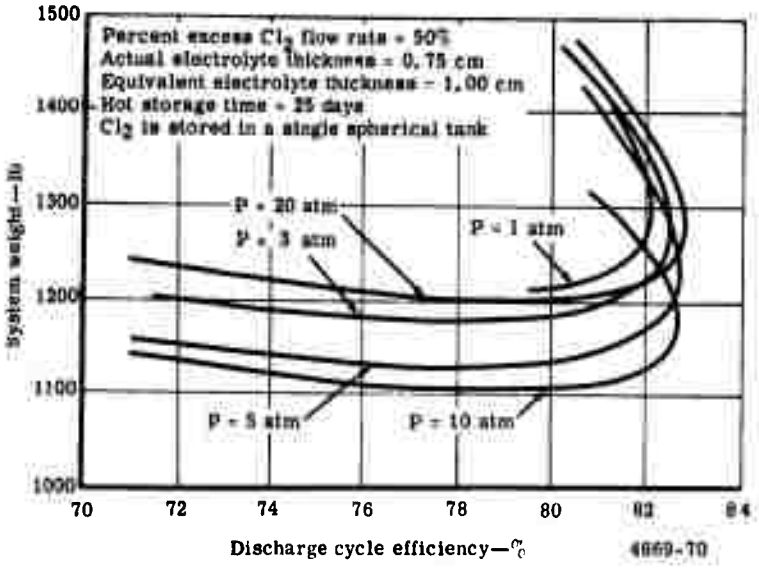

Figure 3-9. System weight versus discharge cycle efficiency.

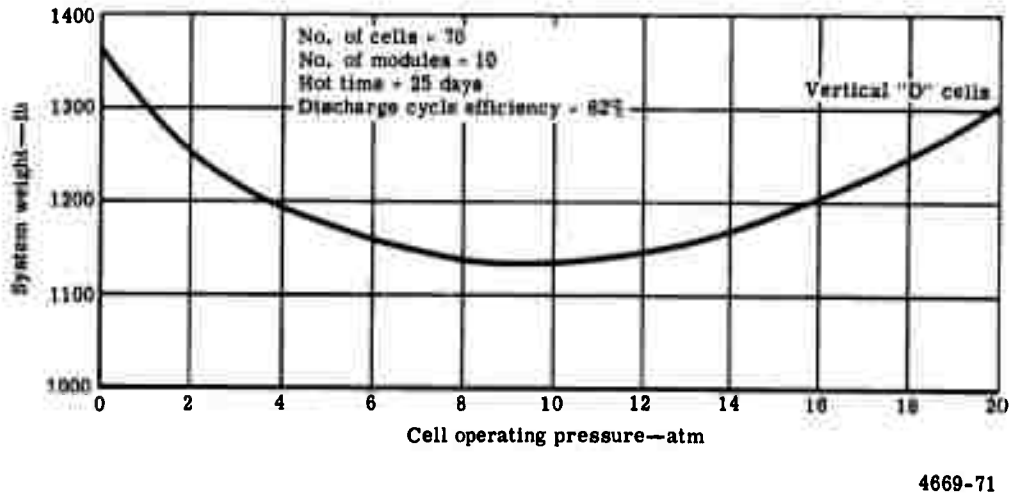

Figure 3-10. System weight versus cell operating pressure.

The apparent trend is that lower system weights can be obtained by using higher system pressures. Since 5 atm appeared to be the optimum pressure for minimum weight considering only cell weight, this curve shows 9 atm to be an optimum. It is planned that further refinements in the computer program will allow an entire system design optimization. After review of alternative design concepts by ERDL, future programs may be directed towards optimization of those concepts which are selected for further development.

APPENDIX 4

SELF-REGULATION OF CHLORINE FLOW

INTRODUCTION

The following analysis is used to show the self-regulating feature of the Cl_2 supply system. Controlling parameters include the regulator outlet pressure, the cell pressure drop, and the jet pump operating characteristics.

CHLORINE FLOW ANALYSIS

Referring to Figures 4-1 and 4-2, assume maximum or design conditions are shown at point A. It remains to determine what will happen at off-design. Assuming a constant inlet pressure, P_1, as power demand is reduced, the flow required is reduced, or $\dot{W}_1$ decreases. It can be noted that all of the flow $\dot{W}_1$ must be consumed by the cell and that $\dot{W}_2 = \dot{W}_1 + \dot{W}_3$. This observation immediately establishes one limit to the flow and pressure, that of zero electrical demand. In this case no flow comes from the tank and the pressures P_1 and P_2 are equal, resulting in zero flow for $\dot{W}_1$, $\dot{W}_2$, and $\dot{W}_3$. This analysis assumes the coulombic efficiency to be 100% for simplicity.

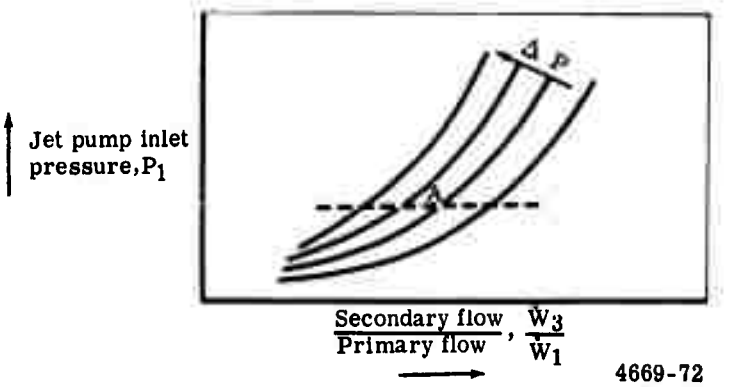

Figure 4-1. Jet pump characteristics.

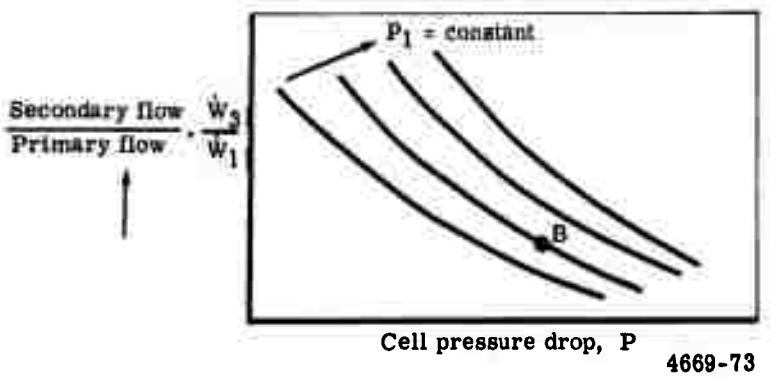

Figure 4-2. Jet pump characteristics—cross plot.

The analysis also shows the cell pressure at zero output equals the pressure regulator output pressure. Next assume 50% maximum power demand. Observe that $\dot{W}_1$, or the flow of the primary stream, must equal the Cl_2 demand of the cell to satisfy the external circuit. This demand is less than design point. The magnitude of the direction taken by $\dot{W}_3/\dot{W}_1$ at constant P_1, as shown in the jet pump characteristics, was not fully established; however, an insight to the resulting secondary flow, $\dot{W}_3$, can be obtained as follows.

- A cross plot of the characteristic jet pump data (Figure 4-2) indicates that by plotting the secondary-to-primary flow ratio, $\dot{W}_3/\dot{W}_1$, to the cell pressure drop, ΔP, with lines of constant supply, pressure, P_1, shows a characteristic that at any constant P_1 value the flow ratio $\dot{W}_3/\dot{W}_1$ increases as the electrode pressure drop decreases. Allison experimental data in Figure 4-3 show that the electrode drop decreases as the current demand decreases.
- In Figure 4-2, if the design point selection were made at point B at 50% excess Cl_2 flow, and with the pressure regulator set for constant outlet pressure, P_1, then the percent excess flow represented by $\dot{W}_3/\dot{W}_1$ would increase with decreasing power demand. It should be observed that the total recirculated flow would decrease with decreasing power demand, but that the ratio of $\dot{W}_3/\dot{W}_1$ would increase.
- If the spread of percent excess Cl_2 flow is considered excessive, then control of the supply pressure, P_1, would be required. This control could be accomplished by using a variable pressure regulator which takes its signal from the cell outlet current. Further analysis will reveal the extent of the excess percent Cl_2 variation over the cell operational spectrum and if any supply pressure control will be required.

CONCLUSIONS

Several conclusions can be drawn from this analysis.

- Chlorine flow will be the amount required by the load and will be set by the resistance of the external load.
- Sufficient excess Cl_2 will be available at all engine power levels to maintain electrode performance.
- The jet pump will provide a means to join the primary and secondary flows during power operation and will provide pressure communication between cell inlet and outlet conditions during standby and shutdown operation. This communication provides cell pressure balance during standby and shutdown and it minimizes LiCl back-flow into the porous carbon electrode.

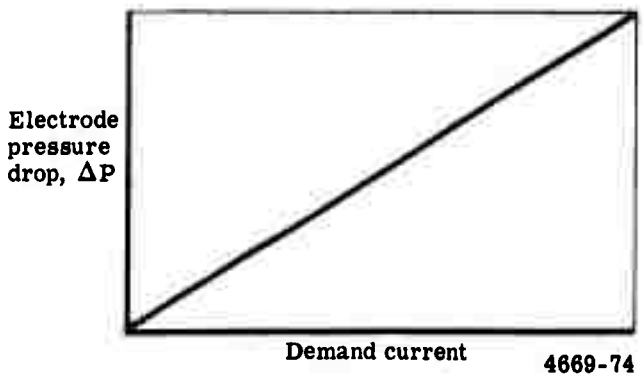

Figure 4-3. Electrode pressure drop characteristics.

APPENDIX 5

CHLORINE ADSORPTION AND DESORPTION DATA

INTRODUCTION

Prior to this contract, investigations of Cl_2 adsorption were in progress at Defense Research Laboratories. Included in these investigations were experiments performed from atmospheric pressure and below for isotherms from 25 to 400°C.

CHLORINE ADSORPTION AND DESORPTION ANALYSIS

The testing apparatus, Figure 5-1, consisted of glass-lined vessels and glass tubing. The charcoal material tested included charcoal types of SGL 8 × 30 and CAL 12 × 40 manufactured by the Pittsburgh Activated Carbon Company.

Isotherm data are presented in Figures 5-2 and 5-3.

Figure 5-4 is a plot showing adsorption-desorption of Cl_2 versus equilibrium time. Adsorption is performed at atmospheric pressure and 25°C except near the end of the adsorption cycle when the pressure is increased to 13 psig. The desorption cycle is started by releasing the pressure to 1 atm. The effects of pressure drop are recorded as the amount of Cl_2 lost. At atmospheric pressure, the temperature of the charcoal is increased over a period of time, and the desorped chlorine is determined for each temperature interval. The desorption cycle was completed at 535°C.

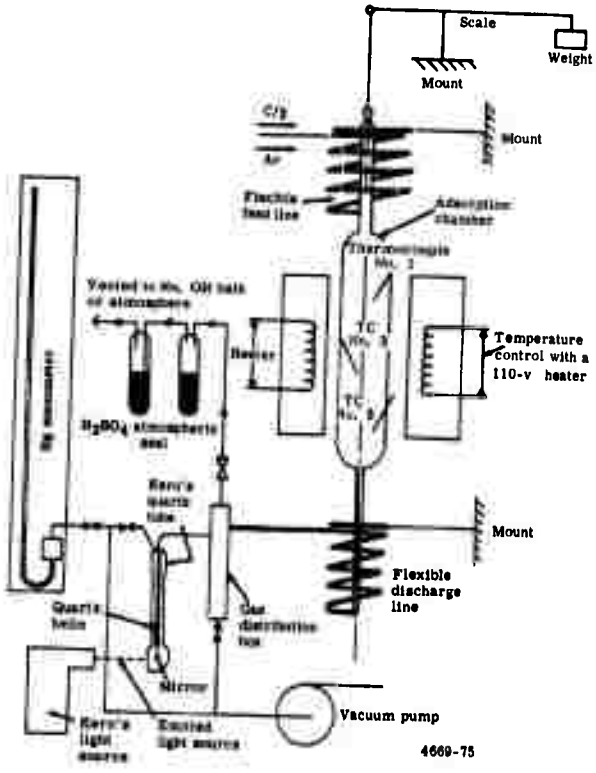

Figure 5-1. Chlorine adsorption system.

BLANK PAGE

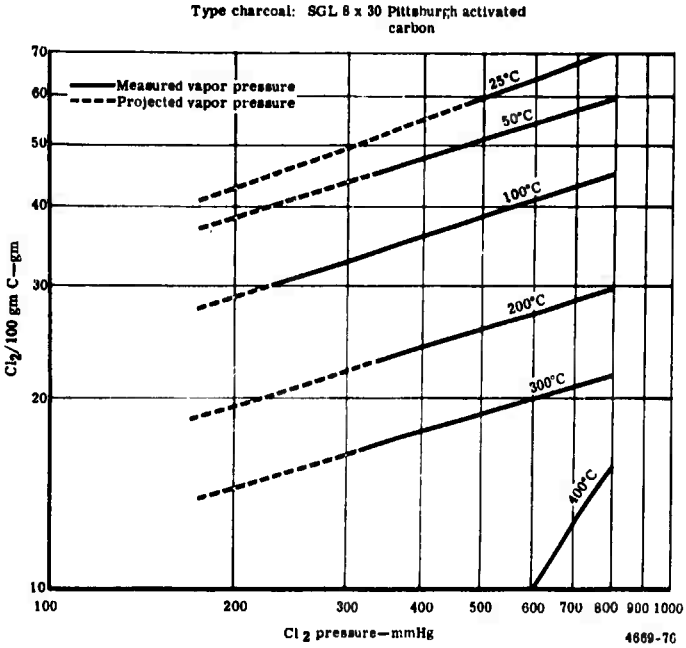

Figure 5-2. Chlorine adsorption isotherms.

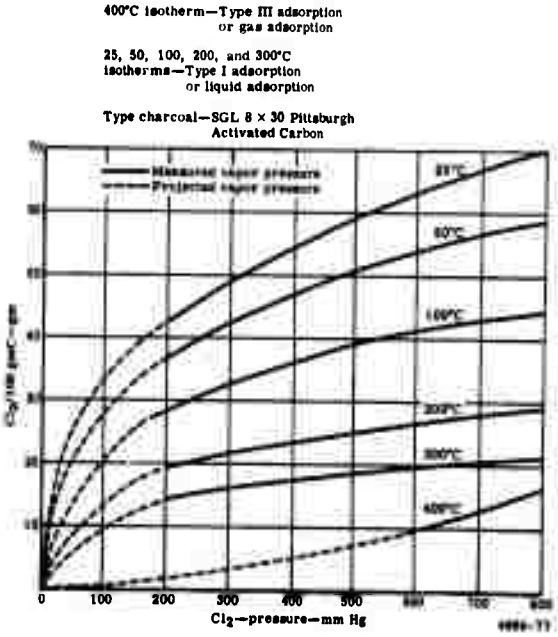

Figure 5-3. Chlorine adsorption isotherms.

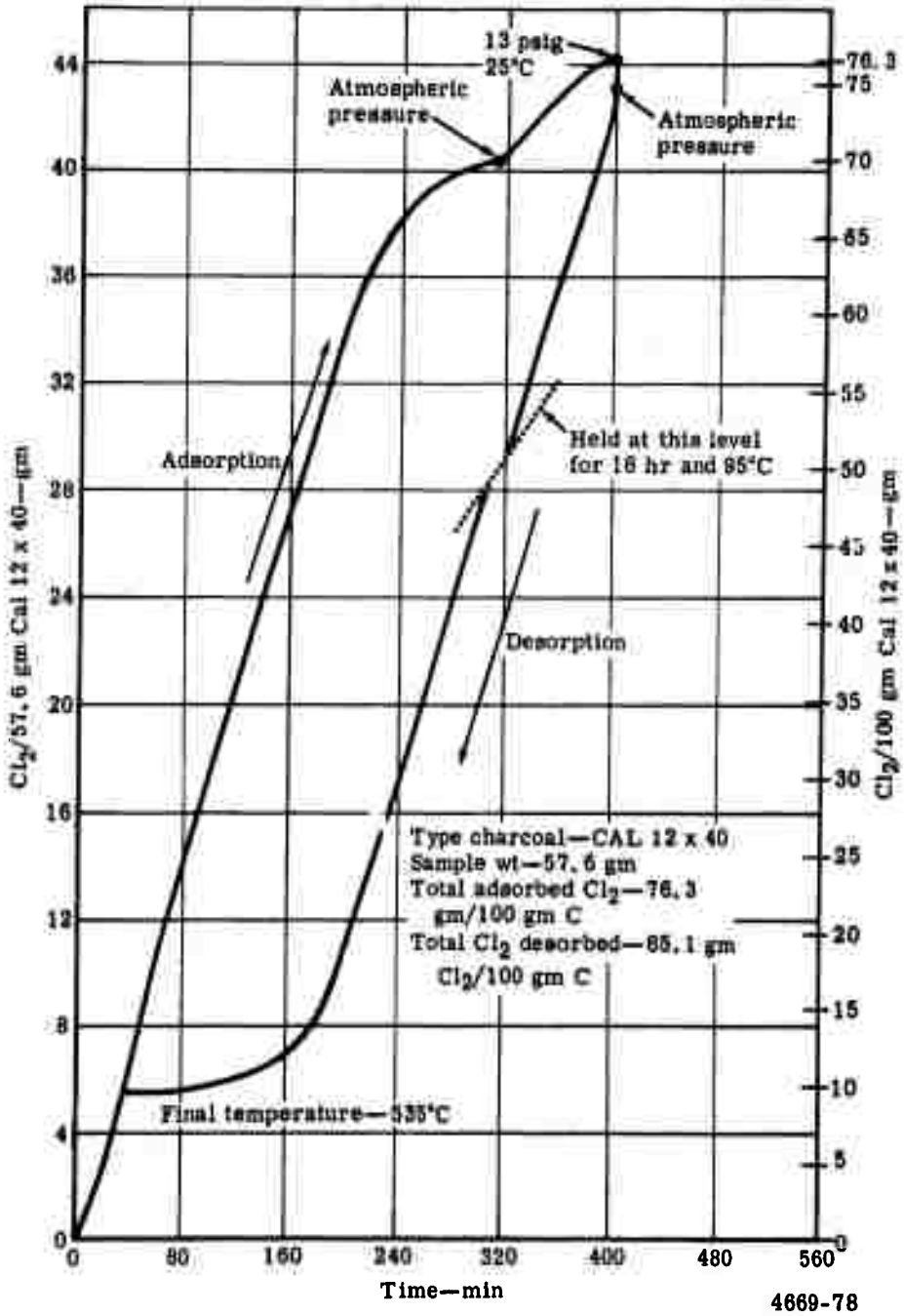

Figure 5-4. Chlorine adsorption-desorption.

Unclassified

Security Classification

DOCUMENT CONTROL DATA - R&D

(Security classification of title, body of abstract and indexing annotation must be entered when the overall report is classified)

1 ORIGINATING ACTIVITY (Corporate author) Allison Division of General Motors P. O. Box 894 Indianapolis, Indiana 46206	2a REPORT SECURITY CLASSIFICATION Unclassified 2b GROUP

3. REPORT TITLE

LITHIUM-CHLORINE ELECTROCHEMICAL ENERGY STORAGE SYSTEM

4 DESCRIPTIVE NOTES (Type of report and inclusive dates)

Interim Technical Report (13 December 1965—13 June 1966)

5 AUTHOR(S) (Last name, first name, initial)

Hietbrink, Earl H. (Editor)

6. REPORT DATE	7a TOTAL NO OF PAGES	7b. NO OF REFS
5 June 1966	126	5

8a. CONTRACT OR GRANT NO. DA-44-009-AMC-1426(T) b. PROJECT NO. c. d.	9a ORIGINATOR'S REPORT NUMBER(S) EDR 4669 9b OTHER REPORT NO(S) (Any other numbers that may be assigned this report)

10. AVAILABILITY/LIMITATION NOTICES

11. SUPPLEMENTARY NOTES	12 SPONSORING MILITARY ACTIVITY U.S. Army Research and Development Laboratories, Fort Belvoir, Virginia 2206

13. ABSTRACT

The objective of the program is to obtain suitable laboratory data to determine the feasibility of a lithium-chlorine electrically rechargeable electrochemical energy storage system for vehicle propulsion. Various methods for increasing the electrochemical charge rate were investigated. At high charging current densities, the cell efficiency was found to drop significantly due to polarization of the Cl_2 electrode. Experimental investigations determined that both geometry and material selection are important in the electrode design and that reverse pulsing enhances the electrode performance, allowing higher charging current density. A laboratory test cell using Li and Cl_2 as reactants was fabricated to evaluate methods for increasing the electrochemical charge rate. An electrical short terminated the first cell test before meaningful data could be obtained. The required design modifications to eliminate this problem are being incorporated into the design. System analytical studies were conducted on two cell concepts. The first was an advanced concept of the Mark IV experimental cell currently being tested. The second was a cylindrical cell design using vertical electrodes. The latter cell was selected as the most advantageous and was developed into a replaceable ten-module engine system to meet the ERDL duty cycle requirements. The system is estimated to weigh 1250 lb and provide 200 kw-hr of energy. System analysis and trade-off studies on a fast charge system concept are in progress. Experimental investigations were initiated to determine the feasibility of Cl_2 adsorption on charcoal.

DD FORM 1 JAN 64 1473

Unclassified

Security Classification

BLANK PAGE

14. KEY WORDS	LINK A		LINK B		LINK C	
	ROLE	WT	ROLE	WT	ROLE	WT
Electric propulsion						
Energy conversion						
Electric power production						
Storage batteries						
Batteries and components						
Power supplies						
Power equipment						
Electrical equipment						
Electrochemistry						
Chemical reactions						
Electrodes						
Electrolytes						

INSTRUCTIONS

1. ORIGINATING ACTIVITY: Enter the name and address of the contractor, subcontractor, grantee, Department of Defense activity or other organization *(corporate author)* issuing the report.

2a. REPORT SECURITY CLASSIFICATION: Enter the overall security classification of the report. Indicate whether "Restricted Data" is included. Marking is to be in accordance with appropriate security regulations.

2b. GROUP: Automatic downgrading is specified in DoD Directive 5200.10 and Armed Forces Industrial Manual. Enter the group number. Also, when applicable, show that optional markings have been used for Group 3 and Group 4 as authorized.

3. REPORT TITLE: Enter the complete report title in all capital letters. Titles in all cases should be unclassified. If a meaningful title cannot be selected without classification, show title classification in all capitals in parenthesis immediately following the title.

4. DESCRIPTIVE NOTES: If appropriate, enter the type of report, e.g., interim, progress, summary, annual, or final. Give the inclusive dates when a specific reporting period is covered.

5. AUTHOR(S): Enter the name(s) of author(s) as shown on or in the report. Enter last name, first name, middle initial. If military, show rank and branch of service. The name of the principal author is an absolute minimum requirement.

6. REPORT DATE: Enter the date of the report as day, month, year; or month, year. If more than one date appears on the report, use date of publication.

7a. TOTAL NUMBER OF PAGES: The total page count should follow normal pagination procedures, i.e., enter the number of pages containing information.

7b. NUMBER OF REFERENCES: Enter the total number of references cited in the report.

8a. CONTRACT OR GRANT NUMBER: If appropriate, enter the applicable number of the contract or grant under which the report was written.

8b, 8c, & 8d. PROJECT NUMBER: Enter the appropriate military department identification, such as project number, subproject number, system numbers, task number, etc.

9a. ORIGINATOR'S REPORT NUMBER(S): Enter the official report number by which the document will be identified and controlled by the originating activity. This number must be unique to this report.

9b. OTHER REPORT NUMBER(S): If the report has been assigned any other report numbers *(either by the originator or by the sponsor)*, also enter this number(s).

10. AVAILABILITY/LIMITATION NOTICES: Enter any limitations on further dissemination of the report, other than those imposed by security classification, using standard statements such as:

(1) "Qualified requesters may obtain copies of this report from DDC."

(2) "Foreign announcement and dissemination of this report by DDC is not authorized."

(3) "U. S. Government agencies may obtain copies of this report directly from DDC. Other qualified DDC users shall request through _____."

(4) "U. S. military agencies may obtain copies of this report directly from DDC. Other qualified users shall request through _____."

(5) "All distribution of this report is controlled. Qualified DDC users shall request through _____."

If the report has been furnished to the Office of Technical Services, Department of Commerce, for sale to the public, indicate this fact and enter the price, if known.

11. SUPPLEMENTARY NOTES: Use for additional explanatory notes.

12. SPONSORING MILITARY ACTIVITY: Enter the name of the departmental project office or laboratory sponsoring *(paying for)* the research and development. Include address.

13. ABSTRACT: Enter an abstract giving a brief and factual summary of the document indicative of the report, even though it may also appear elsewhere in the body of the technical report. If additional space is required, a continuation sheet shall be attached.

It is highly desirable that the abstract of classified reports be unclassified. Each paragraph of the abstract shall end with an indication of the military security classification of the information in the paragraph, represented as *(TS)*, *(S)*, *(C)*, or *(U)*.

There is no limitation on the length of the abstract. However, the suggested length is from 150 to 225 words.

14. KEY WORDS: Key words are technically meaningful terms or short phrases that characterize a report and may be used as index entries for cataloging the report. Key words must be selected so that no security classification is required. Identifiers, such as equipment model designation, trade name, military project code name, geographic location, may be used as key words but will be followed by an indication of technical context. The assignment of links, rules, and weights is optional.